UNIVERSIDADE FEDERAL DE SÃO CARLOS

CENTRO DE CIÊNCIAS EXATAS E DE TECNOLOGIA
DEPARTAMENTO DE QUÍMICA
PROGRAMA DE PÓS-GRADUAÇÃO EM QUÍMICA

"MAGNETIC IMMOBILIZED ENZYMES MICROREACTORS FOR IN-VITRO METABOLISM ASSAYS AND/OR BIOCATALYSIS APPLICATIONS"

Izadora Liranço Furlani*

Tese apresentada como parte dos requisitos para obtenção do título de DOUTOR EM CIÊNCIAS, área de concentração: QUÍMICA.

Orientadora: Profa. Dra. Quezia Bezerra Cass

Coorientadora: Profa. Dra. Regina Vincenzi Oliveira

*** bolsista FAPESP (2018/03035-3 e 2021/10410-8)**

São Carlos – SP

2023

UNIVERSIDADE FEDERAL DE SÃO CARLOS

Centro de Ciências Exatas e de Tecnologia
Programa de Pós-Graduação em Química

Folha de Aprovação

Defesa de Tese de Doutorado da candidata Izadora Liranço Furlani, realizada em 31/03/2023.

Comissão Julgadora:

Profa. Dra. Quezia Bezerra Cass (UFSCar)

Profa. Dra. Maria Emília da Silva Pereira de Sousa (U.Porto)

Profa. Dra. Maria Elizabeth Tiritan (U.Porto)

Profa. Dra. Lidia Moreira Lima (UFRJ)

Profa. Dra. Carmen Lúcia Cardoso (FFCLRP/USP)

O Relatório de Defesa assinado pelos membros da Comissão Julgadora encontra-se arquivado junto ao Programa de Pós-Graduação em Química.

Dedico esta tese de doutorado aos meus pais e melhores amigos, ***Edna e Edgard.*** ∞

Obrigada, pai e mãe por cada conselho e por me mostrar que a maior herança é o conhecimento.

AGRADECIMENTOS

À Profa. Dra. Quezia Bezerra Cass por abrir as portas de seu laboratório e acompanhar meus primeiros passos como cientista. Obrigada por compartilhar seu conhecimento e pela amizade.

À Profa. Dra. Regina Vincenzi de Oliveira por aceitar ser minha coorientadora e acompanhar de perto toda a evolução do projeto. Agradeço por compartilhar seu conhecimento e experiências em laboratório. Obrigada também pelas conversas e todo incentivo.

Ao Prof. Dr. Serge Rudaz da Universidade de Genebra por me acolher em seu laboratório e me proporcionar a oportunidade da realização de um sonho. Agradeço pelos ensinamentos, conselhos e desafios a mim confiados.

À Dra. Isabel Meister por acompanhar de perto meu período na Universidade de Genebra. Obrigada Isa pela paciência, por todo conhecimento compartilhado e por me mostrar a beleza da metabolômica e lipidômica.

Aos meus queridos amigos do núcleo de pesquisa em cromatografia, Separare e agregados, pela amizade, momentos de café, discussões científicas, apoio e incentivo. Agradeço pelos momentos de descontração dentro e fora do laboratório.

Aos meus queridos amigos da Universidade de Genebra que me receberam de braços abertos. Obrigada pelas discussões científicas, acolhimento e aperols.

Ao Fernando Gonçalves de Almeida pelo companheirismo e apoio em um dos momentos mais importantes da minha carreira.

Agradeço incondicionalmente aos meus pais, Edgard e Edna, minha irmã Débora Carla, meus sobrinhos, Yuri e Miguel. Obrigada pelo amor,

apoio, puxões de orelha, velas acesas e por sempre estarem comigo em todos os momentos. A vocês, eu dedico todo meu amor, carinho e gratidão.

Aos docentes e ao corpo técnico e administrativo do Departamento de Química da Universidade Federal de São Carlos e da Universidade de Genebra.

Ao Prof. Dr. Wladimir Rafael Beck do Departamento de Ciências Fisiológicas da Universidade Federal de São Carlos, pela doação de fígados de ratos Wistar.

Ao Prof. Dr. Anderson Rodrigo Moraes de Oliveira da Faculdade de Filosofia Ciências e Letras de Ribeirão Preto – USP, pela doação de diclofenaco e bufuralol.

À Ouro Fino Saúde Animal pela doação de albendazol sulfóxido.

À Fundação de Amparo à Pesquisa do Estado de São Paulo (FAPESP) pelas bolsas de Doutorado Direto (2018-03035-3) e Bolsa Estágio de Pesquisa no Exterior - BEPE (2021/10410-1).

Agradeço ao apoio financeiro da Coordenação de Aperfeiçoamento de Nível Superior – Brasil (CAPES) – Código de Financiamento 001 e, ao Conselho Nacional de Desenvolvimento Científico e Tecnológico – CNPq.

LIST OF ABBREVIATIONS

CYP	Cytochrome P450
NADPH	Nicotinamide adenine dinucleotide phosphate reduced
$NADP^+$	Nicotinamide adenine dinucleotide phosphate oxidized
G6PDH	Glucose-6-phosphate dehydrogenase
G6PDH-Mbs	Glucose-6-phosphate dehydrogenase immobilized onto magnetic beads
RLM	Rat liver microsomal fraction
RLM-Mbs	Rat liver microsomal fraction immobilized onto magnetic beads
LC-UV	Liquid-chromatography coupled to ultraviolet detector
LC-MS	Liquid-chromatography coupled to mass spectrometer
ABZ	Albendazole
ABZSO	Albendazole sulfoxide
G6PDH-HLM-Mbs	Dual one pot system containing G6PDH-Mbs and HLM-Mbs
CL	Metabolic clearance
DDI	Drug-drug interaction
DME	Drug metabolite enzymes
NCE	New Chemical Entities
rCYP	Human cytochrome recombinant enzymes
HLM	Human liver microsomes
HLM-Mbs	Human liver microsomal fraction immobilized onto magnetic beads
DNA	Deoxyribonucleic acid
FMO	Flavin-containing monooxygenases
UGT	UDP-glucuronsyl transferases
SULTs	sulfotransferases

GSTs	glutathione S-transferases
NATs	N-acetyltransferases
UDPGA	Uridine diphosphate glucuronic acid
V_0	Velocity of reaction
K_m	Michaelis-Menten constant
V_{max}	Maximum rate achieved by the system
[S]	Concentration of a substrate S
K_{prime}	Constant comprising the interaction factor
H	Hill's coefficient
CLint	Metabolic intrinsic clearance
EDES	electrochemically-driven enzymatic system
QqQ	Triple-quadrupole mass spectrometer analyser
SRM	Selection reaction monitoring

LIST OF TABLES

LIST OF FIGURES

RESUMO

IMOBILIZAÇÃO DE ENZIMAS EM MICROREATORES MAGNÉTICOS COM APLICAÇÃO EM ENSAIO DE METABOLISMO *IN VITRO* E BIOCATÁLISE

Citocromo P450s é uma superfamília de hemeproteínas amplamente utilizada para estudar reações de fase I em ensaios de metabolismo *in vitro* de fármacos e, correlacionar com resultados *in vivo*. Além disso, esta classe de enzimas pode estar envolvida na biossíntese de compostos de alto valor e, portanto, apresenta grande interesse industrial. As reações catalisadas por CYPs são complexas e envolvem várias etapas. Além disso, problemas relacionados com à falta de atividade catalítica e o fornecimento constante do cofator nicotinamida adenina dinucleotídeo fosfato (NADPH) são alguns desafios a serem superados. Considerando esses aspectos, novas alternativas analíticas devem ser implementadas para transformar os ensaios convencionais usando CYPs em uma abordagem mais viável. A imobilização de enzimas tem sido utilizada há vários anos e ainda representa uma estratégia inteligente para aumentar a atividade catalítica, a estabilidade e, quando possível, proporcionar a reutilização do alvo imobilizado. Para atender a esse objetivo, a primeira parte do trabalho aqui apresentado, consistiu na imobilização da enzima glicose-6-fosfato desidrogenase (G6PDH) em partículas magnéticas (G6PDH-Mbs). Um método LC-UV foi desenvolvido e qualificado para quantificar a produção de NADPH. O biorreator biocatalítico G6PDH-Mbs foi caracterizado através de estudos cinéticos onde o perfil sigmoidal foi obtido. A aplicação de G6PDH-Mbs foi demonstrada em ensaios de metabolismo *in vitro* utilizando albendazol e fiscalina B. A implementação de G6PDH-Mbs como sistema gerador aumentou em 3 vezes a produção dos metabólitos quando comparado ao uso de NADPH comercial. A segunda parte do trabalho, está relacionada à imobilização de CYPs. Para isso,

frações microssomais de fígado de rato (do inglês, *rat liver microsomes* - RLM) foram usadas como uma alternativa econômica para modular as condições de imobilização das CYPs em esferas magnéticas. Em seguida, o procedimento de imobilização otimizado foi aplicado à frações microssomais de fígado humano (do inglês, *human liver microsomes* - HLM) para produzir o biorreator biocatalítico HLM-Mbs. As reações de biotransformação usando HLM-Mbs foram testadas monitorando a biotransformação de albendazol (ABZ) em albendazol-sulfóxido (ABZ-SO) e, a temperatura foi avaliada para aumentar a produção de metabólitos e a reutilização de HLM-Mbs em múltiplos ciclos. A aplicação de HLM-Mbs em ensaios de metabolismo *in vitro* foi demonstrada por estudos cinéticos e de inibição. Além disso, as atividades catalíticas para CYP2C9 e CYP2D6 foram testadas avaliando as reações de hidroxilação de diclofenaco e bufuralol como substratos. Como contribuição final deste trabalho, um biorreator bicatalítico dual (G6PDH-HLM-Mbs) foi criado misturando o sistema gerador de NADPH (G6PDH-Mbs) com HLM-Mbs.

ABSTRACT

MAGNETIC IMMOBILIZED ENZYMES MICROREACTORS FOR IN-VITRO METABOLISM ASSAYS AND/OR BIOCATALYSIS APPLICATION

Cytochrome P450s are a superfamily of hemeproteins widely used to study phase I reactions in *in vitro* drug metabolism assays and to correlate them with *in vivo* outcomes. In addition, this class of enzymes can be involved in the biosynthesis of high-value complex compounds and thus, has emerged as a key asset within industrial interest. Reactions catalyzed by CYPs are complex and routinely involve several steps. Moreover, problems related to the lack of catalytic activity and the constant supply of the cofactor nicotinamide adenine dinucleotide phosphate (NADPH) are some drawbacks to be overcome. Considering these aspects, new analytical alternatives should be implemented to transform conventional assays using CYP into a more valuable approach. Enzyme immobilization has been used for several years and it still represents a clever strategy to increase catalytic activity, stability, and when possible, to provide the reuse of the immobilized target. To meet this end, as the first part of the work herein described, the enzyme glucose-6-phosphate dehydrogenase (G6PDH) was covalently immobilized onto magnetic beads (G6PDH-Mbs). An LC-UV method was developed and qualified to quantify the production of NADPH. The biocatalyst bioreactor G6PDH-Mbs was characterized through kinetic studies where a sigmoidal profile was obtained. The application of G6PDH-Mb was demonstrated in *in vitro* metabolism assays using albendazole and fiscalin B. The implementation of G6PDH-Mb as a generator system increased 3-folds the production of the metabolites when compared to the use of commercial NADPH. The second part of the work is related to CYP immobilization. For that, rat liver microsomes (RLM) were used as a cost-effective alternative to modulating the immobilization conditions for CYP onto magnetic beads. Next, the optimized

immobilization procedure was applied to human liver microsomal (HLM) to produce the biocatalytic bioreactor HLM-Mbs. Biotransformation reactions using HLM-Mbs were tested by monitoring the biotransformation of albendazole (ABZ) into albendazole-sulfoxide (ABZ-SO), and the temperature was evaluated to increase the production of the metabolites and the reuse of HLM-Mbs in multiple cycles. The application of HLM-Mbs in *in vitro* metabolism assays was demonstrated by kinetic and inhibition studies. In addition, catalytic activities for CYP2C9 and CYP2D6 were tested by evaluating the hydroxylation reactions of diclofenac and bufuralol as substrates. As a final contribution of this work, a dual biocatalyst bioreactor (G6PDH-HLM-Mbs) was created by mixing the generator system of NADPH (G6PDH-Mbs) with HLM-Mbs.

TABLE OF CONTENTS

Chapter I

Introduction

Chapter I | Introduction

1.1 Cytochrome P450 enzymes: Structures, Properties and Application

Cytochrome P450 (CYP) enzymes are a superfamily of hemoproteins belonging to the enzymatic subclass of monooxygenases (EC 1.14.14.1). These enzymes were identified in the 1960s by Omura and Sato.[1,2] The name "cytochromes P450" was attributed due to the maximum absorbance at 450 nm when CYPs are in the reduced form and in the presence of carbon monoxide.[2] CYPs have been identified in almost all animal species, plants, fungi, and bacteria. Several families and subfamilies are listed according to the degree of homology in the peptide sequence. For their nomenclature, the root "CYP" is used followed by a family number (> 40 % identity in amino acid sequence), a family letter (> 55 % identity), and another number designating to the individual enzyme.[3] In humans, CYP is mainly present in the liver, particularly in hepatocytes. Their presence has also been demonstrated in other organs such as skin, lungs, kidneys, brain, and intestine.[3,4] Currently, 18 families of human CYP are listed, encoded by 57 different genes. Among these 57 isozymes, 13 are considered "orphans" because their metabolic function is still unknown.[4]

CYPs are integrated into the phospholipid membrane of the smooth endoplasmic reticulum of many cells and require the presence of two electron transfer proteins, the NADPH-P450 reductase[5,6] and the cytochrome b5. The electron transfer chain is as follows: NADPH > NADPH-P450 reductase > CYP. In this sense, the role of cytochrome b5 is still uncertain but it seems to have a second electron transfer properties.[7,8]

The main steps of the catalytic cycle of CYPs are agreed upon in the literature and are depicted in FIGURE 1.1.[9] Catalysis begins with the binding of the substrate (RH) to cytochrome P450 in the oxidized form (Fe^{3+}), and the binary complex P450-($F3^{+3}$)-RH is formed **(a)**, which is reduced through two sequential oxido-reduction steps, where the cofactor NADPH donates an electron to cytochrome P450 via a flavoprotein called NADPH-cytochrome P450 reductase, which in turn reduces the RH-P450 complex (Fe^{3+}), and forms the complex RH-P450-(Fe^{2+}) **(b)**. Thus, the RH-P450-(Fe^{2+}) complex binds to molecular oxygen to form the RH-P450-(Fe^{2+})-O_2 complex **(c)**, which accepts a second electron introduced by NADPH, reducing the molecular oxygen and forming a highly reactive and unstable complex **(d)**. Next, the protonation of the complex occurs resulting in cleavage of the O-O bond **(e)** and releasing water **(f)**. A P450-Fe^{+3}O-RH complex is formed, followed by the removal of a hydrogen atom from the substrate **(g)**. Ultimately, the oxygenated substrate dissociates, regenerating the oxidized form of cytochrome P450.[10–12]

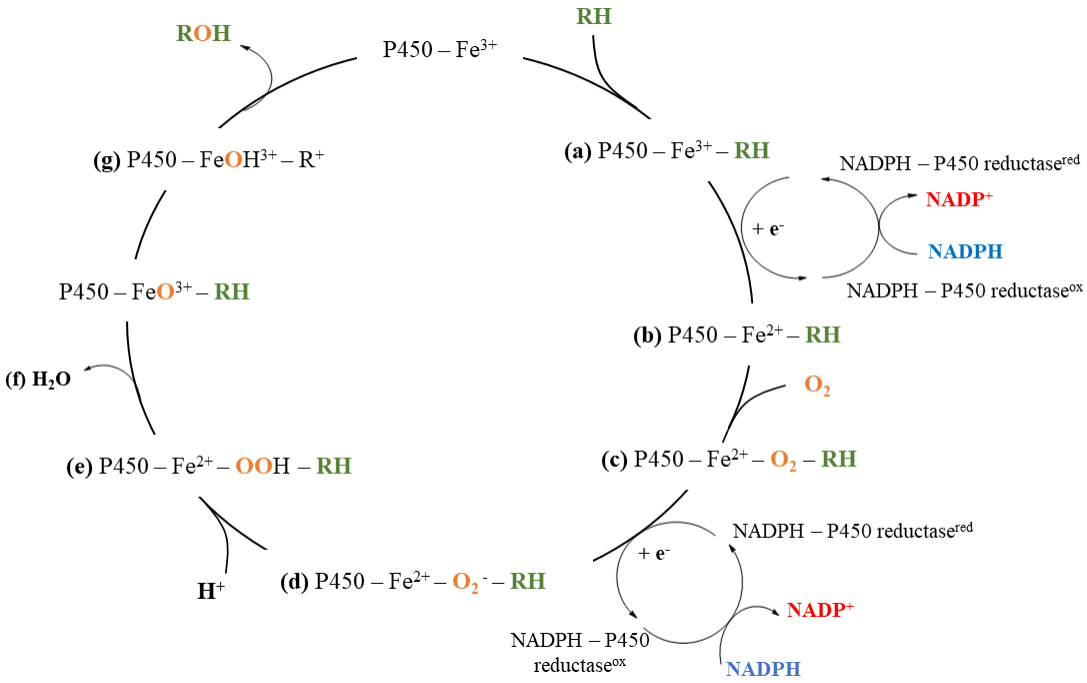

FIGURE 1.1. Diagram representing general aspects of the catalytic cycle of cytochrome P450 enzymes. RH is the substrate and ROH is the metabolite formed. Adapted from Guengerich.[9]

As depicted in FIGURE 1.1, reactions catalyzed by CYPs must occur in the presence of the nicotinamide adenine dinucleotide phosphate reduced (NADPH) and are known as hydroxylation or monooxygenation reactions due to the ability of cytochrome P450 to mediate the transfer of one oxygen to the substrate and reduction of the other oxygen into water, resulting in compounds that are hydrophilic and more susceptible to elimination or further phase II reactions.[13] Thus, the main role of CYPs are to catalyze various reactions in the metabolism of endogenous (*e.g.*, steroid hormones, cholesterol, and fatty acids), and/or exogenous/xenobiotics molecules (*e.g.*, drugs, air pollutants, and pesticides).[14] The catalytic diversity demonstrated to interact with a large number of substrates is due to the expression of various isozymes with complementary selectivity.

It is estimated that CYPs are responsible for about 75 – 80 % of the metabolism of drugs currently available in the market and this class of enzymes is mainly involved in the phase I reactions. Considering the expression rate of the various isozymes in the human liver, only three families (CYP1, CYP2, and CYP3) are significantly involved in this process. The most important isozymes contributing in a total to more than 95 % of the drug bioconversion mediated by all CYPs are: CYP1A1, CYP1A2, CYP2B6, CYP2C9, CYP2C19, CYP2D6, CYP2E1, CYP3A4, and CYP3A5.[15–17] FIGURE 1.2 represents the contribution of different isoforms in drug metabolism.[18,19]

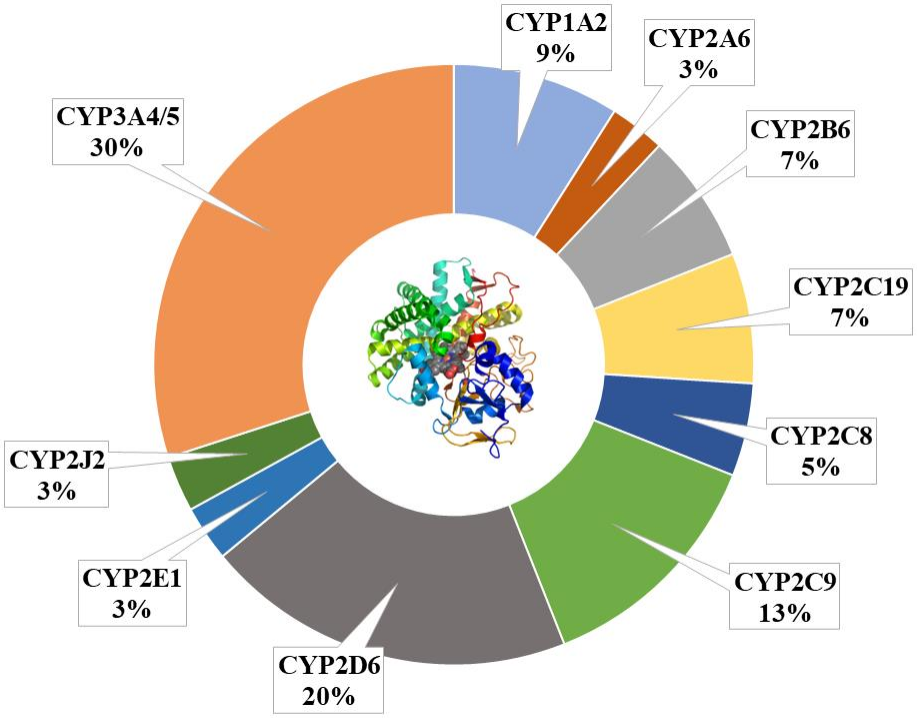

FIGURE 1.2. Percentage contribution of different CYP's isozymes in the metabolism of drugs commercially available.[18,19]

During the early stages of drug discovery and development, the knowledge of drug metabolic properties involving CYPs is crucial to establish a drug profile considering safety, efficacy, and toxicity. This scenario led to the rapid introduction of a number of *in vitro* metabolism assays aiming to promote the development of new, robust, efficient, and safer drug therapies.[20] Elucidation of the metabolic stability of a drug to predict its clearance (CL) and to assess potential drug-drug interactions (DDIs) remain two main important goals in conducting *in vitro* metabolism assays. Other goals include (i) elucidation and determination of principal metabolic routes, (ii) identification of major metabolites, (iii) mapping of major drug metabolite enzymes (DMEs) responsible for the main biotransformation pathways, and (iv) assessment of their quantitative contributions to the overall metabolic profile.[21]

In this sense, the advantage of *in vitro* drug metabolism methods is the possibility of understanding and predicting mostly all *in vivo* situations without administering the drugs to humans or unnecessarily sacrificing animals.[22] Furthermore, some approaches such as metabolic stability and CYP inhibition,

can be easily incorporated into cost and time-effective high throughput methodologies.

In addition, CYPs also display a significant role in the synthesis of compounds. In this context, protein engineering has been promoting great efforts to improve the catalytic activity of CYPs, increase the stability and explore other non-natural reactions catalyzed by CYPs. In the biocatalysis field, bacterial CYPs are the most applied set of enzymes due to their high turnover, readily expressed in *E. coli*, and the use of oxygen more efficiently (high couple efficiency). Recently studies have focused on enzymatic/chemo-enzymatic multistep cascades involving CYPs for producing valuable organic compounds with higher structural and functional diversification.[17,23]

1.2 NADPH as an important cofactor in reactions catalyzed by CYP

As previously discussed, nicotinamide adenine dinucleotide phosphates ($NADP^{+}_{(ox)}$/$NADPH_{(red)}$) play an essential role as electron donors, not only in reactions catalyzed by CYP, but in several anabolic and catabolic reactions.[13,14] It is also useful in most biosynthetic enzymatic reactions, including those responsible for all major cell components, such as DNA and lipids. Due to this essential role in biosynthesis, the availability of NADPH represents a great interest to the industry. However, a constant NADPH supply would be too expensive for large-scale applications.[24]

Using a generator system for the *in situ* production of NADPH is an alternative to overcome the expensive values associated with its use. As generator systems, some strategies can be adopted, such as chemical, electrochemical, photochemical, and enzyme-based methods.[24,25] Considering the application to *in vitro* drug metabolism, the most common generator systems are **electrochemical** and **enzyme based-methods**.

Electrochemical methods are the most direct, requiring few to no intermediate steps. However, some challenges include the formation of inactive forms, the need for high potentials; which can leads to corrosion and degradation of electrodes, and the requirement of an expensive catalyst such as Rh, Ru, or Pt.[26,27] Recently, novel photoelectrochemical surface modifications are being applied to electrochemically regenerate active NADPH from $NADP^+$, as demonstrated by Kadowaki *et. al.*[25] Nevertheless, in the case of cascade reactions, the use of electrochemical methods can be frequently incompatible with other components from the enzymatic reactions.[28]

Enzymatic methods are still a gold standard for the generation of NADPH applied to *in vitro* drug metabolism. These methods involve the conversion of $NADP^+$ to NADPH mediated by glucose-6-phosphate dehydrogenase (G6PDH) or 6-phosphogluconate dehydrogenase (6PGD). Both enzymes are involved in the pentose phosphate pathway and its route is presented in FIGURE 1.3.[24] Considering the application of *in vitro* studies, the conversion carried out by G6PDH is the most reported.[29–31] Briefly, the G6PDH uses glucose-6-phosphate (G6P) and $NADP^+$ as substrates to produce 6-phospho-d-glucono-1,5-lactone and NADPH.

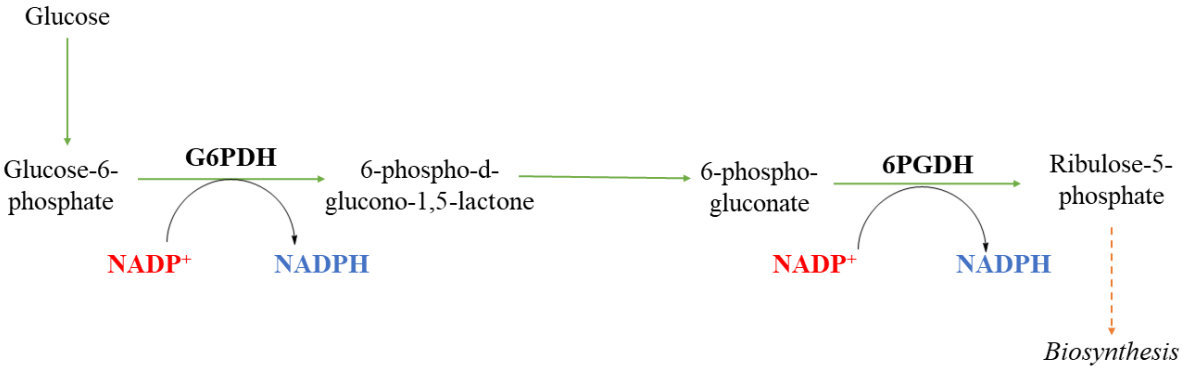

FIGURE 1.3. Summary of the pentose phosphate pathway. NADPH generation by glucose-6-phosphate dehydrogenase (G6PDH) and 6-phosphogluconate dehydrogenase (6PGDH). Adapted from Spaans et. al.[20]

Although the use of a generator system is an interesting strategy, it should fulfill some requirements. For example, easy manipulation, amount of enzymes and other reagents used, and the system stability under operational conditions.[24,32] In addition, it is recommended to monitor the amount of NADPH that is being produced by the generator system. CYPs are cofactor-dependent enzymes, therefore their function is directly related to the amount of NADPH furnished.

1.3 *In vitro* models to study human hepatic drug metabolism

In general, human CYP recombinant enzymes (rCYP), human liver microsomes (HLM), and hepatocytes are the most used hepatic models for selectively studying *in vitro* CYP activities.[33]

Human CYP recombinant enzymes (rCYP) are recombinant enzymes or liposomes containing a single selective CYP isoform. These *in vitro* systems are generally prepared from insect cells infected with recombinant baculovirus containing a cDNA insert encoding for the human CYP metabolic enzyme. They are commercially named Baculosomes® or Supersomes®. In addition, allelic variants are also available, and baculovirus often includes supplemental genes for NADPH-P450 reductase and cytochrome b5.[34,35] In some alternative reconstituted systems (*e.g.*, RECO®), these CYP-related proteins are associated to purified recombinant human CYP isoform obtained in the bacterium as *Escherichia coli* (Bactosomes®) or yeast cells.[36] Expression systems using mammalian cells are less employed due to the lower expression level and/or low yield in producing cells.[34] Recombinant enzymes are usually applied to study the activity of selective enzymes separately and are routinely used for phenotyping reactions (CYP mapping), metabolic stability and clearance determination, drug-drug interaction (DDI) related enzyme inhibition, or mechanistic investigations.[37]

Moreover, considering their higher activity compared to human liver microsomes (HLM), this model could be useful for generating additional metabolic data.[35]

Human liver microsomes (HLM) are obtained by the homogenization of the liver, followed by two-step differential centrifugation of the homogenate. The first centrifugation at 9000 x g yields a supernatant fraction named S9, which in turn is ultracentrifuged at 100,000 x g to produce the "microsomal pellet".[38] Microsomes are vesicles of hepatocyte-derived smooth endoplasmic reticulum containing the enzymes responsible for phase I oxidation, including the CYPs and flavin-containing monooxygenases (FMOs). UDP-glucuronsyl transferases (UGTs), and most phase II enzymes (sulfotransferases (SULTs), glutathione S-transferases (GSTs), N-acetyltransferases (NATs), carboxylesterases (CES), and methyltransferases) are cytosolic and therefore, they are absent from HLM and mainly included in S9 or cytosolic fractions.[39] The use of HLM allows for assessment and discrimination between CYPs/FMOs and UGTs activities by supplementing them with the relevant cofactor (NADPH or uridine diphosphate glucuronic acid (UDPGA)).[38] HLM can be prepared from a single donor for the characterization of interindividual variability (*e.g.*, gender and allelic variant) in hepatic metabolism or can be mixed from different donors obtained as a pool for mimicking the metabolism of an average person in the population.[40] Commonly, HLMs are the most popular *in vitro* model due mainly to their easy application, well-established procedures, stability during prolonged storage at –80 °C, suitability for high-throughput screening methodologies, commercial availability, and for extrapolation from the *in vitro* to *in vivo* results.[41] CYP activity in microsomes, however, is rapidly inactivated after several freeze/thaw cycles and upon contact with organic solvents.[40,42]

Primary intact **human hepatocytes** are isolated from livers through a procedure named two-step collagenase digestion and can be used either as a cell suspension or as primary cell cultures. This *in vitro* model contains all hepatic metabolic enzymes (both microsomal and cytosolic) as well as all cofactors,

including those required for the phase I oxidation and phase II conjugation and transporters, at similar levels with those under *in vivo* physiological conditions.[19] The restricted availability of fresh livers and the limited viability after the isolation are, however, the main disadvantage of using suspended fresh hepatocytes. Besides, lack of cell polarity, cell-cell, and cell-matrix contact could decrease their *in vivo* resemblance. Thus, monolayer cultures allow for the overcoming of these drawbacks and offer better viability of freshly isolated hepatocytes, even if the specific liver functions such as metabolic activities are reduced over time.[43] Mixtures of hepatocytes from multiple donors are generally used for metabolic stability and clearance studies, metabolites profiling, liver toxicity investigations and represent the most important *in vitro* model for studies on inductive DDI.[44]

In vitro assays are usually performed in solution by the incubation of the molecule of interest with HLM or rCYP at 37 °C in pH 7.4 buffer. The biotransformation is initialized by the presence of NADPH as a cofactor or NADPH generator system.[15,26,29] For specific tests (*e.g.*, in enzymatic inhibition studies or to determine which isozymes are responsible for the biotransformation), a substrate or a selective inhibitor for a particular isozyme must also be added to the reaction mixture.[15,45] Reactions are conducted for a certain time, and it is quenched by adding an organic solvent or by changing the pH, followed by the centrifugation step.[45,46] Then, the supernatant is usually analyzed by LC-UV or LC-MS/MS methods. FIGURE 1.4 illustrates the scheme for *in vitro* metabolism assays conducted in solution.

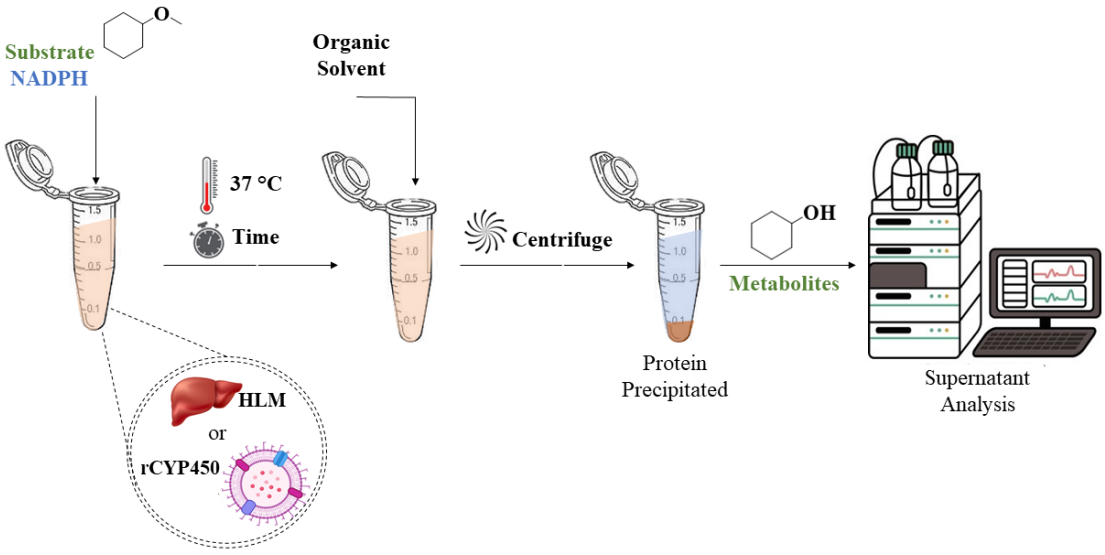

FIGURE 1.4. Simplified scheme of in vitro drug metabolism experiments carried out in solution with HLM or rCYP.

Control samples are also important for the analysis of *in vitro* drug metabolism. In this case, control samples are usually obtained in the absence of cofactors, matrix or at the time point zero. Data analysis is conducted by comparing the results obtained in the control samples with the test samples, and it allows to simplify the interpretation of results, mainly for the identification of new metabolites in a new chemical entity (NCE).[45,46] Among *in vitro* metabolic tests, it is highlighted (1) the metabolic stability and metabolite identification studies, (2) enzyme kinetic studies, and (3) phenotyping studies.[9,45–47]

1.3.1 Metabolic stability and metabolite identification studies

Metabolic stability studies are conducted to determine the biotransformation susceptibility of compounds in the context of selecting or designing drugs with favorable pharmacokinetic properties.[18,48] Different derivatives of the same molecule can be tested to select that one which is not metabolized or which presents a limited and/or predictable metabolism. These tests are performed by incubating the molecule of interest at different times and in the presence of microsomes. The substrate concentration corresponds to the K_m

value or around 1 μmol L^{-1}, if the K_m has not been determined yet.[48] The use of HLMs allows the evaluation of phase I reactions. Therefore, it is recommended to use hepatocytes (fresh or cryopreserved) for screening the metabolic stability of a compound due to the presence of all phase I and phase II enzymes.[18,49]

The data analysis usually follow-up the substrate consumption and the percentage is reported according to incubation times. From these results, it is possible to estimate the *in vitro* half-life, which can be used to estimate the *in vitro* intrinsic clearance (CL_{int}), and then scaled to an *in vivo* CL_{int} using physiologically based parameters.[35,50]

The identification of metabolites is performed by monitoring common metabolic reactions from phase I and/or phase II (*e.g.*, hydroxylation or demethylation). Currently, there are a number of *in silico* tools to predict the biotransformation reaction products. As the analytical platforms, it is possible to use mass analyzers of high- and/or low-resolution.[51,52] The latter is often carried out in a triple-quadrupole (QqQ) operating in the selected reaction monitoring (SRM) acquisition mode, in which substrate and metabolites are analyzed using multiple transitions.[51]

1.3.2 Kinetic studies

During the early stages of drug discovery and development, enzymatic kinetic assays are performed to determine kinetic parameters, such as K_m and V_{max}. In addition, these experiments are important to understand the pharmacodynamic consequences that an isozyme can cause by exposure of one or multiple drugs.[18,53]

In general, the Michaelis-Menten equation (EQUATION 1.1) is used to determine K_m and V_{max} values. The model describes the rate of enzymatic reaction by correlating initial velocity (V_0) to the concentration of substrate [S]. FIGURE 1.5 illustrates the curve profile of an enzyme which corresponds to the

Michaelis-Menten equation. K_m gives an idea of the enzyme-substrate affinity and information about the saturating substrate concentration. The last point is important because the enzyme's saturation can give rise to non-linear kinetics which can cause difficulties in predicting dose-response effects.[53–55]

$$V_0 = \frac{V_{max}[S]}{K_m + [S]} \qquad \text{EQUATION 1.1}$$

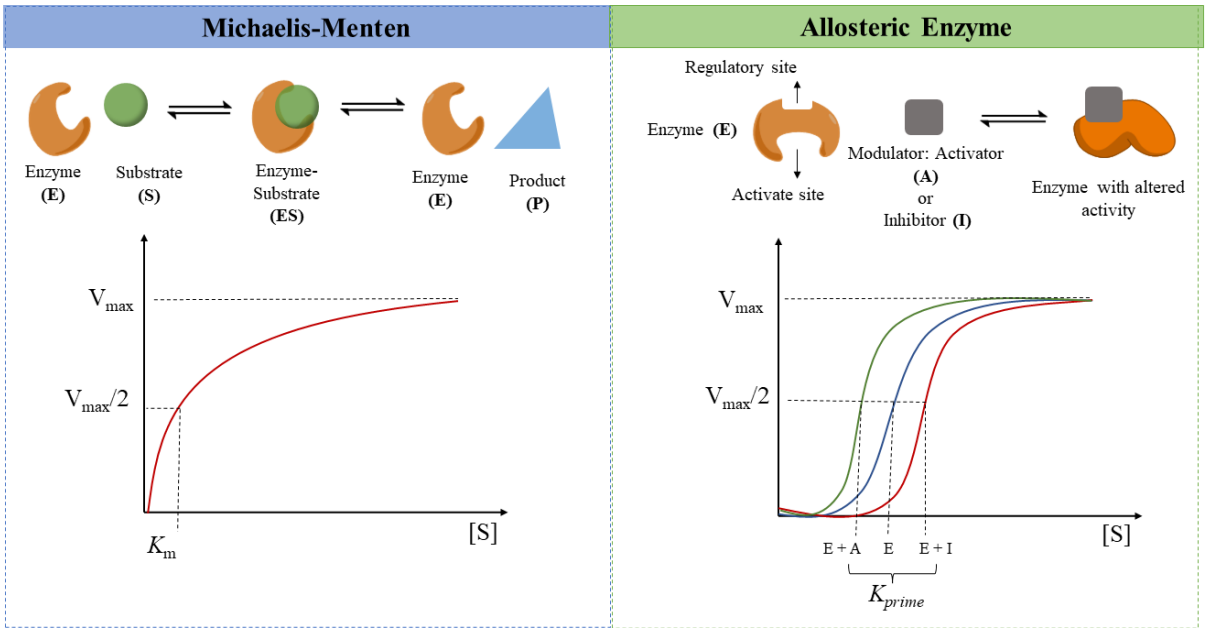

FIGURE 5.5. Kinetic profile of a Michaelis-Menten and allosteric enzymes. Adapted from Copeland.[53]

Nevertheless, a non-Michaelis-Menten profile can be obtained for some enzymes, which is a result of an allosteric effect that commonly yields a sigmoidal velocity saturation curve. In this case, the binding of one substrate molecule induces structural or electronic changes in the enzymes that result in an altered affinity and/or increase the rate of product formation for a second substrate-binding site. In this sense, the velocity curve will display the kinetic characteristic of an allosteric enzyme.[56] Hill's equation (EQUATION 1.2) is

applied to generate kinetic parameters, and it gives an appropriate fit to experimental data. As presented in FIGURE 1.5, in a low substrate concentration range, velocity response is slower than in Michaelis-Menten kinetics. While at intermediate specific velocities, the sigmoidal response provides more sensitive control by variations of the substrate concentration.[53,56]

$$V_0 = \frac{V\mathrm{max} * [\mathrm{S}]^{\mathrm{H}}}{K\mathrm{prime} + [\mathrm{S}]^{\mathrm{H}}}$$

EQUATION 1.2

Hill's equation can be used to determine the co-operativity significance in substrate binding. In this sense, K_{prime} is a constant comprising the interaction factors and no longer equals K_{m}. Hill's coefficient (H) is used to describe the degree of cooperativity. Thus, an H equal to 1, there is no cooperativity, and the enzyme follows the Michaelis-Menten equation. H >1 indicates positive cooperativity and H < 1 there is negative cooperativity.[53,56]

1.3.2 CYP reaction phenotyping studies

Phenotyping assays are carried out to determine which enzyme(s) are responsible for the metabolism of a molecule of interest. In addition, these experiments have an important role to evaluate the safety of a new drug, understanding the drug-drug interactions (DDIs), and the interaction effects of interspecies related to the drug metabolism.[21,46,57]

Different strategies can be applied for these experiments, such as (i) the use of rCYPs; (ii) selective chemical inhibitors for CYP isoforms, and (iii) selective antibodies for CYP isoforms.[21,33]

By the use of **rCYPs,** it is possible to identify which CYP isoforms are responsible for the drug metabolism of the interest compound. This reaction can be measured by following the formation of metabolites, or by consumption of

the substrate. However, this method did not ensure *in vivo* outcomes, because the *in vitro* metabolism assays are carried out using just one isoform.[15,58,59]

Methods using **selective chemical inhibitors** consist of the inhibition of a selective CYP isoform by using a well-known chemical inhibitor. Briefly, a selective chemical inhibitor for the CYP isoform is incubated with HLMs and the target molecule. Control samples are prepared without the chemical inhibitor, and the metabolite formation is measured. If the metabolite formation is lower or not observed in the presence of the selective chemical inhibitor, the inhibited isoform may be involved in the metabolism of the target molecule under study.[58,59] TABLE 1.1 present a summary of the most common substrates and selective chemical inhibitors used for phenotyping assays.

Table 1.1. List of examples of specific substrates and inhibitors of the major isoforms of CYPs involved in drug metabolism in humans.

Isozymes	Substrate	Metabolite monitored	Inhibitor
CYP1A2	Phenacetin	Acetaminophen	Furafylline[60], norfloxacine
CYP2A6	Coumarin	7'-hydroxy-coumarin	Letrozole[61], pilocarpine[62]
CYP2B6	Bupropione	Hydroxy-bupropione	Thiotepa[63], ritonavir, efavirenz
CYP2C8	Paclitaxel	6α-hydroxy-paclitaxel	Quercetin[64], trimethoprim[65], simvastatine
CYP2C9	Diclofenac	4-hydroxy-diclofenac	Sulfaphenazole[66], fluconazole, metronidazole

CYP2C19	S-mephenytoin	4-hydroxy-mephenytoin	Ticlopine[67], omeprazole, fluconazole
CYP2D6	Dextromethorphan	Dexthorphan	Quinidine[67], chloroquine
CYP2E1	Chlorzoxazone	6-hydroxy-chlorzoxazone	Diethyldithiocarbamate[68], disulfram
CYP3A4	Testosterone	6-β-hydroxy-testosterone	Ketoconazole[66], troleandomycin[69]

Monoclonal antibodies can also be used in phenotyping studies, through the inhibition of CYP's isoforms. The main advantage is the selectivity compared to the average of CYP enzymes. However, there is a lack of selectivity for some important isoforms, such as CYP3A4. In addition, these experiments present a high cost and low commercial availability. Also, some monoclonal antibodies are made based on mouse isoforms, and their results cannot be useful to compare with *in vivo* outcomes.[59]

It is important to highlight that using just one of these approaches described above is not effective to identify which isoform(s) are responsible for the biotransformation of an NCE. Therefore, it is recommended to use at least two of them in phenotyping studies.[70]

1.4 Enzyme immobilization

Enzyme immobilization has been studied for several years as a clever strategy to replace biological processes using enzymes in solution. Benefits associated with enzyme immobilization include the improvement of functional properties and mainly the enzyme's reuse. Therefore, the implementation of this strategy is even more common in industrial processes.[71,72]

The crucial technical advantage of enzyme immobilization is the heterogenization of the catalytic reaction. In other words, the enzyme keeps

insoluble by incorporation onto or into the support. In this sense, development of biocatalyst bioreactors should consider some properties, such as appropriate immobilization chemistry, suitable solid carrier matrix, and whenever possible, mimic the biological conditions. Those parameters are crucial to determine the activity, specificity, selectivity, and stability of the immobilized enzyme.[72–74]

In summary, the immobilization of enzymes can be classified into physical or chemical methods. **Physical methods** include hydrogen bonds, affinity bonding, Van der Waals forces, hydrophobic interactions, and ionic bonding between enzymes and support. **Chemical methods** involve the formation of covalent bonds of the support with amino acid residues from the enzyme, or through cross-links where proteins are directly immobilized using cross-linked reagents, such as glutaraldehyde. In addition, proteins can also be entrapped/encapsulated into the support.[73,75,76] FIGURE 1.6 depicted the most typical immobilization methods used.

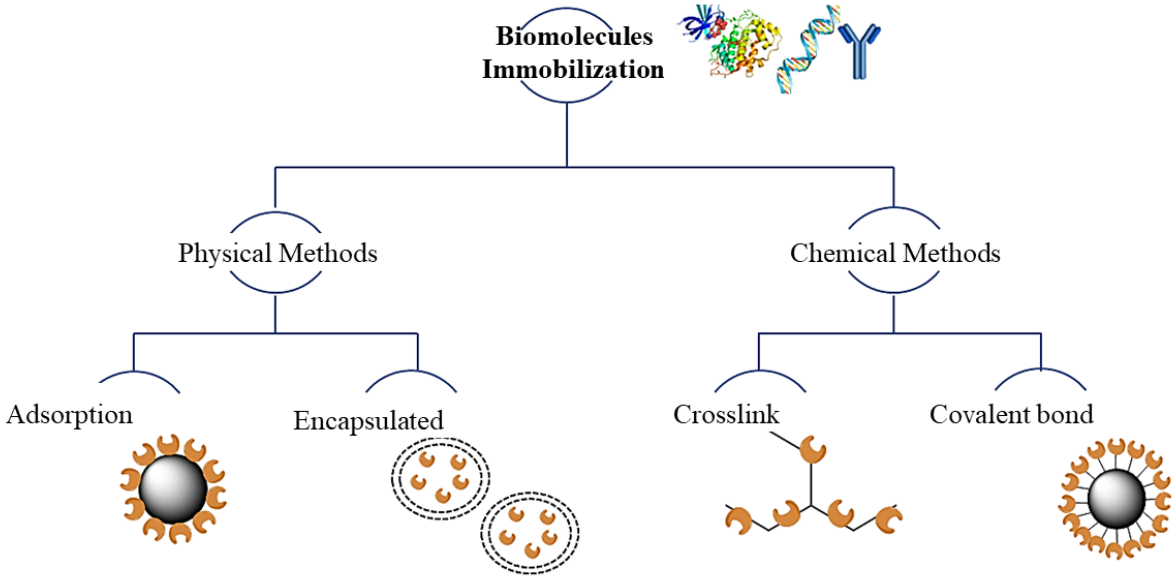

FIGURE 6.6. Immobilization methods for biomolecules. Adapted from Furlani et. al.[76]

In general, **adsorption methods** allow immobilization under mild conditions, and usually there are no structural modifications of the biomolecule,

which can keep a high enzymatic activity even after the immobilization process. However, the interaction of enzyme-support is random and can occur with desorption through variations in temperature, pH, and ionic strength. As alternatives, is common to implement chemical modifications on the support surface or use the ionic exchange as a strategy.[72–77]

Entrapment/Encapsulated are physical methods where the enzyme is encapsulated in support by the sol-gel process. Entrapment methods require polymeric synthesis in the presence of the enzyme. This immobilization method protects the enzyme from direct contact with the reaction medium and thus minimizes enzyme inactivation by organic solvents or by other enzymes such as proteases. Nevertheless, during the synthesis process, the enzyme can undergo a conformational change, which can change kinetic properties and result in the lack of substrate specificity.[72–77]

Crosslink method is a sort of irreversible immobilization and it is not necessary to use solid support. Basically, this technique uses bi – or multifunctional reagents to attach enzyme-enzyme or enzyme-inactive proteins and form a complex three-dimensional structure. It is a laborious technique and can cause low mechanical stability, poor reproducibility, and a reduction of 50 % in the catalytic activity. [72–77]

Covalent bond is one of the most applied immobilization methods described in the literature. This technique is based on the covalent bonds between functional groups present on the support surface and the functional groups of amino acid residues of the enzyme. To meet this end, the first step is the activation of the biomolecule or the support. The first case is used to promote immobilization in a specific region of the biomolecule. On the other hand, the activation of the support is widely applied through chemical reactions, such as Schiff base, epoxide, amide bond formation, N-hydroxysuccinimide, carbonyl diimidazole, cyanogen bromide, etc. The advantages associated with the covalent bond approach are

related to thermal stability improvement and avoiding enzyme dissociation alongside the use of the bioreactor.[72–77]

Supports are also another important factor for the immobilization of biomolecules and should take into account some characteristics, such as having an adequate surface for the biomolecule attachment, pore and particle size, mechanical resistance, chemical and microbiological stability, reusability, low toxicity, and low cost. Supports can be classified into organic and inorganic according to their chemical characteristics and subdivided into a natural or synthetic.[72,73,75,76]

Currently, different supports are commercially available. Magnetic beads, silica, chitosan, nylon fibers, and cellulose are widely described in the literature.[72,75] Magnetic beads, for example, have received special attention due to their wide chemistry versatility, high surface area, easy separation of beads from the reaction medium by the use of an external magnetic field, and great biocompatibility.[78,79]

In summary, there is no universal support, but the adequate choice, as well as the appropriate immobilization technique, should be optimized according to the targeted biomolecule and the study goal. More details about different supports and techniques for the immobilization of biomolecules can be found in the literature.[72–75,80,81]

1.4.1 Challenges in the immobilization of CYPs

In the field of *in vitro* phase I metabolism, several efforts have been made to improve conventional *in vitro* methods to novel and alternative methods to ensure rapid, reliable, and cost-effective metabolic studies.[17,82,83] Therefore, a variety of innovative CYP engineering, as described in section 1.3 is commercially available, as well as new models based on the immobilization of cytochrome P450 systems.[17,23,84] The choice of the *in vitro* methodology depends

mainly on the type of drug metabolism study and takes into account some factors. For example (i) the need for high-throughput procedures, (ii) the balance of practical advantages/limitations, and (iii) the required degree of *in vivo* resemblance.[17,23,85,86]

Currently, there are two distinct *in vitro* systems based on the approach of immobilized CYPs for drug metabolism and biocatalysis (FIGURE 1.7): (i) CYP-biosensors, and (ii) immobilized biocatalytic systems, which can be shared into on-line and off-line bioreactors.[87,88]

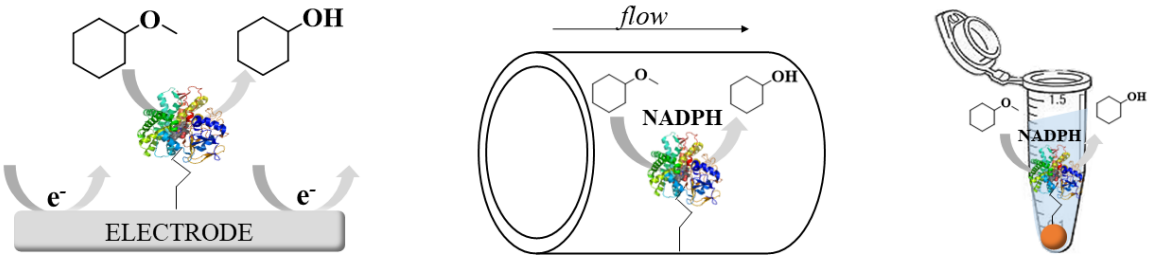

CYP-biosensors **On-line** **Off-line**

FIGURE 7.7. Main biocatalytic bioreactors using CYPs immobilized for *in vitro* drug metabolism assays and biocatalysis.

CYP-biosensors act for the detection of potential CYP-mediated redox reactions by the immobilization of CYPs on the electrode surface.[23,89] For example, the electrochemically driven enzymatic system (EDES) replaces the natural electron-supply source (*i.e.*, NADPH) with an electrode. In this case, the electrode will be used as an artificial redox partner, transferring electrons to CYPs. Systems based on EDES allow performing of a simple kinetic and DDI studies. Also, it can be useful for screening toxic metabolites using reliable enzymatic catalytic activity.[17,90] Nevertheless this system currently has some problems with application due to the adsorptive denaturation of proteins, rate-limiting diffusion of the substrate to the electrode, and structural changes of enzymes during the immobilization process.[88] Another alternative is the use of photochemical mechanisms as a source of potential redox to supply NADPH and additional redox

CYP-associated proteins. Although it is a great approach, the generated oxidative activity is inconsistent with the natural redox system and represents the major issue of these methods for drug metabolism simulations.[90,91] Therefore, perspective application areas of these biosensors mainly include biosynthesis, medical diagnostic, and environmental engineering.[17,84,92]

Immobilized biocatalytic systems using human-liver microsomes or recombinant CYP could be used by off-line and on-line approaches combined with LC-UV or LC-MS instruments.[85,93] The on-line approach allows automation, reduction of incubation volumes, and elimination of sample handling. The enzymatic reaction takes place in a flow-through system which can be directly coupled to analytical platforms for analysis. Although it is an interesting strategy mainly for high-throughput screening, the compatibility of immobilized CYPs with the inner environment of chromatographic supports such as monolithic columns is a challenge and should be carefully optimized.[85,94,95]

For this reason, biocatalytic off-line incubations remain a gold standard for drug metabolism and biocatalysis. This strategy applied the immobilized CYPs in an environment that can mimic similar incubation conditions to *in vivo*.[93] Moreover, by decoupling metabolic incubation from the chromatography analysis, the overall *in vitro* methodology can be optimized by choosing the appropriate sample preparation and analytical strategy.[95] In our laboratory, the use of magnetic beads as solid support has been already demonstrated.[32,93,96–98] Minor modifications in the immobilization procedure should always be pinpointed taking into consideration, not only the protein target but also the study proposal. Lima et al.[99], for example, evaluated the immobilization of acetylcholinesterase (AChE) in different sizes of magnetic beads. The study demonstrated that a higher surface area improved the catalytic activity for immobilized AChE, however, magnetic beads of 1 µm were the best option for affinity experiments.

Particularities of CYP systems should be taken into account to obtain a fully functional and stable biocatalytic bioreactor.[17,23,92] In general, CYPs are complex systems and the catalytic cycle depends on multiple reactions, as illustrated in FIGURE 1.1. Therefore, the biocatalytic bioreactor composed of CYPs requires the correct quaternary assembly by an orientation that will benefit the access of the substrate, the electron source (*e.g.*, NADPH), and the product release. Constantly substrate and cofactors supply are important to ensure the biocatalytic application of the immobilized CYPs. In addition, control and/or minimizing the lack of stability is still an undergo topic for these sets of enzymes.[17,23]

Therefore, herein, the immobilization of CYP enzymes onto magnetic beads were carried out in order to develop a biocatalytic bioreactor for *in vitro* drug metabolism assays and biocatalysis proposals. The immobilization conditions were optimized with rat liver microsomal fractions as a low-cost alternative and then, successfully applied for human liver microsomal fraction immobilization. In addition, a generator system of NADPH was also developed based on the immobilization onto magnetic beads of glucose-6-phosphate dehydrogenase. Both biocatalytic bioreactors were individually developed and then mixed into one-pot conditions in order to mimic similar *in vivo* conditions.

References

1. OMURA, T. & SATO, R. "The Carbon Monoxide-binding Pigment of Liver Microsomes: I. EVIDENCE FOR ITS HEMOPROTEIN NATURE". J. Biol. Chem., **239**, 2370–2378, 1964.
2. OMURA, T. & SATO, R. "A New Cytochrome in Liver Microsomes". J. Biol. Chem., **237**, PC1375–PC1376, 1962.
3. LOWE FURGE, L. & GUENGERICH, F. P. "Cytochrome P450 Enzymes in Drug Metabolism and Chemical Toxicology ". Biochem. Mol. Biol. Educ., **34**, 66–74, 2006.
4. GUENGERICH, F. P., WU, Z. L. & BARTLESON, C. J. "Function of human cytochrome P450s: characterization of the orphans". Biochem. Biophys. Res. Commun., **338**, 465–469, 2005.
5. WANG, M. *ET AL.* "Three-dimensional structure of NADPH-cytochrome P450 reductase: prototype for FMN- and FAD-containing enzymes". Proc. Natl. Acad. Sci. U. S. A., **94**, 8411–8416, 1997.
6. MULLER-ENOCH, D., CHURCHILL, P., FLEISHER, S. & GUENGERICH, F. P. "Interaction of liver microsomal cytochrome P-450 and NADPH-cytochrome P-450 reductase in the presence and absence of lipid.". J. Biol. Chem., **259**, 8174–8182, 1984.
7. YAMAZAKI, H., JOHNSON, W. W., UENG, Y. F., SHIMADA, T. & GUENGERICH, F. P. "Lack of electron transfer from cytochrome b5 in stimulation of catalytic activities of cytochrome P450 3A4. Characterization of a reconstituted cytochrome P450 3A4/NADPH-cytochrome P450 reductase system and studies with apo-cytochrome b5". J. Biol. Chem., **271**, 27438–27444, 1996.
8. YAMAZAKI, H. *ET AL.* "Roles of cytochrome b5 in the oxidation of testosterone and nifedipine by recombinant cytochrome P450 3A4 and by human liver microsomes". Arch. Biochem. Biophys., **325**, 174–182, 1996.

9. GUENGERICH, F. P. "Cytochrome P450 and chemical toxicology". Chem. Res. Toxicol., **21**, 70–83, 2008.
10. LOHMANN, W. & KARST, U. "Biomimetic modeling of oxidative drug metabolism : Strategies, advantages and limitations". Anal. Bioanal. Chem., **391**, 79–96, 2008.
11. GUENGERICH, F. P. "Common and uncommon cytochrome P450 reactions related to metabolism and chemical toxicity". Chem. Res. Toxicol., **14**, 611–650, 2001.
12. ISIN, E. M. & GUENGERICH, F. P. "Complex reactions catalyzed by cytochrome P450 enzymes". Biochim. Biophys. Acta, **1770**, 314–329, 2007.
13. AV, P., CE, F., PANDEY, A. V. & FLÜCK, C. E. "NADPH P450 oxidoreductase: structure, function, and pathology of diseases". Pharmacol. Ther., **138**, 229–254, 2013.
14. NEBERT, D. W. & RUSSELL, D. W. "Clinical importance of the cytochromes P450". Lancet (London, England), **360**, 1155–1162, 2002.
15. DONATO, M. T., CASTELL, J. V., MT, D. & JV, C. "Strategies and molecular probes to investigate the role of cytochrome P450 in drug metabolism: focus on in vitro studies". Clin. Pharmacokinet., **42**, 153–178, 2003.
16. ZANGER, U. M. & SCHWAB, M. "Cytochrome P450 enzymes in drug metabolism: regulation of gene expression, enzyme activities, and impact of genetic variation". Pharmacol. Ther., **138**, 103–141, 2013.
17. VALIKHANI, D., BOLIVAR, J. M. & PELLETIER, J. N. "An Overview of Cytochrome P450 Immobilization Strategies for Drug Metabolism Studies, Biosensing, and Biocatalytic Applications: Challenges and Opportunities". ACS Catal., **11**, 9418–9434, 2021.
18. BARANCZEWSKI, P. *ET AL.* "Introduction to in vitro estimation of metabolic stability and drug interactions of new chemical entities in drug discovery and development". Pharmacol. Reports, **58**, 453–472, 2006.
19. HEWITT, N. J. *ET AL.* "Primary hepatocytes: Current understanding of the

regulation of metabolic enzymes and transporter proteins, and pharmaceutical practice for the use of hepatocytes in metabolism, enzyme induction, transporter, clearance, and hepatotoxicity studies". Drug Metab. Rev., **39**, 159–234, 2007.

20. EMOTO, C., MURAYAMA, N., ROSTAMI-HODJEGAN, A. & YAMAZAKI, H. "Methodologies for investigating drug metabolism at the early drug discovery stage: prediction of hepatic drug clearance and P450 contribution". Curr. Drug Metab., **11**, 678–685, 2010.
21. ZHANG, H., DAVIS, C. D., SINZ, M. W. & RODRIGUES, A. D. "Cytochrome P450 reaction-phenotyping: an industrial perspective". Expert Opin. Drug Metab. Toxicol., **3**, 667–687, 2007.
22. PELKONEN, O., TURPEINEN, M., UUSITALO, J., RAUTIO, A. & RAUNIO, H. "Prediction of drug metabolism and interactions on the basis of in vitro investigations". Basic Clin. Pharmacol. Toxicol., **96**, 167–175, 2005.
23. GILLAM, E. & HAYES, M. "The evolution of cytochrome P450 enzymes as biocatalysts in drug discovery and development". Curr. Top. Med. Chem., **13**, 2254–2280, 2013.
24. SPAANS, S. K., WEUSTHUIS, R. A., VAN DER OOST, J. & KENGEN, S. W. M. "NADPH-generating systems in bacteria and archaea". Front. Microbiol., **6**, 1–27, 2015.
25. KADOWAKI, J. T., JONES, T. H., SENGUPTA, A., GOPALAN, V. & SUBRAMANIAM, V. V. "Copper oxide-based cathode for direct NADPH regeneration". Sci. Reports 2021 111, **11**, 1–12, 2021.
26. WANG, X. *ET AL.* "Cofactor NAD(P)H Regeneration Inspired by Heterogeneous Pathways". Chem, **2**, 621–654, 2017.
27. UPPADA, V., BHADURI, S. & NORONHA, S. B. "Cofactor regeneration-an important aspect of biocatalysis". Curr. Sci., **106**, 946–957, 2014.
28. HEATH, R. S. & TURNER, N. J. "Recent advances in oxidase biocatalysts: Enzyme discovery, cascade reactions and scale up". Curr. Opin. Green

Sustain. Chem., **38**, 2022.

29. PEROVANI, I. S., SANTOS BARBETTA, M. F., MOREIRA DA SILVA, R., LOPES, N. P. & MORAES DE OLIVEIRA, A. R. "In vitro-in vivo correlation of the chiral pesticide prothioconazole after interaction with human CYP450 enzymes". Food Chem. Toxicol., **163**, 112947, 2022.
30. CARRÃO, D. B., DOS REIS GOMES, I. C., BARBOSA JUNIOR, F. & DE OLIVEIRA, A. R. M. "Evaluation of the enantioselective in vitro metabolism of the chiral pesticide fipronil employing a human model: Risk assessment through in vitro-in vivo correlation and prediction of toxicokinetic parameters". Food Chem. Toxicol., **123**, 225–232, 2019.
31. DE ALBUQUERQUE, N. *ET AL.* "In Vitro Metabolism of Artepillin C by Rat and Human Liver Microsomes". Planta Med., **83**, 737–745, 2017.
32. FURLANI, I. L., OLIVEIRA, R. V. & CASS, Q. B. "Glucose-6-phosphate dehydrogenase immobilized onto magnetic beads (G6PDH-Mb) as a generator system for production of NADPH: Development and application in metabolism studies". J. Pharm. Biomed. Anal., **219**, 114901, 2022.
33. PLANT, N. "Strategies for using in vitro screens in drug metabolism". **9**, 328–336, 2004.
34. FRIEDBERG, T. *ET AL.* "Merits and limitations of recombinant models for the study of human P450-mediated drug metabolism and toxicity: an intralaboratory comparison". Drug Metab. Rev., **31**, 523–544, 1999.
35. STRINGER, R. A., STRAIN-DAMERELL, C., NICKLIN, P. & HOUSTON, J. B. "Evaluation of recombinant cytochrome P450 enzymes as an in vitro system for metabolic clearance predictions". Drug Metab. Dispos., **37**, 1025–1034, 2009.
36. YUN, C.-H., YIM, S.-K., KIM, D.-H. & AHN, T. "Functional Expression of Human Cytochrome P450 Enzymes in Escherichia coli". Curr. Drug Metab., **7**, 411–429, 2006.
37. FOTI, R., WIENKERS, L. & WAHLSTROM, J. "Application of cytochrome P450

drug interaction screening in drug discovery". Comb. Chem. High Throughput Screen., **13**, 145–158, 2010.

38. LI, A. P. "Screening for human ADME/Tox drug properties in drug discovery". Drug Discov. Today, **6**, 357–366, 2001.
39. ROSS, M. K. & CROW, J. A. "Human carboxylesterases and their role in xenobiotic and endobiotic metabolism". J. Biochem. Mol. Toxicol., **21**, 187–196, 2007.
40. PARKINSON, A., MUDRA, D. R., JOHNSON, C., DWYER, A. & CARROLL, K. M. "The effects of gender, age, ethnicity, and liver cirrhosis on cytochrome P450 enzyme activity in human liver microsomes and inducibility in cultured human hepatocytes". Toxicol. Appl. Pharmacol., **199**, 193–209, 2004.
41. OBACH, R. S. *ET AL.* "The Prediction of Human Pharmacokinetic Parameters from Preclinical and In Vitro Metabolism Data". J. Pharmacol. Exp. Ther., **283**, 46–58, 1997.
42. LI, D. *ET AL.* "Effect of regular organic solvents on cytochrome P450-mediated metabolic activities in rat liver microsomes". **38**, 1922–1925, 2010.
43. HENGSTLER, J. G. *ET AL.* "Cryopreserved primary hepatocytes as a constantly available in vitro model for the evaluation of human and animal drug metabolism and enzyme induction". Drug Metab. Rev., **32**, 81–118, 2000.
44. LI, A. P. "Human hepatocytes: Isolation, cryopreservation and applications in drug development". Chem. Biol. Interact., **168**, 16–29, 2007.
45. SVENSSON, U. S. H. & ASHTON, M. "Identification of the human cytochrome P450 enzymes involved in the in vitro metabolism of artemisinin". Br. J. Clin. Pharmacol., **48**, 528, 1999.
46. WALSKY, R. L. & OBACH, R. S. "Validated assays for human cytochrome P450 activities". Drug Metab. Dispos., **32**, 647–660, 2004.
47. VENKATAKRISHNAN, K. *ET AL.* "Comparison between Cytochrome P450 (CYP) Content and Relative Activity Approaches to Scaling from cDNA-

Expressed CYPs to Human Liver Microsomes: Ratios of Accessory Proteins as Sources of Discrepancies between the Approaches". Drug Metab. Dispos., **28**, 1493–1504, 2000.

48. TRUNZER, M., FALLER, B. & ZIMMERLIN, A. "Metabolic soft spot identification and compound optimization in early discovery phases using MetaSite and LC-MS/MS validation". J. Med. Chem., **52**, 329–335, 2009.
49. OLESON, F. B., BERMAN, C. L. & LI, A. P. "An evaluation of the P450 inhibition and induction potential of daptomycin in primary human hepatocytes.". Chem. Biol. Interact., **150**, 137–147, 2004.
50. BOWMAN, C. M. & BENET, L. Z. "In Vitro-In Vivo Extrapolation and Hepatic Clearance-Dependent Underprediction". J. Pharm. Sci., **108**, 2500–2504, 2019.
51. GU, H., ZHANG, P., ZHU, J. & RAFTERY, D. "Globally Optimized Targeted Mass Spectrometry: Reliable Metabolomics Analysis with Broad Coverage". Anal. Chem., **87**, 12355–12362, 2015.
52. HECHT, E. S., SCIGELOVA, M., ELIUK, S. & MAKAROV, A. "Fundamentals and Advances of Orbitrap Mass Spectrometry". in *Encyclopedia of Analytical Chemistry* 1–40, (Wiley, 2019). doi:10.1002/9780470027318.a9309.pub2.
53. COPELAND, R. A. *Enzymes : a practical introduction to structure, mechanism, and data analysis*. (Wiley, 2000).
54. TRACY, T. S. & HUMMEL, M. A. "Modeling Kinetic Data from In Vitro Drug Metabolism Enzyme Experiments". Drug Metab. Rev., **36**, 231–242, 2004.
55. OBACH, R. S. & REED-HAGEN, A. E. "Measurement of Michaelis constants for cytochrome P450-mediated biotransformation reactions using a substrate depletion approach". Drug Metab. Dispos., **30**, 831–837, 2002.
56. SHOU, M. *ET AL.* "Sigmoidal kinetic model for two co-operative substrate-binding sites in a cytochrome P450 3A4 active site: an example of the metabolism of diazepam and its derivatives.". Biochem. J., **340**, 845, 1999.
57. VENKATAKRISHNAN, K., VON MOLTKE, L. L. & GREENBLATT, D. J. "Human

drug metabolism and the cytochromes P450: application and relevance of in vitro models". J. Clin. Pharmacol., **41**, 1149–1179, 2001.

58. JIA, L. & LIU, X. "The Conduct of Drug Metabolism Studies Considered Good Practice (II): In Vitro Experiments". Curr. Drug Metab., **8**, 829, 2007.
59. ZIENTEK, M. A. & YOUDIM, K. "Reaction Phenotyping: Advances in the Experimental Strategies Used to Characterize the Contribution of Drug-Metabolizing Enzymes". Drug Metab. Dispos., **43**, 163–181, 2015.
60. CLARKE, S. E., AYRTON, A. D. & CHENERY, R. J. "Characterization of the inhibition of P4501A2 by furafylline". Xenobiotica., **24**, 517–526, 1994.
61. JEONG, S., WOO, M. M., FLOCKHART, D. A. & DESTA, Z. "Inhibition of drug metabolizing cytochrome P450s by the aromatase inhibitor drug letrozole and its major oxidative metabolite 4,4'-methanol-bisbenzonitrile in vitro". Cancer Chemother. Pharmacol., **64**, 867–875, 2009.
62. KINONEN, T. *ET AL.* "Competitive inhibition of coumarin 7-hydroxylation by pilocarpine and its interaction with mouse CYP 2A5 and human CYP 2A6". Br. J. Pharmacol., **116**, 2625–2630, 1995.
63. RAE, J. M., SOUKHOVA, N. V., FLOCKHART, D. A. & DESTA, Z. "Triethylenethiophosphoramide is a specific inhibitor of cytochrome P450 2B6: implications for cyclophosphamide metabolism". Drug Metab. Dispos., **30**, 525–530, 2002.
64. WALSKY, R. L., OBACH, R. S., GAMAN, E. A., GLEESON, J. P. R. & PROCTOR, W. R. "SELECTIVE INHIBITION OF HUMAN CYTOCHROME P4502C8 BY MONTELUKAST". Drug Metab. Dispos., **33**, 413–418, 2005.
65. HRUSKA, M. W. *ET AL.* "The effect of trimethoprim on CYP2C8 mediated rosiglitazone metabolism in human liver microsomes and healthy subjects". Br. J. Clin. Pharmacol., **59**, 70–79, 2005.
66. BALDWIN, S. J. *ET AL.* "Ketoconazole and sulphaphenazole as the respective selective inhibitors of P4503A and 2C9". Xenobiotica., **25**, 261–270, 1995.
67. KO, J. W., DESTA, Z., SOUKHOVA, N. V., TRACY, T. & FLOCKHART, D. A. "In

vitro inhibition of the cytochrome P450 (CYP450) system by the antiplatelet drug ticlopidine: potent effect on CYP2C19 and CYP2D6". Br. J. Clin. Pharmacol., **49**, 343–351, 2000.

68. CHANG, T. K. H., GONZALEZ, F. J. & WAXMAN, D. J. "Evaluation of Triacetyloleandomycin, α-Nasymphthoflavone and Diethyldithiocarbamate as Selective Chemical Probes for Inhibition of Human Cytochromes P450". Arch. Biochem. Biophys., **311**, 437–442, 1994.
69. CHANG, T. K. H., GONZALEZ, F. J. & WAXMAN, D. J. "Evaluation of Triacetyloleandomycin, α-Nasymphthoflavone and Diethyldithiocarbamate as Selective Chemical Probes for Inhibition of Human Cytochromes P450". Arch. Biochem. Biophys., **311**, 437–442, 1994.
70. "Federal Register :: Drug-Drug Interaction Assessment for Therapeutic Proteins; Draft Guidance for Industry; Availability". https://www.federalregister.gov/documents/2020/08/10/2020-17412/drug-drug-interaction-assessment-for-therapeutic-proteins-draft-guidance-for-industry-availability.
71. SILMAN, I. & KATCHALSKI, E. "Water-insoluble derivatives of enzymes, antigens, and antibodies". Annu. Rev. Biochem., **35**, 873–908, 1966.
72. SHELDON, R. A. & DEPARTMENT OF BIOTECHNOLOGY JULIANALAAN 136, 2628 BL DELFT, THE NETHERLANDS, FAX: (+31)-15-278-1415, D. U. OF T. "Enzyme Immobilization: The Quest for Optimum Performance". Adv. Synth. Catal., **349**, 1289–1307, 2017.
73. SHELDON, R. A. & VAN PELT, S. "Enzyme immobilisation in biocatalysis: Why, what and how". Chem. Soc. Rev., **42**, 6223–6235, 2013.
74. DATTA, S., CHRISTENA, L. R. & RAJARAM, Y. R. S. "Enzyme immobilization: an overview on techniques and support materials". 3 Biotech, **3**, 1–9, 2013.
75. SHELDON, R. A. "Enzyme immobilization: The quest for optimum performance". *Advanced Synthesis and Catalysis* vol. 349 1289–1307, at https://doi.org/10.1002/adsc.200700082 (2007).

76. FURLANI, I., AMARAL, B., OLIVEIRA, R. & CASS, Q. "IMOBILIZAÇÃO ENZIMÁTICA: CONCEITO E EFEITOS NA PROTEÓLISE". Quim. Nova, **43**, 463–473, 2020.
77. KATCHALSKI-KATZIR, E. "Immobilized enzymes - learning from past successes and failures". Trends Biotechnol., **11**, 471–478, 1993.
78. AGUILAR-ARTEAGA, K., RODRIGUEZ, J. A. & BARRADO, E. "Magnetic solids in analytical chemistry: A review". Anal. Chim. Acta, **674**, 157–165, 2010.
79. MEHTA, R. V. "Synthesis of magnetic nanoparticles and their dispersions with special reference to applications in biomedicine and biotechnology". Mater. Sci. Eng. C, **79**, 901–916, 2017.
80. ABOLPOUR HOMAEI, A., SARIRI, R., VIANELLO, F. & STEVANATO, R. "Enzyme immobilization: an update". J. Chem. Biol., **6**, 185–205, 2013.
81. CAO, S. *ET AL.* "Recent advances in immobilized enzymes on nanocarriers". Chinese J. Catal., **37**, 1814–1823, 2016.
82. DE OLIVEIRA CARDOSO, J., OLIVEIRA, R. V., LU, J. B. L. & DESTA, Z. "In vitro metabolism of montelukast by cytochrome P450S and UDP-glucuronosyltransferases". Drug Metab. Dispos., **43**, 1905–1916, 2015.
83. TANVIR, S., PANTIGNY, J., MORANDAT, S. & PULVIN, S. "Development of immobilization technique for liver microsomes". Colloids Surfaces B Biointerfaces, **68**, 178–183, 2009.
84. SCHNEIDER, E. & CLARK, D. S. "Cytochrome P450 (CYP) enzymes and the development of CYP biosensors". Biosens. Bioelectron., **39**, 1–13, 2013.
85. NICOLI, R., BARTOLINI, M., RUDAZ, S., ANDRISANO, V. & VEUTHEY, J. L. "Development of immobilized enzyme reactors based on human recombinant cytochrome P450 enzymes for phase I drug metabolism studies". J. Chromatogr. A, **1206**, 2–10, 2008.
86. LI, Z. *ET AL.* "Engineering cytochrome P450 enzyme systems for biomedical and biotechnological applications". J. Biol. Chem., **295**, 833–849, 2020.
87. FASINU, P., J. BOUIC, P. & ROSENKRANZ, B. "Liver-Based In Vitro

Technologies for Drug Biotransformation Studies - A Review". Curr. Drug Metab., **13**, 215–224, 2012.

88. NOWAK, P., WOŹNIAKIEWICZ, M. & KOŚCIELNIAK, P. "Simulation of drug metabolism". TrAC - Trends Anal. Chem., **59**, 42–49, 2014.
89. BISTOLAS, N., WOLLENBERGER, U., JUNG, C. & SCHELLER, F. W. "Cytochrome P450 biosensors - A review". Biosens. Bioelectron., **20**, 2408–2423, 2005.
90. HUANG, M., XU, X., YANG, H. & LIU, S. "Electrochemically-driven and dynamic enhancement of drug metabolism via cytochrome P450 microsomes on colloidal gold/graphene nanocomposites{". RCS Adv., **2**, 12844–12850, 2012.
91. JENSEN, K., JENSEN, P. E. & MØLLER, B. L. "Light-driven cytochrome P450 hydroxylations". ACS Chem. Biol., **6**, 533–539, 2011.
92. BERNHARDT, R. & URLACHER, V. B. "Cytochromes P450 as promising catalysts for biotechnological application: chances and limitations". Appl. Microbiol. Biotechnol., **98**, 6185–6203, 2014.
93. FURLANI, I. L., OLIVEIRA, R. V. & CASS, Q. B. "Immobilization of cytochrome P450 enzymes onto magnetic beads: An approach to drug metabolism and biocatalysis". Talanta Open, **7**, 2023.
94. SCHEJBAL, J., ŘEMÍNEK, R., ZEMAN, L., MÁDR, A. & GLATZ, Z. "On-line coupling of immobilized cytochrome P450 microreactor and capillary electrophoresis: A promising tool for drug development". J. Chromatogr. A, **1437**, 234–240, 2016.
95. DE MORAES, M. C., CARDOSO, C. L. & CASS, Q. B. "Solid-Supported Proteins in the Liquid Chromatography Domain to Probe Ligand-Target Interactions". *Frontiers in Chemistry* vol. 7 at https://doi.org/10.3389/fchem.2019.00752 (2019).
96. VANZOLINI, K. L., VIEIRA, L. C. C., CORRÊA, A. G., MOADDEL, R. & CASS, Q. B. "Acetylcholinesterase immobilized on modified magnetic beads as a

tool for screening a compound library". Microchim. Acta, **182**, 2209–2213, 2015.

97. VANZOLINI, K. L. *ET AL.* "Rapid ligand fishing for identification of acetylcholinesterase-binding peptides in snake venom reveals new properties of dendrotoxins". Toxicon, **152**, 1–8, 2018.
98. VANZOLINI, K. L. L. *ET AL.* "Acetylcholinesterase affinity-based screening assay on Lippia gracilis Schauer extracts". J. Pharm. Biomed. Anal., **153**, 232–237, 2018.
99. DE LIMA, J. M., FURLANI, I. L., DA SILVA, L. R. G., VALVERDE, A. L. & CASS, Q. B. "Micro- And nano-sized amine-terminated magnetic beads in a ligand fishing assay". Anal. Methods, **12**, 4116–4122, 2020.
100. WANG, M. *ET AL.* "Three-dimensional structure of NADPH–cytochrome P450 reductase: Prototype for FMN- and FAD-containing enzymes". Proc. Natl. Acad. Sci., **94**, 8411–8416, 1997.
101. O'REILLY, E., KÖHLER, V. & FLITSCH, S. L. "Cytochromes P450 as useful biocatalysts: addressing the limitations". Chem. Commun. (Camb)., **47**, 2490–2501, 2011.
102. SHUMYANTSEVA, V. V., KUZIKOV, A. V., MASAMREKH, R. A., BULKO, T. V. & ARCHAKOV, A. I. "From electrochemistry to enzyme kinetics of cytochrome P450". Biosens. Bioelectron., **121**, 192–204, 2018.
103. LU, J., CUI, D., LI, H., ZHANG, Y. & LIU, S. "Cytochrome P450 bienzymes assembled on Au/chitosan/reduced graphene oxide nanosheets for electrochemically-driven drug cascade metabolism". Electrochim. Acta, **165**, 36–44, 2015.
104. WU, K. *ET AL.* "Preparation of cytochrome P450 enzyme-cobalt phosphate hybrid nano-flowers for oxidative coupling of benzylamine". Enzyme Microb. Technol., **131**, 109386, 2019.
105. BECKWITT, C. H. *ET AL.* "Liver 'organ on a chip'". Exp. Cell Res., **363**, 15–25, 2018.

106. NERIMETLA, R., PREMARATNE, G., LIU, H. & KRISHNAN, S. "Improved electrocatalytic metabolite production and drug biosensing by human liver microsomes immobilized on amine-functionalized magnetic nanoparticles". Electrochim. Acta, **280**, 101–107, 2018.
107. BELAZ, K. R. A., CASS, Q. B. & OLIVEIRA, R. V. "Determination of albendazole metabolites by direct injection of bovine plasma and multidimensional achiral-chiral high performance liquid chromatography". Talanta, **76**, 146–153, 2008.
108. ROBERTA A. BELAZ, K. & V. OLIVEIRA, R. "HPLC-fluorescence Determination of EROD Activity in Wistar Rat Liver Microsomes Obtained by Two Different Extraction Procedures". Curr. Pharm. Anal., 2013 doi:10.2174/1573412138048060 34.
109. BRADFORD, M. M. "A rapid and sensitive method for the quantitation of microgram quantities of protein utilizing the principle of protein-dye binding". Anal. Biochem., **72**, 248–254, 1976.
110. TAN, C. Y. *ET AL.* "Immobilization of a Bacterial Cytochrome P450 Monooxygenase System on a Solid Support". Angew. Chem. Int. Ed. Engl., **55**, 15002–15006, 2016.
111. URLACHER, V. B. & GIRHARD, M. "Cytochrome P450 monooxygenases: An update on perspectives for synthetic application". Trends Biotechnol., **30**, 26–36, 2012.
112. BARBOSA, O. *ET AL.* "Glutaraldehyde in bio-catalysts design: a useful crosslinker and a versatile tool in enzyme immobilization". RSC Adv., **4**, 1583–1600,.
113. VEISI, H. *ET AL.* "In Situ Green Synthesis of Pd Nanoparticles on Tannic Acid-Modified Magnetite Nanoparticles as a Green Reductant and Stabilizer Agent: Its Application as a Recyclable Nanocatalyst (Fe 3 O 4 @TA/Pd) for Reduction of 4-Nitrophenol and Suzuki Reactions". ChemistrySelect, **3**, 1820–1826, 2018.

114. CERQUEIRA, U. M. F. M. *ET AL.* "Doehlert design in the optimization of procedures aiming food analysis – A review". Food Chem., **364**, 130429, 2021.

115. FERREIRA, S. L. C., DOS SANTOS, W. N. L., QUINTELLA, C. M., NETO, B. B. & BOSQUE-SENDRA, J. M. "Doehlert matrix: A chemometric tool for analytical chemistry - Review". Talanta, 2004 doi:10.1016/j.talanta.2004.01.015.

116. J. RICHARDSON, S., BAI, A., A. KULKARNI, A. & F. MOGHADDAM, M. "Efficiency in Drug Discovery: Liver S9 Fraction Assay As a Screen for Metabolic Stability". Drug Metab. Lett., **10**, 83–90, 2016.

117. DAYAN, A. D. "Albendazole , mebendazole and praziquantel . Re v iew of non-clinical toxicity and pharmacokinetics". **86**, 141–159, 2003.

118. NAGAR, S., ARGIKAR, U. A. & TWEEDIE, D. J. "Enzyme kinetics in drug metabolism: Fundamentals and applications". Methods Mol. Biol., **1113**, 1–6, 2014.

119. DORAN, A. C. *ET AL.* "Defining the Selectivity of Chemical Inhibitors Used for Cytochrome P450 Reaction Phenotyping: Overcoming Selectivity Limitations with a Six-Parameter Inhibition Curve-Fitting Approach". Drug Metab. Dispos., DMD-AR-2022-000884, 2022 doi:10.1124/DMD.122.000884.

120. WALSKY, R. & BOLDT, S. "In vitro cytochrome P450 inhibition and induction". Curr. Drug Metab., **9**, 928–939, 2008.

121. MINDER, E. I., MEIER, P. J., MÜLLER, H. K., MINDER, C. & MEYER, U. A. "Bufuralol metabolism in human liver: a sensitive probe for the debrisoquine-type polymorphism of drug oxidation". Eur. J. Clin. Invest., **14**, 184–189, 1984.

122. ARANA-PEÑA, S. *ET AL.* "Enzyme co-immobilization: Always the biocatalyst designers' choice…or not?". *Biotechnology Advances* 107584, at https://doi.org/10.1016/j.biotechadv.2020.107584 (2020).

Chapter II

Research Articles

Chapter II | Research Articles

The first article for this Thesis discusses the immobilization of glucose-6-phosphate dehydrogenase onto magnetic beads (G6PDH-Mbs) as a generator system for *in situ* NADPH production. To that, a liquid-chromatography UV method was developed and qualified in order to monitor the production of NADPH through the enzymatic reaction catalyzed by glucose-6-phosphate dehydrogenase in the presence of $NADP^+$ and glucose-6-phosphate. The chromatography separation of $NADP^+$ and NADPH represented a great challenge, considering the physical-chemical properties of those compounds. Then, the biocatalyst bioreactor was characterized in terms of catalytic activity and kinetic studies. The efficiency of G6PDH-Mbs in the production of NADPH, which is the essential cofactor for CYPs reactions, was demonstrated by the *in vitro* metabolism assays of albendazole and fiscalin B.

The second article explains the immobilization of enzymes from cytochrome P450 onto magnetic beads. The immobilization conditions were modulated using rat liver microsomal fractions (RLM-Mbs) as a low-cost alternative, and then successfully applied to the immobilization of human liver microsomes (HLM-Mbs). The HLM-Mbs were characterized according to the catalytic activity, kinetic and inhibition studies for CYP3A4. In addition, enzymatic activities for CYP2C9 and CYP2D6 on HLM-Mbs were evaluated by monitoring the hydroxylation reactions of diclofenac and bufuralol as substrates.

The second article also describes the one-pot used strategy to form the dual biocatalyst bioreactor G6PDH-HLM-Mbs. In this case, the characteristics of both systems were combined, promoting a unique environment to produce NADPH *in situ* and *in vitro* metabolism by CYP-mediate reactions.

2.1. Research Article I

Glucose-6-phosphate dehydrogenase immobilized onto magnetic beads (G6PDH-Mb) as a generator system for production of NADPH: Development and application in metabolism studies

Journal of Pharmaceutical and Biomedical Analysis 219 (2022) 114901

Izadora Liranço Furlani • Regina Vincenzi Oliveira • Quezia Bezerra Cass

Glucose-6-phosphate dehydrogenase immobilized onto magnetic beads (G6PDH-Mb) as a generator system for production of NADPH: Development and application in metabolism studies

Izadora Liranço Furlani, Regina Vincenzi Oliveira and Quezia Bezerra Cass*

SEPARARE – Núcleo de Pesquisa em Cromatografia, Departamento de Química, Universidade Federal de São Carlos, Rodovia Washington Luiz, km 235, 13565-905

Abstract

Reduced nicotinamide adenine dinucleotide phosphate (NADPH) participates in several anabolic and catabolic pathways, being essential in numerous biochemical reactions involving energy release. Most of these reactions require a high amount of NADPH, which can be expensive from an industry point of view. Thus, biotechnology industries developed a great interest in NADPH production. Currently, there are different ways to obtain NADPH *in situ*, however, the most common is by enzymatic reactions, known as generator systems. Although this approach can be beneficial in terms of cost, the major drawback is the impossibility of reusing the enzyme. To overcome this, enzyme immobilization is a proven alternative. Herein, we report the use of glucose-6-phosphate dehydrogenase immobilized onto magnetic beads (G6PDH-Mb) through glutaraldehyde coupling to produce high amounts of NADPH. The G6PDH-Mbs were kinetically characterized showing a sigmoidal curve. Besides, the stability was evaluated, and their reuse was demonstrated for a period superior to 40 days. The G6PDH-Mb was used to *in situ* production of the NADPH metabolism experiments, using human liver microsome solutions and either albendazole or fiscalin B as model targets. The production of *in vitro* metabolites from albendazole and fiscalin B was evaluated by comparing the use of NADPH generated *in situ* with those obtained by commercial NADPH. Moreover, the

activity of the G6PDH-Mb was monitored after using it for five consecutive albendazole metabolism reactions, with only a minor decrease in the enzyme activity (3.58 ± 1.67 %) after the fifth time of use. The higher concentration obtained when using the designed G6PDH-Mb generator system demonstrated proof of the concept and its applicability.

Keywords

Immobilized enzyme; NADPH generator system; magnetic beads, cofactors separation, *in vitro* metabolism.

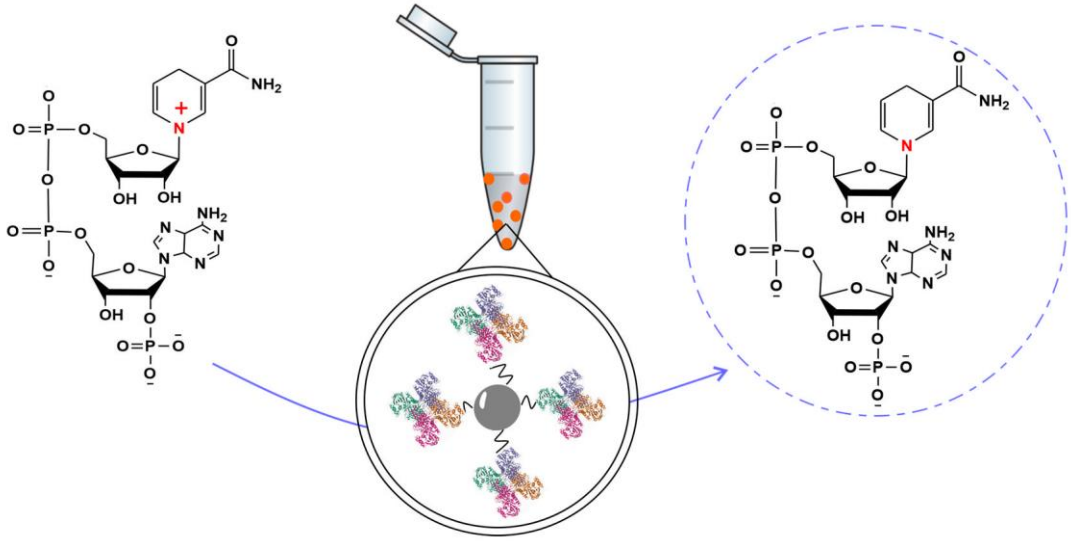

Graphic Abstract.

Glucose-6-phosphate dehydrogenase immobilized onto magnetic particles and its application in the production of NADPH.

1. Introduction

Nicotinamide adenine dinucleotides (NAD/NAD^+/NADH) and nicotinamide adenine dinucleotide phosphates ($NADP^+$/NADPH) are key electron donors that play an essential role in all organisms. NAD(H) and NADP(H) mediates a number of anabolic and catabolic reactions being important cofactors for various oxidoreductase enzymes, playing critical roles for transferring and reserving reduction potential [1]. NADPH exclusively drives the anabolic synthesis of important biomolecules, such as sugars, amino acids, lipids, and the reduction of glutathione [2]. Due to its importance in biosynthesis and its increasing role in human health and major diseases [3], NADPH has been of great interest to the biotechnology industries [4].

Nowadays, many industrial processes use biocatalytic reactions, where the consumption of NADPH would be substantially high and expensive from an industrial point of view [1]. In this regard, *in situ* production can minimize manufacturing costs. Currently, there have been a variety of strategies for producing NADPH *in situ*, including chemical [5], electrochemical [6], photochemical [7], enzymatic, and catalytic reactions [8].

The major enzymatic source of NADPH in the cell basically consists of $NADP^+$ and different enzymes involved in the oxidative pentose phosphate metabolic pathway, such as glucose-6-phosphate dehydrogenase (G6PDH) and 6-phosphogluconate dehydrogenase (6PGD) [1]. In mitochondria, NADPH production includes three major routes catalyzed by NADP-linked isocitrate dehydrogenase 2 (IDH2), NADP-linked malic enzyme, and mitochondrial transhydrogenase [1,9,10]. Glucose-6-phosphate dehydrogenase is, however, the most used route and for that G6P and $NADP^+$ are used as the substrates to produce 6-phospho-D-glucono-1,5-lactone and NADPH [1,11]. This reaction is shown in Fig. 1.

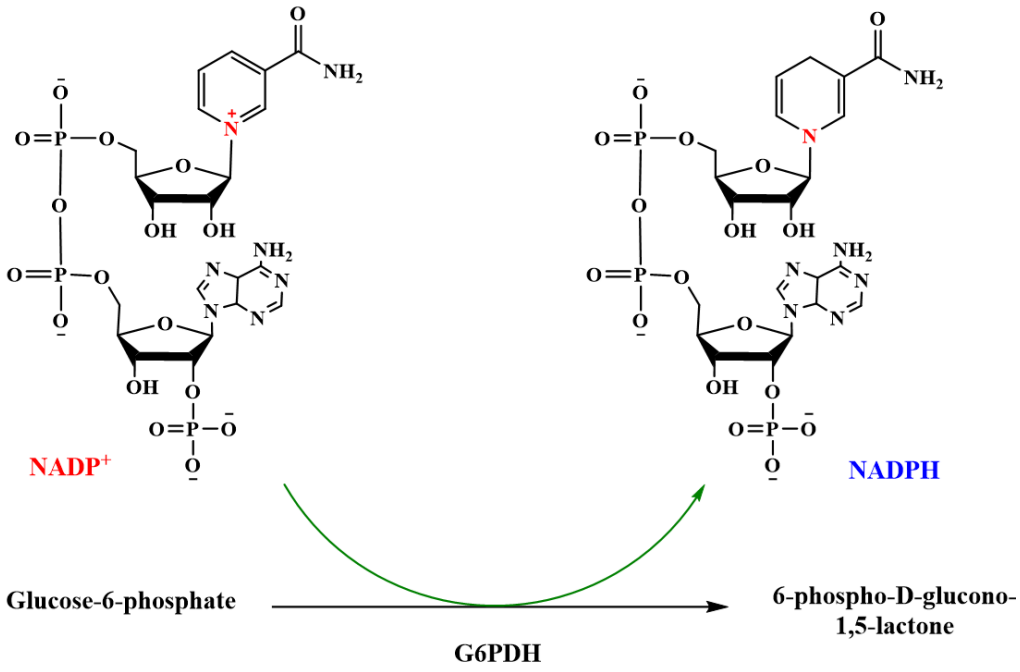

Fig. 1. NADPH production by glucose-6-phosphate dehydrogenase (G6PDH). Chemical structures of $NADP^+$ and NADPH

The *in situ* production of NADPH by glucose-6-phosphate dehydrogenase is usually carried out with the free enzyme in solution [1]. Although this is regarded as a sustainable approach, it implies most of the time in lack of long-term operational enzyme stability, difficult recovery, and re-use of the enzyme. These disadvantages can be overcome through the immobilization technique [12,13].

Enzyme immobilization is usually tailored made to the purpose of the application, and for that, several solid supports are available. As a role, they provide easy separation of the products, enhancing recovery and reuse of the enzyme. Moreover, it improves stability under manipulation and storage, enabling repeated reuse [12,13].

Different support such as magnetic beads, silica, chitosan, nylon fibers, and others show as main advantages the versatility of chemistry surface, the size, and high surface area [14,15]. In the case of magnetic beads, it promotes the easy separation from the reaction medium by use of an external magnetic field, besides, it has excellent biocompatibility [15,16].

The immobilization of glucose-6-phosphate dehydrogenase through different techniques and for diverse applications has already been reported in the literature, as summarized in the reference of Srivastava and Singh [17]. Nevertheless, the immobilization of G6PDH aiming to produce *in situ* NADPH in biotransformation reaction is still not well explored [18].

Herein we report the *in situ* production of NADPH by the use of glucose-6-phosphate dehydrogenase immobilized onto magnetic beads to generate immobilized biocatalysts (G6PDH-Mbs). The concentration of the produced NADPH was quantified by liquid chromatography and ultraviolet detection (LC-UV), under reversed-phase elution mode at 260 nm. The G6PDH-Mb was kinetically characterized and then, used in two different *in vitro* metabolism experiments. The first one was carried out with albendazole as a model drug. The quantification of its major metabolite, albendazole sulfoxide, was analyzed by a liquid chromatography-mass spectrometry method (LC-MS/MS). The second metabolism assay was carried out with fiscalin B, which is a quinazolinone alkaloid and has been reported for its neuroprotective, antitumor, and antimalarial effects [19–22]. The biotransformation reactions for fiscalin B were evaluated by liquid chromatography coupled to quadrupole time-of-flight high resolution mass spectrometry (LC-HRMS).

2. Methods and Materials

2.1 Reagents

Glucose-6-phosphate dehydrogenase – 500 U (from baker's yeast (S. cerevisiae – E.C: 1.1.1.49)), amine-terminated silane-coated magnetic beads (50 mg mL^{-1}, 1µm diameter), nicotinamide adenine dinucleotide phosphate reduced (NADPH), nicotinamide adenine dinucleotide phosphate ($NADP^+$), glucose-6-phosphate (G6P), ammonium acetate, potassium phosphate, glutaraldehyde, formic acid, hydrochloric acid (HCl), tris(hydroxymethyl)aminomethane (Tris), and albendazole (ABZ) were all purchased from Sigma-Aldrich (St. Louis, MO, USA). Human liver microsomes from 50 different individual donors were purchased from Thermo Fischer Scientific. Albendazole sulfoxide (ABZ-SO) was generously supplied by Ouro Fino Saúde Animal (Ribeirão Preto, SP, Brazil). Albendazole sulfone (ABZ-SO_2) and albendazole-2-amine-sulfone (ABZ-SO_2-NH_2) were synthesized in our laboratory, in accordance with Belaz et. al [23]. Fiscalin B was synthesized and furnished by Prof. Dr. Emilia Souza, Universidade do Porto, Portugal [22].

The chromatographic columns used were Phenomenex® Phenyl-Hexyl (50 x 2.1 mm; 5.0 µm), SeQuant® Zic-HILIC (150 x 2,1 mm; 5 µm), and XSelect® HSS T3 (100 x 2.1 mm; 3.5 µm). A C8 (100 x 4.1 mm; 10 µm) column was packed in-house by the ascending slurry method using octyl silica (Luna®, 10 µm particle size, 120 Å pore size) and methanol for slurry preparation (50 mL) and for packing. The packing was carried out at a pressure of 7500 psi and the column was conditioned for about 12 hours with methanol at a flow rate of 0.8 mL min^{-1} [24]. Methanol was HPLC grade from Merck (Darmstadt, HE, Germany) and the water used for all experiments was ultrapure and deionized in a Millipore Milli-Q system from Merck (Darmstadt, HE, Germany).

2.2 Chromatographic conditions for separation of $NADP^+$ and NADPH

Chromatographic analysis was carried out on a Shimadzu HPLC system (Shimadzu Kyoto, Japan), which consisted of the two LC-20AD pumps, a SIL 20A autosampler with a 50 µL loop, a DGU-20A5 degasser, an SPD-M20AD UV-Vis detector, and CBM-20A interface.

Different chromatographic separations were evaluated and are summarized in Table S1. Briefly, hydrophilic interaction liquid chromatography (HILIC) mode was tested with a SeQuant® Zic-HILIC (150 x 2.1 mm, i.d; 5 µm) using a flow rate of 0.2 mL min^{-1} and acetonitrile:ammonium acetate (10 mmol L^{-1}, pH 8.0) as mobile phase. The isocratic elution was also changed by testing 70 and 75 % of the organic modifier.

Reversed-phase liquid chromatography (RPLC) was also evaluated with different stationary phases such as: XSelect® C18 HSST3 (100 x 2.1 mm, i.d; 3.5 µm) with a flow rate of 0.2 mL min^{-1}; Luna® Phenyl-hexyl (100 x 2.1 mm, i.d; 10 µm) using a flow rate of 0.5 mL min^{-1}; and a C8 (100 x 4.6 mm, i.d; Luna® C8 10 µm) column and a flow rate of 0.8 mL min^{-1}. For the RPLC separations, the mobile phases tested used methanol as the organic modifier and ammonium acetate (10 mmol L^{-1}, pH 8.0, and pH 6.0) as the aqueous solvent. Due to the high polarity of the analytes, the concentration of the organic solvent was kept at 1 or 3 %.

2.3 LC-UV method qualification for monitoring NADPH production

The linearity of the method was evaluated by constructing an analytical calibration curve with external standards for quantification. A stock solution of NADPH at a concentration of 1600 µmol L^{-1} was prepared in ammonium acetate (10 mmol L^{-1}, pH 7.4). Calibration standards and quality controls (QCs) were prepared in triplicate by diluting the NADPH stock solution in ammonium acetate (10 mmol L^{-1}, pH 7.4) to give final concentrations at 5; 10; 20; 40; 80; 160; 320; 640 and 800 µmol L^{-1}.

The intra- and inter-day accuracy and precision of the LC-UV method were evaluated by analyzing QCs at three different concentrations at 6; 360 and 680 µmol L^{-1}. Five samples of each concentration were individually prepared and analyzed in three non-consecutive days. The limit of quantification (LOQ) was determined based on the variability obtained from repeated injections (n=3), which had to be less than 20%. The limit of detection (LOD) was calculated based on a signal-to-noise ratio at about 3. Chromatographic analysis of blank samples constituted of ammonium acetate (10 mmol L^{-1}, pH 7.4) was analyzed to assess the impact of any carryover immediately after the highest calibration standard was analyzed.

2.4 Immobilization on the magnetic beads

Glucose-6-phosphate dehydrogenase was covalently linked on the surface of magnetic beads, following a previously reported protocol [25]. Briefly, 25 mg of magnetic beads were washed three times with 1.0 mL of phosphate buffer (100 mmol L^{-1}, pH 7.0) using a magnetic separator. The supernatant was discarded, and the magnetic beads were suspended in 1.0 mL of phosphate buffer (100 mmol L^{-1}, pH 7.0) containing 5% of glutaraldehyde and then shaken for 3 hours at room temperature. After magnetic separation, the magnetic beads were washed three more times with 1.0 mL of phosphate buffer (100 mmol L^{-1}, pH 7.0), followed by the addition of 500 µL of G6PDH solution (4 µg mL^{-1}) prepared in phosphate buffer (100 mmol L^{-1}, pH 7.0). The reaction was kept for 16 hours at 4.0 ºC under gentle rotation using a Rotary laboratory mixer Revolver™ (Labnet International – New Jersey, USA). After that, the supernatant was collected, and the beads were washed three times with 1.0 mL of Tris-HCl buffer (10 mmol L^{-1}, pH 8.0). The obtained immobilized magnetic bead (G6PDH-Mb) batch was divided into five aliquots of 5 mg each and stored in the same solution at 4.0 ºC. Three of them were used for the kinetic assays and metabolism experiments, while the other two

were used in stability assays. Fig. S1 showed the immobilization reaction for G6PDH.

The immobilization efficiency was evaluated in terms of enzymatic activity measured in the enzymatic solution before and after immobilization of G6PDH onto the magnetic beads. The G6PDH-Mb stability was evaluated by periodically monitoring its activity over 40 days after immobilization. The same batch of G6PDH-Mb was reused during the stability evaluation.

For preparing G6PDH-Mb-controls, the immobilized biocatalysts were heated to 80 °C for 20 min in a water bath, for denaturalization.

2.5 Enzymatic activity assay in solution

Enzymatic activities were measured in the enzymatic solution before and after the G6PDH immobilization on the magnetic beads. In brief, 10 µL of G6PDH solution (4 µg mL^{-1}) were incubated for 4 minutes with 20 µL of G6P 200 mmol L^{-1}, 40 µL of $NADP^+$ 2.0 mmol L^{-1} and 130 µL of ammonium acetate (10 mmol L^{-1}, pH 7.4), totalizing a final volume of 200 µL. Stock solutions for G6PDH, G6P and $NADP^+$ were prepared in ammonium acetate (10 mmol L^{-1}, pH 7.4). The reaction was interrupted by increasing the temperature to 80 °C for 2 minutes, then followed by centrifugation at 7,267 g for 5 minutes. The supernatants were collected and analyzed by the LC-UV described in the session 2.3.

2.6 Enzymatic activity assay for G6PDH-Mb

For measuring the enzymatic activity of the G6PDH-Mb the following conditions were used: G6PDH-Mb (0.4 U/5 mg beads) was incubated with 140 µL of ammonium acetate (10 mmol L^{-1}, pH 7.4), 20 µL of G6P 200 mmol L^{-1}, and 40 µL of $NADP^+$ 2.0 mmol L^{-1}. Stock solutions for G6P and $NADP^+$ were also prepared in ammonium acetate (100 mmol L^{-1}, pH 7.4). The mixture was gently agitated using a Rotary laboratory mixer Revolver™ (Labnet International – New Jersey, USA) for 4 minutes at room temperature. Then, the G6PDH-Mb was

placed on the magnetic separator for 2 min, and the supernatant was collected and analyzed by LC-UV as described in session 2.3. The same activity assay procedure was carried out for monitoring the stability of G6PDH-Mb.

2.7 Kinetic characterization of G6PDH-Mb

The kinetic characterization of the immobilized G6PDH-Mb was carried out in triplicate. $NADP^+$ solutions ranging from 5 to 2160 µmol L^{-1} were tested, while the G6P was maintained in a fixed concentration of 20 mmol L^{-1}. Both $NADP^+$ and G6P solutions were prepared in ammonium acetate (10 mmol L^{-1}, pH 7.4). $NADP^+$ (40 µL) and G6P (20 µL) solutions were added to G6PDH-Mb (0.4 U/ 5 mg beads) placed in 140 µL of ammonium acetate (10 mmol L^{-1}, pH 7.4) and the reaction was carried out for 4 min before placing the reaction vessel to a magnet during 2 min for G6PDH-Mb separation. Aliquots of the supernatant were collected, transferred to autosampler vials, and a volume of 10 µL was injected into the LC-UV system (session 2.3). In the end of each kinetic reaction, the G6PDH-Mb was washed 3 times with ammonium acetate (10 mmol L^{-1}, pH 7.4), then the immobilized biocatalyst was reused. The formation of NADPH related to the variation of $NADP^+$ concentration was plotted, according to Hill's equation (Equation 1). The *K*prime value and Hill's coefficient were estimated using GraphPad Prism® software (version 5.0) by nonlinear regression analysis. Experimental conditions are summarized in Table S2.

Equation 1

$$y = \frac{V\text{max} * X^H}{K\text{prime} + X^H}$$

2.8 LC-MS/MS method for drug metabolism

The analysis of the *in vitro* drug metabolism was conducted using a Phenomenex® Phenyl-Hexyl column (50 x 2.1 mm; 5.0 µm), using methanol:water containing 0.1% of formic acid (35:65 v/v) as mobile phase; column temperature of 35 °C,

and flow rate of 0.2 mL min^{-1}. The injection volume was 10 µL. The LC-MS/MS analysis was performed using an Acquity Binary pump (Waters, Milford, USA), an autosampler model 2777C (Waters), coupled with a XEVO TQ-MS (Waters Corporation, Milford, MA, USA) equipped with an electrospray ionization (ESI) source operating in the positive mode. Data acquisition and processing were performed by using MassLynx 4.1 and TargetLynx software (Waters Corporation, Milford, MA, USA), respectively. The mass spectrometry conditions were: capillary voltage 2.40 kV, cone voltage 29 V, source temperature at 150 °C, desolvation gas temperature at 350 °C, and desolvation gas flow at 490 L h^{-1}.

The analyses were performed in selected reaction monitoring (SRM). For each albendazole's metabolite, two SRM transitions were optimized as quantifiers. Precursor to product ions transitions and collision energies are listed in Table 1.

Table 1

LC-MS/MS parameters for albendazole and its metabolites.

Compound	Precursor (*m/z*) $[M+H]^+$	SRM transitions	Cone (V)	Collision (V)
ABZ	265.90	234.05	10	24
		191.16	10	38
ABZ-SO	282.10	159.04	26	38
		207.90	26	24
ABZ-SO_2	298.11	159.03	32	38
		266.00	32	20
ABZ-SO_2-NH_2	240.10	105.86	34	38
		133.08	34	30

2.9 LC-MS/MS method qualification for quantification of albendazole sulfoxide

The linearity of the method was evaluated by constructing an analytical calibration curve with external standards for quantification. A stock solution of albendazole sulfoxide (3.5 mmol L^{-1}) was prepared in methanol. Seven working standard solutions were prepared in ammonium acetate (10 mmol L^{-1}) at 10000, 8500, 6500, 2500, 1000, 400, and 200 nmol L^{-1}. Three quality controls working solutions were prepared at 8200, 5000, and 300 nmol L^{-1}. Calibration standards and quality controls (QCs) samples were prepared by aliquoting 10 µL of the appropriate working solution into 80 µL of ammonium acetate (10 mmol L^{-1}, pH 7.4) containing 10 µL of microsomal fraction 10 mg mL^{-1}, which were deactivated by heating at 80 °C for 20 min in a water bath for protein denaturalization. The samples were mixed for 30 seconds by vortex, and the protein was precipitated with 80 µL of acetonitrile following by centrifugation at 7,267 g for 5 min. After that, 50 µL of the reaction solution was diluted with 50 µL of water and 10 µL was injected into the LC-MS/MS system. The final concentrations of the calibration standards were 20, 40, 100, 250, 650, 850, and 1000 nmol L^{-1} and the final concentrations of the QC samples were 30, 500, and 820 nmol L^{-1}.

The intra and inter-day precision and accuracy of the LC-MS/MS method for quantification of albendazole sulfoxide was determined by analyzing five replicates of each QC sample (30, 500, and 820 nmol L^{-1}). The precision results were expressed as coefficient of variation (CV %) of the responses obtained for each level of concentration evaluated and the accuracy of the method was evaluated as the percentage recovery of albendazole sulfoxide when comparing the calculated and the nominal concentrations.

The limit of detection (LOD) was calculated as the minimum detectable amount of compound, with a signal-to-noise (S/N) ratio of ≥three. The LOQ was determined as the lowest calibration level of the standard calibration curve that could be determined with acceptable precision and accuracy (≤ 20 %).

The method was applied to analyze the production of albendazole sulfoxide metabolite through the *in vitro* metabolism. During data acquisition, the

calibration curve and quality control samples were analyzed before and after the biotransformation samples.

2.10 LC-HRMS/MS analysis – Metabolite Identification

For fiscalin B, the *in vitro* metabolism experiments were monitored using a high-resolution mass spectrometer (HRMS) containing a quadrupole time-of-flight mass analyzer (QTOF). The MS analysis was performed using an Impact HD QTOF™ mass spectrometer (Bruker Daltonics, Bremen, Germany) equipped with an electrospray (ESI) interface operating in positive ion mode.

The optimal parameters were set as follows: positive ion mode, capillary voltage, 3.6 kV; end plate offset, 450 V; nebulizer, 4 bar; dry gas flow, 8 L min^{-1}; dry heater temperature, 180 °C; collision cell energy, 5 eV, and full MS scan range, *m/z* 100–1100. The mass spectrometer was programmed to perform data-dependent acquisition (DDA) MS/MS mode using a dynamic method of 3 sec of cycle time, release after 0.9 min, and exclusion *m/z* after 1 spectrum. MS acquisition rate of 2.00 Hz and MS/MS acquisition rate of 2.00 Hz for low precursor ions (50,000 cts.) and 4.00 Hz for high precursor ions (100,000 cts) were used. The experiments used a dynamic range of collision energy from 25 eV to 62.5 eV for all *m/z* range analyzed.

The chromatographic separation for the *in vitro* metabolism of fiscalin B was carried out with a Phenomenex® Phenyl-Hexyl column (50 × 2.1 mm; 5 µm). The mobile phase consisted of 0.1% of formic acid either in water (solvent A) and acetonitrile (solvent B). A linear gradient was set as follows: 20–95% B, 0–8 min; 95–20% B, 8.01–11 min. The flow rate was 0.2 mL min^{-1} and the sample injection volume was 5 µL.

Internal mass-spectrometer calibration was performed with 1 mmol L^{-1} of sodium formate prepared in acetonitrile, using quadratic high-precision calibration (HPC) regression mode. The calibration solution was injected at the end of the analytical run (8.01–9 min) and all spectra were calibrated before compound identifications.

For the metabolite structural elucidation, the analyses were acquired in MS/MS mode and the fragments spectra were compared to fiscalin B [22]. The MetabolitePredict® Software was also used as a tool for in silico prediction of metabolites.

2.11 G6PDH-Mb application to in situ NADPH production in drug metabolism experiments of albendazole

For the *in situ* production of the NADPH, 20 µL of G6P (200 mmol L^{-1}) and 65 µL of $NADP^+$ (2 mmol L^{-1}), both prepared in ammonium acetate (10 mmol L^{-1}, pH 7.4), were added in an Eppendorf tube to G6PDH-Mb (0.4 U/5 mg beads) placed in 115 µL of ammonium acetate (10 mmol L^{-1}, pH 7.4), and mixed under gentle rotation for 4 min using a Rotary laboratory mixer Revolver™ (Labnet International – New Jersey, USA). The reaction was maintained for 4 min at room temperature and then placed in a magnetic separator for 2 min prior to collecting an aliquot of 20 µL of the supernatant for monitoring by LC-UV the production of NADPH (session 2.3). The *in vitro* metabolism experiment was based on Solida et. al. [22] with minor changes. Thus, a stock solution of albendazole 3.77 mmol L^{-1} (1mg mL^{-1}) was prepared in methanol and diluted to 200 µmol L^{-1} with ammonium acetate (10 mmol L^{-1}, pH 7.4). A 10 mg mL^{-1} human liver microsome solution was also prepared in ammonium acetate (10 mmol L^{-1}, pH 7.4). Then, to conduct the *in vitro* metabolism, 10 µL of microsomal fraction (10 mg mL^{-1}), 10 µL of albendazole 200 µmol L^{-1} and 80 µL of ammonium acetate (10 mmol L^{-1}, pH 7.4) were added to the mixture containing the G6PDH-Mb and the produced NADPH. The Eppendorf was agitated under gentle rotation at 36 °C for 30 minutes in a water bath to carry out the metabolism assay. The G6PDH-Mb was magnetically separated (2 min) and, then 80 µL of acetonitrile was added to 100 µL of the collected supernatant and centrifuged for 5 minutes at 7,267 g. For the LC-MS/MS analysis, 50 µL of the supernatant was collected and diluted with 50 µL of water. The experimental condition is summarized in Table S3.

The recovered G6PDH-Mb was washed 3 times with ammonium acetate (10 mmol L^{-1}, pH 7.4) and immediately reused. Five consecutive metabolism reactions were carried out using the recycled G6PDH-Mb to monitor its stability during the experiments. The production of NADPH was measured after each *in vitro* metabolism experiment using the LC-UV method (session 2.3).

To compare the performance of the *in situ* generation of NADPH, additional *in vitro* metabolism experiments were also carried out using the same conditions previously described but using commercial NADPH purchased from Sigma-Aldrich®. Briefly, 400 µmol L^{-1} of NADPH was prepared in ammonium acetate (10 mmol L^{-1}, pH 7.4), followed by the addition of 10 µL of microsomal fraction (10 mg mL^{-1}), 10 µL of albendazole 200 µmol L^{-1} and 80 µL of ammonium acetate (10 mmol L^{-1}, pH 7.4). The reaction was maintained during 30 minutes at 36 °C in water bath. The reaction was stopped by the addition of 80 µL of acetonitrile in the reaction mixture, followed by centrifugation for 10 min at 7,267 g. Then, 50 µL of supernatant was diluted with 50 µL of water prior the analysis by LC-MS/MS method (session 2.9). The experimental condition is summarized in Table S4.

Using the same experimental procedure described above, two blank samples were also prepared and evaluated. The blank samples used ammonium acetate (10 mmol L^{-1}, pH 7.4) instead of $NADP^+$ (BS-1) or the commercial NADPH (BS-2).

2.12 G6PDH-Mb application to in situ NADPH production in drug metabolism experiments of fiscalin B

The *in vitro* metabolism of fiscalin B was conducted using the same experimental procedure described in section 2.11 for albendazole, with minor changes. Briefly, a stock solution of fiscalin B 2.59 mmol L^{-1} (1mg mL^{-1}) was prepared in acetonitrile and diluted to 200 µmol L^{-1} using ammonium acetate (10 mmol L^{-1}, pH 7.4). A solution of human liver microsomes from 50 different individual donors (10 mg mL^{-1}) was prepared in ammonium acetate (10 mmol L^{-1}, pH 7.4).

The *in situ* NADPH production was carried by the addition of a solution contained 80 µL of ammonium acetate (10 mmol L^{-1}, pH 7.4), 10 µL of human liver microsome solution (10 mg mL^{-1}), and 10 µL of fiscalin B (200 µmol L^{-1}). The reaction was agitated under gentle rotation at 36 °C for 60 minutes in a water bath. The G6PDH-Mb was magnetically separated (2 min) and, then 80 µL of acetonitrile was added to a 100 µL of the collected supernatant and centrifuged for 5 minutes at 7,267 g. The supernatant was transferred to an autosampler vial for the LC-HRMS/MS analysis.

The experiment was also carried out using commercial NADPH (Sigma-Aldrich®). Thus, 400 µmol L^{-1} of NADPH prepared in ammonium acetate (10 mmol L^{-1}, pH 7.4), followed by the addition of 10 µL of human liver microsome solution (10 mg mL^{-1}), 10 µL of fiscalin B solution (200 µmol L^{-1}), and 80 µL of ammonium acetate (10 mmol L^{-1}, pH 7.4) was maintained during 60 min at 36 °C in a water bath. The reaction was stopped by adding 80 µL of acetonitrile in 100 µL of the collected supernatant, then centrifuged for 10 min at 7,267 g, and analyzed using the LC-HRMS/MS method.

Blank samples for both systems (*in situ* generated NADPH and commercial NADPH) were prepared from the reaction mixtures at time 0 min.

3 Results and Discussion

3.1 Chromatographic separation conditions for monitoring $NADP^+$ and NADPH

To measure NADPH production, an analytical method for the chromatographic separation of the cofactors $NADP^+$ and NADPH was developed considering different separation mechanisms and stationary phases.

Initially, considering the polarity of the analytes, hydrophilic interaction chromatography (HILIC) was chosen to provide orthogonal analyte selectivity compared to reverse-phase. Thus, a SeQuant® Zic-HILIC was selected for its

zwitterionic stationary phase and due to its large number of applications in separations of small polar molecules, proteomic analysis, metabolomics, aminoglycosides, and glycopeptides [26].

The chromatographic separation of $NADP^+$ and NADPH with the SeQuant® Zic-HILIC column resulted in poor resolution and chromatographic efficiencies under the experimental conditions examined. Thus, reversed-phase elution mode was considered. For that, an XSelect® HSS T3 column was chosen due to its compatibility with high aqueous mobile phase content, supporting up to 100% aqueous mobile phase, which makes it suitable for separation of polar compounds [27]. Ortmayr et. al. [28] reported the analysis of NADPH in yeast, using an Atlantis T3 column (Waters), which is similar to the XSelect HSS T3 column, showing an Fs = 1.42, according to PQRI Database [29]. The authors described a good chromatographic resolution for quantifying $NADP^+$/NADPH using an LC-MS/MS method. However, the low chromatographic resolution observed for the separation of $NADP^+$/NADPH demonstrated that the XSelect HSS T3 column was not appropriate for the intended analysis by LC-UV.

The highest selectivity was achieved using an *in-house* packed Luna® C8 column (100 x 4.6 mm; Luna® 10 µm) with methanol:ammonium acetate (10 mmol L^{-1}, pH 6.0) (1:99 v/v) as mobile phase. The flow rate was 0.8 mL min^{-1}, and the analysis was monitored at 260 nm. This chromatographic condition provided retention factors (k) for $NADP^+$ and NADPH of 0.4 and 1.18, respectively, separation factor (α) of 2.71, and resolution of (Rs) of 2.42.

The identification of the NADPH chromatographic band was confirmed by injecting a separated standard solution of NADPH and $NADP^+$, at the same chromatography conditions, and comparing their retention times. Fig. 2 illustrates the obtained chromatographic separation for $NADP^+$ and NADPH. Since the main objective of the LC-UV analysis was to monitor NADPH production in high concentrations, a column with a larger particle size (10 µm) showed adequate to

overload conditions. Moreover, the LC-UV method obtained is simple since non-volatile buffers or ion-pair reagents are used.

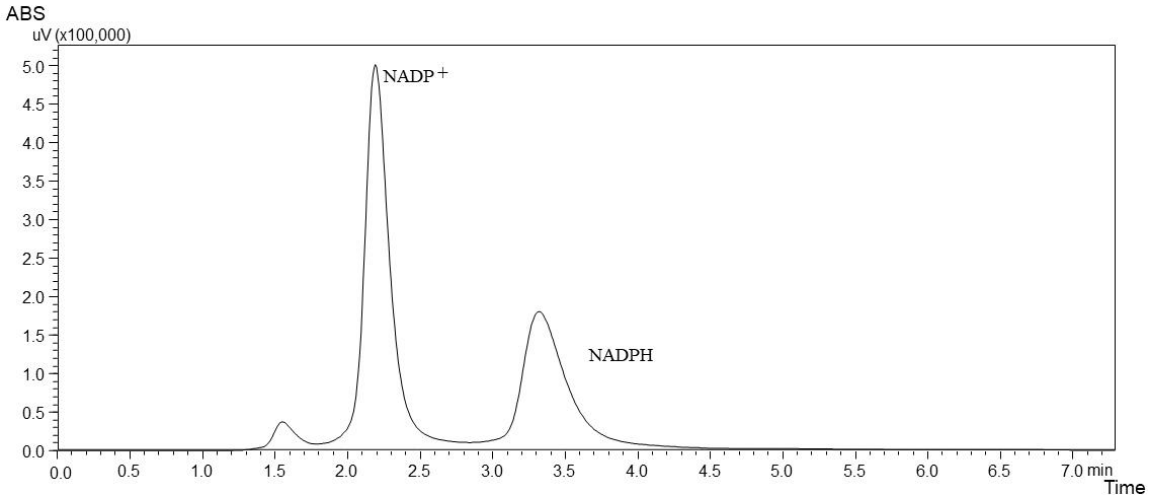

Fig 2. LC-UV chromatogram of $NADP^+$ and NADPH separation by a Luna® C8 analytical column (100 x 4.6 mm; 10 µm); mobile phase: methanol:ammonium acetate (10 mmol L^{-1}, pH 6.0) (1:99 v/v); flow rate: 0.8 mL min^{-1} and wavelength: 260 nm. $NADP^+$ and NADPH resuspended in water to 0.2 mg ml^{-1}; injection volume of 10 µL.

3.2 Qualification of the LC-UV and LC-MS/MS methods

For monitoring of the NADPH, the LC-UV method was qualified considering parameters for selectivity, linearity, inter- and intra-day precision and accuracy, limit of quantification, limit of detection, and carryover. The method showed to be precise and accurate, with a linearity range from 8 to 800 µmol L^{-1}, and a linear correlation between the peak area against concentrations of NADPH of $r^2 = 0.99$ ($y = 6042.3x - 19688$). The inter- and intraday precision showed coefficients of variation (CV%) ranging from 2.8 to 8.7 % and the accuracy from 90.3 to 109 %. The detection limit for NADPH determination was 2 µmol L^{-1} and the limit of quantification was 5 µmol L^{-1}. No interferences with NADPH or carryover from the highest concentration evaluated were observed. The proposed method demonstrated to be very precise and accurate, sensitive, and robust.

For the quantification of albendazole sulfoxide, the LC-MS/MS method was qualified as well, considering the selectivity, linearity, inter- and intra-day

precision and accuracy, limit of quantification, limit of detection, and carryover. The calibration curve obtained for ABZ-SO was linear with a correlation coefficient value of r^2 =0.993 and calibration equation y = 37.4038x – 125.445 (n=3). The precision (CV%) ranged from 8.1 to 11.7 % and the accuracy from 96.6 to 102.9 %. The limit of detection for albendazole sulfoxide was 10 nmol L^{-1}, and the limit of quantification was 20 nmol L^{-1}.

3.3 Immobilization and stability of G6PDH-Mbs

The G6PDH was covalently immobilized on the surface of magnetic beads via glutaraldehyde groups, generating the immobilized biocatalyst G6PDH-Mbs. This procedure was chosen due to its easy experimental procedure and successful rate [30,31].

In order to evaluate the immobilization efficiency of the G6PDH, the following assays were carried out: i) the activities of the enzyme solution prior to immobilization and the residual enzymatic activities of the supernatant after immobilization; ii) activity of prepared G6PDH-Mbs.

The comparison of the residual activity of the G6PDH in the supernatant after the immobilization procedure to the initial enzymatic solution was 42.2 ± 2.1 %, showing that about 55% of the enzyme was immobilized during the process. The G6PDH-Mb prepared showed an *in situ* production of NADPH of 268 ± 3.62µmol L^{-1}, which was maintained for more than 40 days and allowed to complete all kinetic and activities experiments over many weeks. The stability of the G6PDH-Mb in terms of the concentration of produced NADPH is illustrated in Fig. 3. The G6PDH-Mb showed high stability over a 40-day period, with reuse

To warranty that the NADPH production was obtained by the immobilized biocatalysts, an activity assay was also carried out with G6PDH-Mb-controls. In the controls experiment, NADPH was not produced.

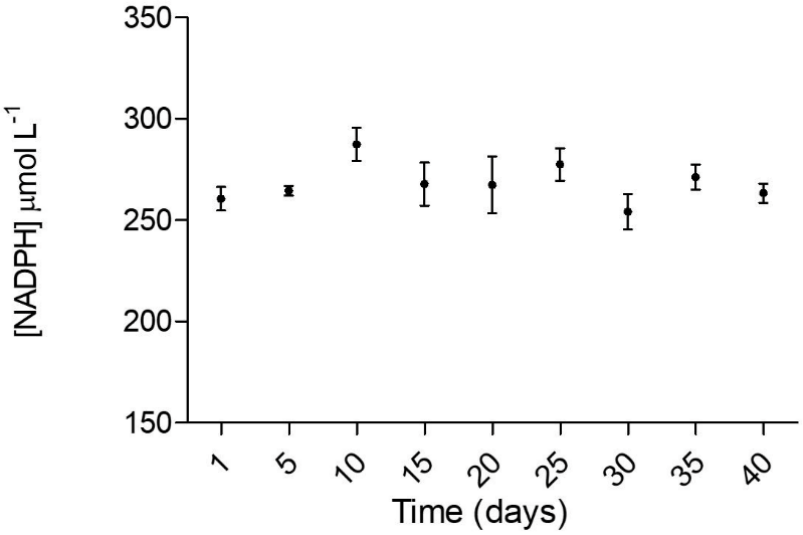

Fig 3. Graphical illustration of the stability of G6PDH-Mb based on the production of NADPH over a period of 40 days, with reuse (mean ± SD). The experimental details are described in section 2.6 for the following concentrations: 400 µmol L^{-1} of $NADP^+$, 20 mmol L^{-1} of glucose-6-phosphate in ammonium acetate 10 mmol L^{-1} pH 7.4.

3.4 Kinetic characterization of G6PDH-Mb for the $NADP^+$ substrate

G6PDH-Mb kinetic parameters were determined by systematic variation of $NADP^+$, while G6P was kept in saturating concentrations, at room temperature and pH 7.4. The best nonlinear regression fit method was used to obtain the kinetic model for the enzyme. Thus, NADPH formation was plotted according to Hill's equation (Equation 1) furnishing a sigmoid curve with Hill's coefficient of 1.48 ± 0.09, K_{prime} of 9975 ± 5414 µmol L^{-1}, and Vmax of 692.2 ± 28.2 µmol L^{-1} (Fig. 4).

A sigmoid kinetic is characteristic of allosteric enzymes. Moreover, Hill's coefficient (H) is used to describe the degree of cooperativity, when H equal to 1, there is no cooperativity, and the enzyme follows the Michaelis-Menten equation. If H > 1, it indicates positive cooperativity, and when H < 1 there is negative cooperativity [33,34]. The characteristic sigmoid curve obtained has already been reported for G6PDH from human erythrocyte, *Candida utilis*, *Leuconostoc mesenteroides*, and rat liver [32,35]. Taking into account the experimental conditions used, the observation of a sigmoid profile occurred mainly in high pH,

ionic strength, temperature, either in the presence of a high concentration of EDTA or glucose-6-phosphate, while $NADP^+$ concentration was varied [34,35], thus, corroborating our results. This model is consistent with an ordered sequential mechanism in which $NADP^+$ is bound first and NADPH released after or later.

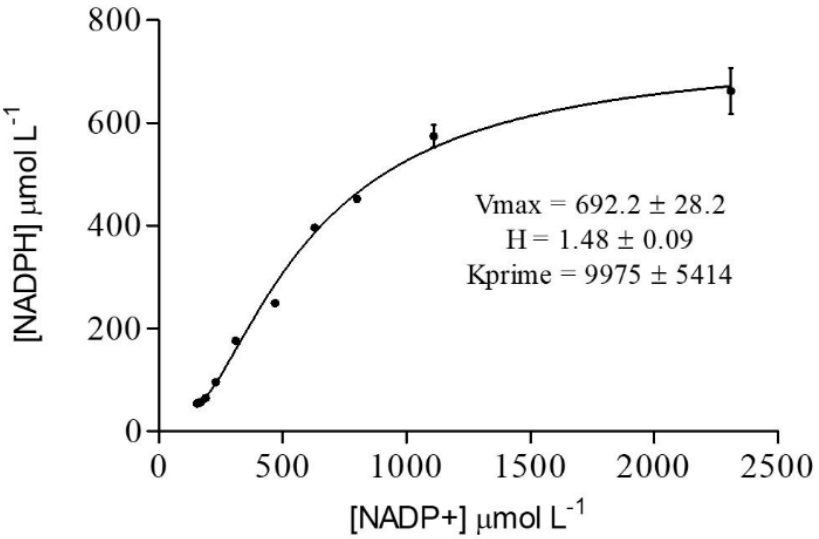

Fig. 4. G6PDH-Mb kinetics obtained to generate NADPH, under a fixed concentration of G6P at 20 mmol L^{-1}, and a range of 5 until 2160 µmol L^{-1} of $NADP^+$. Experiments were carried out in ammonium acetate 10 mmol L^{-1} pH 7.4, the reaction time of 4 min, and temperature of 25 °C.

3.5 Application of G6PDH-Mbs to NADPH production in in vitro metabolism studies

As proof of concept for the utilization of G6PDH-Mbs to effectively generate NADPH *in situ*, its application in *in vitro* metabolism experiments was designed, as illustrated in Fig.5, to produce albendazole sulfoxide.

The G6PDH-Mb kinetic was taken into consideration to calculate the concentration of $NADP^+$ to produce 400 µmol L^{-1} of NADPH in solution. To this end, 650 µmol L^{-1} of $NADP^+$ and 20 mmol L^{-1} of G6P were used.

For comparison, a parallel albendazole metabolism experiment was carried out in the same reaction conditions used with the G6PDH-Mbs, but now with commercial NADPH (400 µmol L^{-1}).

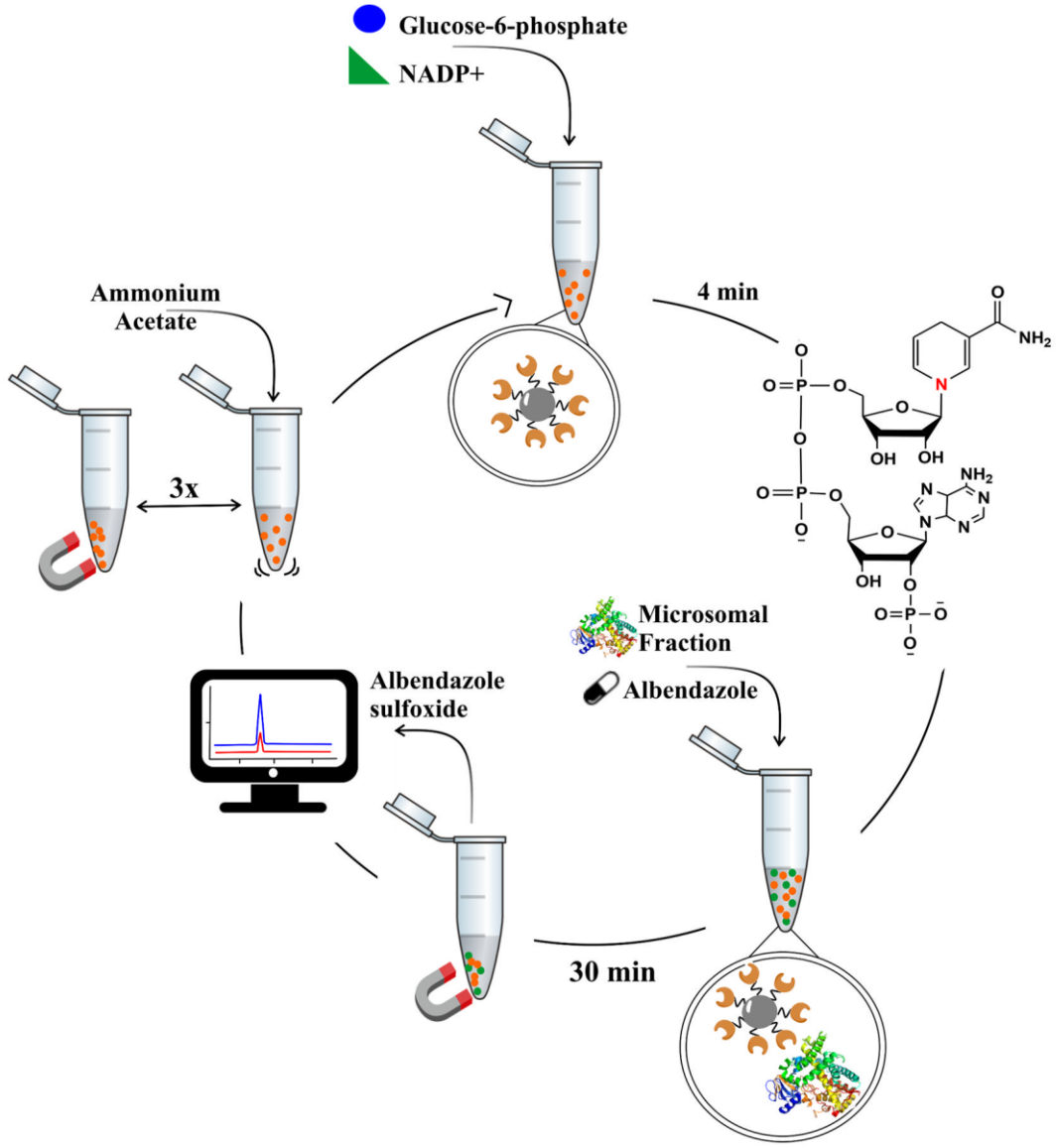

Fig. 5. *In vitro* metabolism through G6PDH-Mbs application to the production of NADPH *in situ*.

ABZ-SO metabolite was individually quantified by the LC-MS/MS method. The use of the commercial NADPH promoted the production of the ABZ-SO in the concentration of 48.02 ± 1.10 nmol L^{-1} while the use of G6PDH-Mb, as the

NADPH generator system, increased the amount of ABZ-SO produced approximately 3-fold, and the final concentration for ABZ-SO was 143.22 ± 0.64 nmol L^{-1}.

Comparative LC-MS/MS chromatograms of the produced ABZ-SO are illustrated in Fig. 6. The production of the minor metabolites, ABZ-SO_2 and ABZ-SO_2-NH_2 were not detected in the examined conditions.

The activity of the G6PDH-Mb was monitored after each time for five consecutive albendazole metabolism reactions. A small decrease in the enzyme activity (3.58 ± 1.67 %) was noted after the fifth time of use, demonstrating the stability and usefulness of developed immobilized biocatalyst by allowing multiple biotransformation reaction experiments.

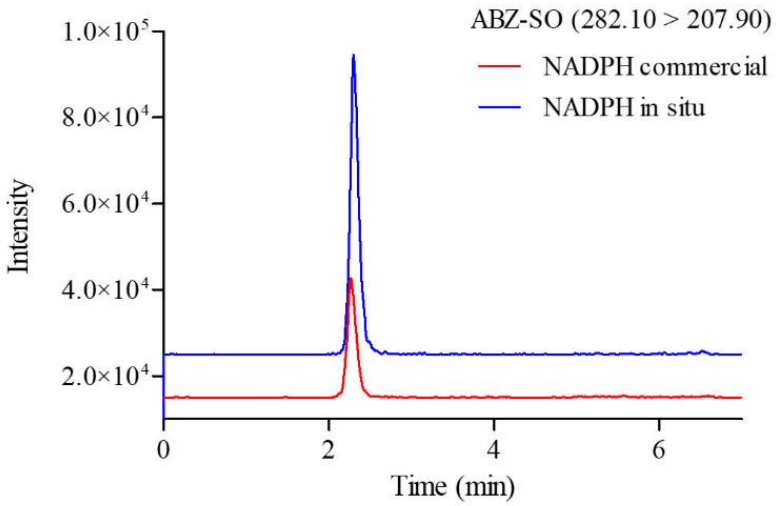

Fig 6. LC-MS/MS chromatogram for the *in vitro* metabolism conducted with NADPH produced *in situ* by the G6PDH-Mb (blue) and the commercial NADPH (red). Transition monitored to ABZ-SO (282.10 > 207.90). The initial concentration of NADPH was 400 µmol L^{-1} for both systems.

The second application using the G6PDH-Mb was used for the *in vitro* metabolism of fiscalin B [20,21]. For this experiment, human liver microsomes were chosen because they promote great contribution to predicting *in vivo* outcomes from *in vitro* metabolism data. Phase I reactions were investigated by using an LC-HRMS data acquisition and processing.

Fiscalin B showed a protonated ion at $[M+H]^+$ 387.1819 (Rt: 4.4 min) corresponding to $[C_{23}H_{23}N_4O_2]^+$ (calcd 387.1816, $\Delta_{m/z\ theoretical}$ = -0.8 ppm). Using the experimental conditions described here, the metabolism of fiscalin B furnished one possible metabolite (Fig. 7). The metabolite designed M1, showed a protonated ion at $[M+H]^+$ 403.1810 (Rt: 3.4 min), consistent with the molecular formula $C_{23}H_{23}N_4O_3$ (calcd 403.1805, $\Delta_{m/z\ theoetical}$ = -1.0 ppm). M1 corresponds to a nominal mass change of 16Da higher than fiscalin B, suggesting a modification by a hydroxylation reaction. According to the MS^2 spectrum, the difference in *m/z* suggests a modification in the indole moiety. The LC-HRMS spectrum for fiscalin B and its metabolite are reported by Long et. al [22].

The use of G6PDH-Mb as NADPH generator provided a gain of 15.5 ± 1.0 % in the M1 production compared to the commercial NADPH. This increase aided in the identification and elucidation of the metabolite.

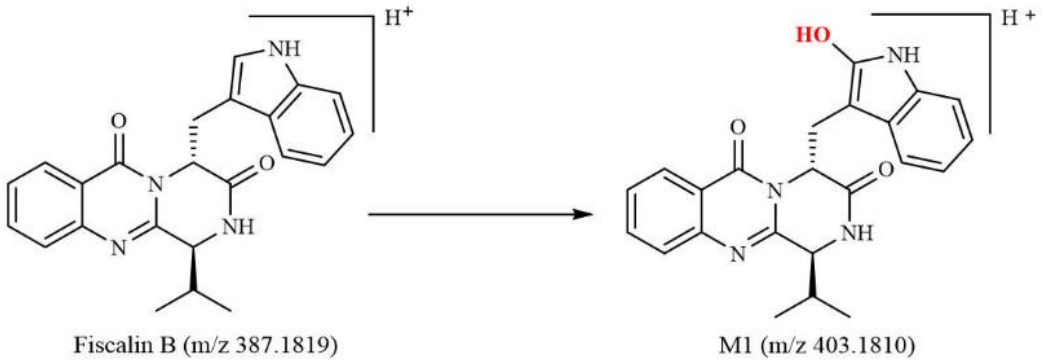

Fig. 7. Inferred *in vitro* metabolite of fiscalin B

In conclusion, in both *in vitro* metabolism experiments, the production of the metabolites was higher using G6PDH-Mb as the generator system than in the experiments with the commercial NADPH. These results suggest that due to the constant supply of cofactor by the immobilized biocatalyst during the assays, it could promote a better production of metabolites.

4 Conclusions

The immobilization of glucose-6-phosphate dehydrogenase onto magnetic beads provided an important strategy to enhance productivity and thus, NADPH supply. Initially, a simple and efficient chromatographic separation was herein described to monitor NADPH production and the G6PDH-Mb activities. The immobilized biocatalyst showed great stability for 40 days allowing its reuse in multiple reaction experiments. The kinetic assay was carried out and a sigmoidal curve was observed with a Hill's coefficient of 1.48 ± 0.09, indicating positive cooperativity for experimental conditions used. The high NADPH turnover obtained with G6PDH-Mb allowed its application to *in vitro* metabolism reactions using albendazole and fiscalin B as models. The higher concentration obtained for ABZ-SO and M1 when compared to the experiments carried out with the commercial NADPH is worth noting since biotransformation reactions are an important toolbox for producing metabolites to a diversity of applications. Also, even after 5 consecutive *in vitro* metabolism experiments, the G6PDH-Mb maintained more than 96 % of activity and could easily be reused for other assays.

Conflicts of interest

The authors declare no conflict of interest.

Author contributions

I.L.F contributed to the study conception, carried out the experiments, and wrote the manuscript. R.V.O and Q.B.C planned the research project, supervised the research activities, reviewed, and edited the draft. All authors have read and approved the final manuscript.

Acknowledgments

The authors gratefully acknowledge support for this work from Fundação de Amparo a Pesquisa do Estado de São Paulo (FAPESP) with the research grants

(FAPESP) (grant number 2014/50244-6, 2014/50249-8, 2020/05965-8) and PhD scholarships 2018/03035-3 and GlaxoSmithKline (GSK). The research grants (302557/2018-0 and 406064/2018-0) from the Conselho Nacional de Desenvolvimento Científico e Tecnológico (CNPq), and the Finance Code 001 from CAPES (Coordenação de Aperfeiçoamento de Pessoal de Nível Superior) are also acknowledged. The authors are grateful to Professor Emilia Souza from the University of Porto, Porto – PT, for furnishing the fiscalin B molecule used in the metabolism experiment.

References

[1] S.K. Spaans, R.A. Weusthuis, J. van der Oost, S.W.M. Kengen, NADPH-generating systems in bacteria and archaea, Front. Microbiol. 6 (2015) 1–27. https://doi.org/10.3389/fmicb.2015.00742.

[2] J. Foreman, V. Demidchik, J.H.F. Bothwell, P. Mylona, H. Miedema, M. Angel Torres, P. Linstead, S. Costa, C. Brownlee, J.D.G. Jones, J.M. Davies, L. Dolan, Reactive oxygen species produced by NADPH oxidase regulate plant cell growth, Nature. 422 (2003) 442–446. https://doi.org/10.1038/nature01485.

[3] J. Hou, N.F. Lages, M. Oldiges, G.N. Vemuri, Metabolic impact of redox cofactor perturbations in Saccharomyces cerevisiae, Metab. Eng. 11 (2009) 253–261. https://doi.org/10.1016/j.ymben.2009.05.001.

[4] T.S. Blacker, Z.F. Mann, J.E. Gale, M. Ziegler, A.J. Bain, G. Szabadkai, M.R. Duchen, Separating NADH and NADPH fluorescence in live cells and tissues using FLIM, Nature Communications. 5 (2014) 1–9. https://doi.org/10.1038/ncomms4936.

[5] H.K. Chenault, G.M. Whitesides, Regeneration of nicotinamide cofactors for use in organic synthesis, Appl. Biochem. Biotechnol. 14 (1987) 147–197. https://doi.org/10.1007/BF02798431.

[6] H. Zhao, W.A. Van Der Donk, Regeneration of cofactors for use in biocatalysis, Curr. Opin. Biotechnol. 14 (2003) 583–589. https://doi.org/10.1016/j.copbio.2003.09.007.

[7] R. Wichmann, D. Vasic-Racki, Cofactor regeneration at the lab scale, Adv. Biochem. Engineering/Biotechnology. 92 (2005) 225–260. https://doi.org/10.1007/b98911.

[8] V. Uppada, S. Bhaduri, S.B. Noronha, Cofactor regeneration - an important aspect of biocatalysis, Curr. Sci. (2014).

[9] N. Pollak, C. Dölle, M. Ziegler, The power to reduce: pyridine nucleotides – small molecules with a multitude of functions, Biochem. J. 402 (2007) 205–218. https://doi.org/10.1042/bj20061638.

[10] W. Ying, NAD^+/NADH and $NADP^+$/NADPH in Cellular Functions and Cell Death: Regulation and Biological Consequences, Antioxid. Redox Signaling. (2008). https://doi.org/10.1089/ars.2007.1672.

[11] D. Hofmann, A. Wirtz, B. Santiago-Schübel, U. Disko, M. Pohl, Structure elucidation of the thermal degradation products of the nucleotide cofactors NADH and NADPH by nano-ESI-FTICR-MS and HPLC-MS, Anal. Bioanal. Chem. 398 (2010) 2803–2811. https://doi.org/10.1007/s00216-010-4111-z.

[12] R.A. Sheldon, S. van Pelt, Enzyme immobilisation in biocatalysis: Why, what and how, Chem. Soc. Rev. 42 (2013) 6223–6235. https://doi.org/10.1039/c3cs60075k.

[13] J.M. Guisan, J.M. Bolivar, F. López-Gallego, J. Rocha-Martín., 2000. Correction to: Immobilization of Enzymes and Cells, Methods in Molecular Biology (Clifton, N.J.). 2100, C1–C1. https://doi.org/10.1007/978-1-0716-0215-7_33.

[14] I. Es, J.D. Vieira, A.C. Amaral, Principles, techniques, and applications of biocatalyst immobilization for industrial application, Appl. Microbiol. Biotechnol. 99 (2015) 2065–2082. https://doi.org/10.1007/s00253-015-6390-y.

[15] M. Bilal, Y. Zhao, T. Rasheed, H.M.N. Iqbal, Magnetic nanoparticles as versatile carriers for enzymes immobilization: A review, Int. J. Biol. Macromol. 120 (2018) 2530–2544. https://doi.org/10.1016/j.ijbiomac.2018.09.025.

[16] E. Gkantzou, M. Patila, H. Stamatis, Magnetic Microreactors with Immobilized Enzymes—From Assemblage to Contemporary Applications, Catalysts. 8, (2018) 282. https://doi.org/10.3390/CATAL8070282.

[17] P.K. Srivastava, S. Singh, Immobilization and applications of glucose-6-phosphate dehydrogenase: a review, Prep. Biochem. Biotechnol. 43 (2013) 376–384. https://doi.org/10.1080/10826068.2012.738274.

[18] S. Tanvir, J. Pantigny, P. Boulnois, S. Pulvin, Covalent immobilization of recombinant human cytochrome CYP2E1 and glucose-6-phosphate dehydrogenase in alumina membrane for drug screening applications, J. Membr. Sci. 329 (2009) 85–90. https://doi.org/10.1016/J.MEMSCI.2008.12.015.

[19] S. M. Wong, L. L. Musza, G. C. Kydd, R. Kullnig, A. M. Gillum, R. Cooper, Fiscalins: new substance P inhibitors produced by the fungus Neosartorya fischeri. Taxonomy, fermentation, structures, and biological properties, J. Antibiot. 46 (1993) 545–553. https://doi.org/10.7164/ANTIBIOTICS.46.545.

[20] S. Long, D. I. S. P. Resende, A. Kijjoa, A. M. S. Silva, A. Pina, T. Fernández-Marcelo, M. H. Vasconcelos, E. Sousa, M. M. M. Pinto, Antitumor Activity of Quinazolinone Alkaloids Inspired by Marine Natural Products, Mar. Drugs. 16 (2018). https://doi.org/10.3390/MD16080261.

[21] S. Long, D.I.S.P. Resende, A. Kijjoa, A.M.S. Silva, R. Fernandes, C.P.R. Xavier, M.H. Vasconcelos, E. Sousa, M.M.M. Pinto, Synthesis of New Proteomimetic Quinazolinone Alkaloids and Evaluation of Their Neuroprotective and Antitumor Effects, Molecules. 24 (2019). https://doi.org/10.3390/MOLECULES24030534.

[22] S. Long, I.L. Furlani, J.M. de Oliveira, D.I.S.P. Resende, A.M.S. Silva, L. Gales, J.A. Pereira, A. Kijjoa, Q.B. Cass, R. V. Oliveira, E. Sousa, M.M.M. Pinto, Determination of the Absolute Configuration of Bioactive Indole-Containing

Pyrazino[2,1-b]quinazoline-3,6-diones and Study of Their In Vitro Metabolic Profile, Molecules. 26 (2021) 5070. https://doi.org/10.3390/molecules26165070.

[23] K.R.A. Belaz, Q.B. Cass, R. V. Oliveira, Determination of albendazole metabolites by direct injection of bovine plasma and multidimensional achiral-chiral high performance liquid chromatography, Talanta. 76 (2008) 146–153. https://doi.org/10.1016/j.talanta.2008.02.013.

[24] M.E. Tiritan, Q.B. Cass, A. Del Alamo, S.A. Matlin, S.J. Grieb, Preparative enantioseparation on polysaccharide phase using microporous silica as a support, Chirality. 10 (1998) 573–577. https://doi.org/10.1002/(SICI)1520-636X(1998)10:7<573::AID-CHIR4>3.0.CO;2-3.

[25] K. Lourenço Vanzolini, Z. Jiang, X. Zhang, L.C. Curcino Vieira, A. Gonçalvez Corrêa, C. Lucia Cardoso, Q. Bezerra Cass, R. Moaddel, Acetylcholinesterase immobilized capillary reactors coupled to protein coated magnetic beads: A new tool for plant extract ligand screening, Talanta. 116 (2013) 647–652. https://doi.org/10.1016/j.talanta.2013.07.046.

[26] B. Buszewski, S. Noga, Hydrophilic interaction liquid chromatography (HILIC)-a powerful separation technique, Anal. Bioanal. Chem. 402 (2012) 231–247. https://doi.org/10.1007/s00216-011-5308-5.

[27] XSelect HSS T3 XP Column, 100Å, 2.5 µm, 2.1 mm X 100 mm, 1/pk - 186006151 : Waters, (n.d.).

https://www.waters.com/nextgen/xg/en/shop/columns/186006151-xselect-hss-t3-xp-column-100a-25--m-21-mm-x-100-mm-1-pk.html (accessed June 8, 2020).

[28] K. Ortmayr, J. Nocon, B. Gasser, D. Mattanovich, S. Hann, G. Koellensperger, Sample preparation workflow for the liquid chromatography tandem mass spectrometry based analysis of nicotinamide adenine dinucleotide phosphate cofactors in yeast, J. Sep. Sci. 37 (2014) 2185–2191. https://doi.org/10.1002/jssc.201400290.

[29] U.S. Pharmacopeial Convention, (n.d.). https://apps.usp.org/app/USPNF/columnsDB.html (accessed June 8, 2020).

[30] K.L. Vanzolini, S. Ainsworth, B. Bruyneel, V. Herzig, M.G.L.L. Seraus, G.W. Somsen, N.R. Casewell, Q.B. Cass, J. Kool, Rapid ligand fishing for identification of acetylcholinesterase-binding peptides in snake venom reveals new properties of dendrotoxins, Toxicon. 152 (2018) 1–8. https://doi.org/10.1016/j.toxicon.2018.06.080.

[31] J.M. De Lima, I.L. Furlani, L.R.G. Da Silva, A.L. Valverde, Q.B. Cass, Micro- And nano-sized amine-terminated magnetic beads in a ligand fishing assay, Anal. Methods. 12 (2020) 4116–4122. https://doi.org/10.1039/d0ay01269f.

[32] S. Singh, A. Anand, P.K. Srivastava, Regulation and properties of glucose-6-phosphate dehydrogenase: A review, Int. J. Plant Physiol. Biochem. 4 (2012) 1–19. https://doi.org/10.5897/IJPPB11.045.

[33] R.Allen. Copeland., 2000. Enzymes : a practical introduction to structure, mechanism, and data analysis, Wiley.

[34] S. A. Adediran, Sigmoid kinetics of human erythrocyte glucose-6-phosphate dehydrogenase, Arch. Biochem. Biophys. 262 (1988) 354–359. https://doi.org/10.1016/0003-9861(88)90198-1.

[35] M.I. Kanji, M.L. Toews, W.R. Carper, A kinetic study of glucose-6-phosphate dehydrogenase, J. Biol. Chem. 8 (1976) 2258-2262. https://doi.org/10.1016/S0021-9258(17)33581-0.

Supplementary Material

Journal of Pharmaceutical and Biomedical Analysis

Glucose-6-phosphate dehydrogenase immobilized onto magnetic beads (G6PDH-Mb) as a generator system for production of NADPH: Development and application in metabolism studies

Izadora Liranço Furlani[1], Regina Vincenzi Oliveira[1] and Quezia Bezerra Cass[1*]

[a]*SEPARARE* – Núcleo de Pesquisa em Cromatografia, Departamento de Química, Universidade Federal de São Carlos, Rodovia Washington Luiz, km 235, 13565-905

Table S1. Chromatography conditions tested to the separation of $NADP^+$ and NADPH.

Column	Mobile phase	Flow rate (mL/min)	%B (v/v)	Elution Mode
Phenomenex® Phenyl-Hexyl (50 x 2.1 mm; 5.0 µm)	Methanol:ammonium acetate 10 mmol L^{-1} pH 8.0 Methanol:ammonium acetate 10 mmol L^{-1} pH 6.0	0.5	1 %	Reverse
SeQuant® Zic-HILIC (150 x 2.1 mm; 5 µm)	ACN:ammonium acetate 10 mmol L^{-1} pH 8.0	0.2	70 and 75 %	HILIC
XSelect® HSS T3 (100 x 2.1 mm; 3.5 µm)	Methanol:ammonium acetate 10 mmol L^{-1} pH 8.0 Methanol:ammonium acetate 10 mmol L^{-1} pH 6.0	0.2	1 and 3 %	Reverse
C8 (100 x 4.6 mm; 10 µm)*	Methanol:ammonium acetate 10 mmol L^{-1} pH 8.0	0.8	1 %	Reverse

	Methanol:ammonium acetate 10 mmol L^{-1} pH 6.0			

* Column packed in-house by the ascending slurry method using octyl silica (Luna®, 10 µm particle size, 120 A pore size) and methanol for slurry preparation (50 mL) and for packing.

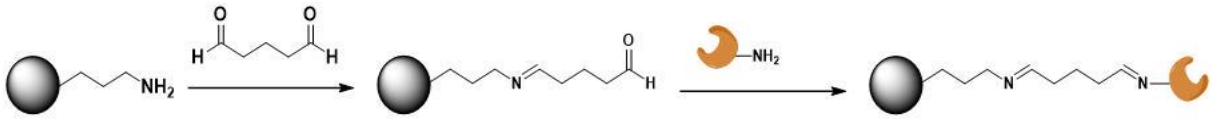

Fig. S1. Immobilization reaction of G6PDH onto magnetic beads.

Table S2. Incubation condition for kinetic characterization of G6PDH-Mb.

Solutions	**Concentrations**	**Volume added (µL)**
NADP+ solutions	5 to 2160 µmol L^{-1}	40
G6P	200 mmol L^{-1}	20
Ammonium acetate pH 7.4	10 mmol L^{-1}	140

* Final volume of 200 µL.

Table S3. Incubation condition for the G6PDH-Mb to *in situ* NADPH production and application in drug metabolism experiments.

Solutions	**Concentrations**	**Volume added (µL)**
First solution: NADPH production by the G6PDH-Mb		
$NADP^+$	2 mmol L^{-1}	65
G6P	200 mmol L^{-1}	20
Ammonium acetate pH 7.4	10 mmol L^{-1}	115
Second solution: in vitro metabolism		
Albendazole	200 µmol L^{-1}	10
Microsomal fraction	10 mg mL^{-1}	10
Ammonium acetate pH 7.4	10 mmol L^{-1}	80

*Final volume 300 µL.

Table S4. Experimental conditions for metabolism experiments using commercial NADPH (Sigma-Aldrich®).

Solutions	Concentrations	Volume added (µL)
NADPH	400 µmol L^{-1}	200
Microsomal fraction	10 mg mL^{-1}	10
Albendazole	200 µmol L^{-1}	10
Ammonium acetate pH 7.4	10 mmol L^{-1}	80

*Final volume 300 µL.

2.2. Research Article II

Immobilization of cytochrome P450 enzymes onto magnetic beads: An approach to drug metabolism and biocatalysis

Talanta Open 7 (2023) 100181

Izadora Liranço Furlani • Regina Vincenzi Oliveira • Quezia Bezerra Cass

Immobilization of cytochrome P450 enzymes onto magnetic beads: an approach to drug metabolism and biocatalysis

Izadora Liranço Furlani[1], Regina Vincenzi Oliveira[1] and Quezia Bezerra Cass[1*]

[1]SEPARARE – Chromatography Research Center, Department of Chemistry, Federal University of São Carlos, São Carlos, Brazil

Abstract

Cytochrome P450 (CYP, P450) presents a wide range of applicability in drug metabolism studies and in biocatalysis as a great alternative to synthesizing compounds. Nonetheless, their lack of stability is one of their major drawbacks. Aiming the possibility of enhancing the catalytic activity and promoting higher stability, liver microsomal fractions have been immobilized on magnetic beads (Mb). The immobilized procedure was modulated by using rat liver microsomal fractions (RLM-Mb). The optimal condition achieved was further employed for the immobilization of the human microsomal fractions on magnetic beads (HLM-Mb). *In vitro* metabolism assays were conducted using albendazole (ABZ) as a model drug, and the formation of albendazole sulfoxide (ABZSO) was monitored. Biotransformation reactions applying the produced HLM-Mb were examined for the best temperature to increase the production of metabolites and their reuse cycles. A kinetic study was carried out for HLM-Mbs monitoring the production of ABZO by the oxidation reaction of ABZ by CYP3A4. The K_M value was 25.6 μmol L^{-1} and V_{max} was 121.0 μmol L^{-1}. Inhibition assays were conducted in the presence of ketoconazole and the production of ABZSO decreased by 46.8 ± 2.5 %. Enzymatic activities for CYP2C9 and CYP2D6 on HLM-Mbs were evaluated by monitoring the hydroxylation reactions of diclofenac and bufuralol as substrates. The immobilization of CYP P450 on magnetic beads increased not only the production of ABZSO metabolites but also the stability of CYP. The use of HLM-Mbs jointly with immobilized glucose-6-phosphate dehydrogenase (G6PDH-Mbs) as a unique generator system for the production of NADPH has

established the one-pot conditions for biocatalysis in a greener approach with reuse of the joint biocatalyst (G6PDH-HLM-Mbs). To this end, the herein reported HLM-Mbs and G6PDH-HLM-Mbs are excellent analytical tools to be explored either in biocatalysis reactions or in *in vitro* metabolism studies.

Keywords

CYP450 immobilization, drug metabolism, biocatalysts, phenotyping, in-vitro assay.

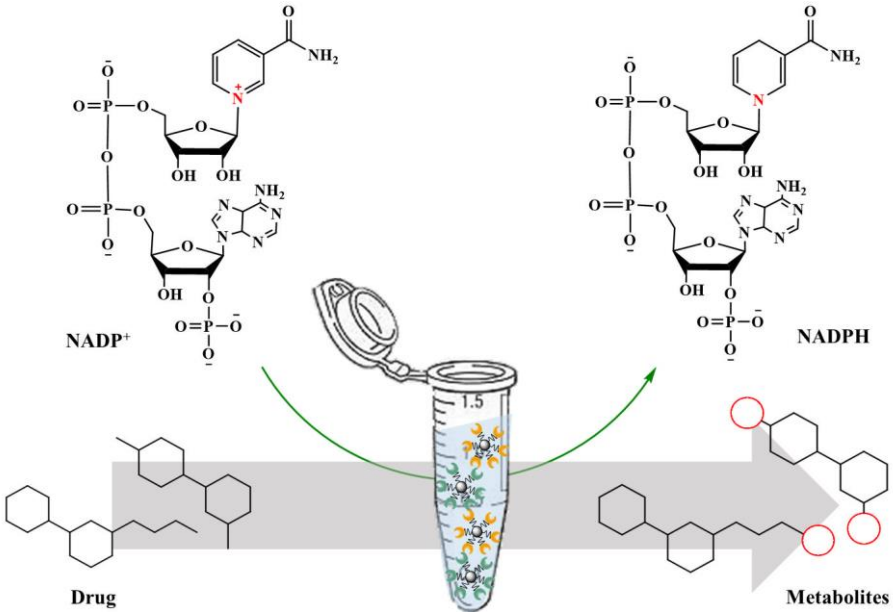

Graphical Abstract.

Dual biocatalyst by the junction of glucose-6-phosphate dehydrogenase immobilized onto magnetic beads and human microsomal fractions immobilized onto magnetic beads to promote a unique bioreactor for the production of NADPH and simultaneous drug metabolism studies.

1. Introduction

Cytochrome P450s (CYP, P450) are a large superfamily of heme proteins that play an essential role in the biosynthesis of natural products, the biosynthesis of steroids, and in the metabolism of a wide range of exogenous and endogenous molecules [15,17]. CYP isoforms are bound to membranes of the endoplasmic reticulum or inner mitochondrial membranes and are associated with their reducing counterparts, the cytochrome (b5) and the cytochrome P450-reductase. Most of the reactions catalyzed by CYPs are known as hydroxylation or monooxygenation due to their ability to mediate the transfer of one atom of molecular oxygen (O_2) into the substrate and reduce the other atom into the water, as shown in Equation 1, where R is a carbon substrate, RO is an oxidized product, nicotinamide adenine dinucleotide phosphate (NAD(P)H) is the reduced form of $NAD(P)^+$ [15,17,100]:

$$NAD(P)H + H^+ + O_2 + \mathbf{RH} \rightarrow NAD(P)^+ + H_2O + \mathbf{ROH} \qquad \textbf{Eq. 1}$$

It is estimated that human CYPs enzymes are responsible for 75-80 percent of all phase-I drug metabolism. Among them, five enzymes, 1A2, 2C9, 2C19, 2D6, and 3A4, account for approximately 80 percent of all CYP-mediated drug biotransformation reactions. During the early stages of drug discovery and development, it is crucial to establish a drug profile regarding safety, efficacy, and toxicity [16,17]. To understand the pharmacokinetics (PK) parameters and to select a drug-like compound that will progress into development, a high number of samples are generated from *in vitro* biotransformation for the assessment of a drug candidate using CYPs.

In biotechnological applications, the regio- and stereoselectivity of the P450 enzymes attracts extensive efforts to the engineering of P450 systems to overcome the intrinsic limitations of the native enzymes [86]. For example, the lack of stability of the enzymes, low catalytic activity, the narrow substrate scope of some P450s,

limited solvent tolerance, dependence on NADPH and O_2, high cost of cofactors (NADPH), and the difficulties to recover the enzymes to allow its reuse, and also the recovery of the metabolism products [17,85,101].

Classical *in vitro* experiments involving drug metabolizing enzymes from the CYPs P450 are usually carried out in solution by incubating the CYPs with specific substrates in the presence of NADPH as a cofactor or by the use of glucose-6-phosphate dehydrogenase (G6PDH) as a generator system for production of NADPH [32]. Despite being well-established procedures, numerous experiments are needed to obtain a metabolic profile of a new drug or to produce a high amount of analytical standard metabolites for analytical application [17]. Therefore, research and industry could benefit from new analytical strategies to overcome the above-mentioned issues with the CYP enzymes, enhancing the efficiency of conventional *in vitro* metabolism assays.

The immobilization of biomolecules onto solid supports is properly settled and widely used for several applications [75,95]. The immobilization of CYP enzymes is also reported and some references focused on the development of biosensors or bioreactors to evaluate drug metabolism and/or biocatalysis by promoting the enhancement of the enzymatic stability, as well as a suitable alternative for enzyme's reuse [94,102]. Lu et al. [103] used AuNP/chitosan/reduced graphene oxide nanocomposite sheets (Au/CS/RGO) to immobilize CYP3A4 and CYP1A2, promoting an electrochemically drive to two consecutive oxidation reactions. Wu et. al. [104] designed a CYP450-$Co_3(PO_4)_2$ hybrid nano-flowers for the oxidative coupling of benzylamine, where the CYP2C9 and $Co_3(PO_4)_2$ were coprecipitated. The application of organ tissue by engineered organoids and microphysiological systems using human liver CYPs is also described by Beckwitt et. al. [105].

For the immobilization of enzymes, magnetic beads have been highlighted because of their wide chemistry versatility, high surface area, easy separation of the beads from the reaction medium by simply using a magnet, and their excellent biocompatibility [17,95]. Nerimetla, R. et. al. [106] reported the immobilization of

human liver microsomes onto magnetic beads by adsorption for metabolite production and drug biosensing. The authors evaluated the biocatalysts of diclofenac and observed a 3-fold increase in metabolite product yield with a half-life of 11 hours.

Although different methods and supports for immobilization are described in the literature, experimental steps need to be optimized according to the targeted biomolecule and the study purpose. Herein we reported the immobilization of rat liver microsomal fractions as a low-cost alternative to modulate and optimize the experimental conditions for the immobilization of CYPs onto magnetic beads (RLM-Mbs). The immobilization parameters evaluated considered the bead's size, the concentration of glutaraldehyde, the concentration of protein, and reaction time. The optimum results obtained for RLM-Mbs were successfully applied in the immobilization of human liver microsomal fractions (HLM-Mbs). Activity assays, stationary kinetic, and inhibition studies were carried out using the produced HLM-Mbs and its applicability was demonstrated by performing *in vitro* drug metabolism of albendazole (ABZ), diclofenac (DCF), and bufuralol (BFL).

To take advantage of the *in situ* production of NADPH for metabolism catalysis by CYPs, the generator system based on glucose-6-phosphate dehydrogenase immobilized onto magnetic beads (G6PDH-Mb) [32] was jointly used with the generator HLM-Mbs, herein referred as G6PDH-HLM-Mbs. The biocatalysis of albendazole into albendazole sulfoxide (ABZSO), which is mediated by CYP3A4, was chosen to monitor the catalytic activity of the G6PDH-HLM-Mbs generator in three cycles. These results are herein fully discussed.

2. Methods and Materials

2.1. Chemicals and materials

Amine-terminated silane-coated magnetic beads (50 mg mL^{-1}, 1µm diameter), nicotinamide adenine dinucleotide 2'-phosphate reduced tetrasodium salt hydrate

(NADPH), nicotinamide adenine dinucleotide phosphate hydrate ($NADP^+$), glucose-6-phosphate (G6P), Glucose-6-phosphate dehydrogenase – 500 U (from baker's yeast (*S. cerevisiae* – E.C: 1.1.1.49)), potassium phosphate, ammonium acetate, glutaraldehyde, formic acid, hydrochloric acid (HCl), tris(hydroxymethyl)aminomethane (Tris), and albendazole (ABZ) were all purchased from Sigma-Aldrich (St. Louis, MO, USA). Methanol was HPLC grade from Merck (Darmstadt, HE, Germany), and ultrapure water from a Millipore Milli-Q system from Merck (Darmstadt, HE, Germany) was used for all experiments. Wistar rat livers were generously provided by Prof. Dr. Wladimir Rafael Beck, Department of Physiological Sciences, Federal University of São Carlos. Human liver microsomes from 50 different individual donors were purchased from Thermo Fischer Scientific™ (catalog number HMMCPL) (São Paulo, SP, Brazil). Albendazole sulfoxide (ABZ-SO) was generously supplied by Ouro Fino Saúde Animal (Ribeirão Preto, SP, Brazil). Albendazole sulfone ($ABZ\text{-}SO_2$) and albendazole-2-amine-sulfone ($ABZ\text{-}SO_2\text{-}NH_2$) were synthesized in our laboratory, in accordance with Belaz et. al. [107]. Captura™ N (25–106 mm diameter) magnetic iron oxide beads coated with silica and functionalized with primary amine groups on the particle surface were generously provided by Kopp Technologies (São Carlos, SP, Brazil). Diclofenac (DCF) and bufuralol (BFL) were kindly provided by Prof. Dr. Anderson Rodrigo Moraes de Oliveira, Faculdade de Filosofia, Ciências e Letras de Ribeirão Preto, University of São Paulo (Ribeirão Preto, SP, Brazil).

2.2. LC-MS/MS method for monitoring of the *in vitro* metabolism

The LC-MS/MS analysis of the *in vitro* drug metabolism of albendazole (ABZ) was conducted using a Phenomenex® Phenyl-Hexyl column (50 x 2.1 mm; 5.0 µm), using methanol:water containing 0.1% of formic acid (35:65 v/v) as the mobile phase; column temperature of 35 °C, and flow rate of 0.2 mL min^{-1}. The injection volume was 10 µL. The LC-MS/MS analysis was performed using an

Acquity Binary pump (Waters, Milford, USA), an autosampler model 2777C (Waters), coupled with a XEVO TQ-MS (Waters Corporation, Milford, MA, USA) equipped with an electrospray ionization (ESI) source operating in the positive mode. Data acquisition and processing were performed by using MassLynx 4.1 and TargetLynx software (Waters Corporation, Milford, MA, USA), respectively. The mass spectrometry conditions were capillary voltage of 2.40 kV, cone voltage of 29 V, source temperature at 150 °C, desolvation gas temperature at 350 °C, and desolvation gas flow at 490 L h^{-1}. Data acquisition was performed in selected reaction monitoring (SRM). For each albendazole's metabolite, two SRM transitions were optimized as quantifiers. Precursor to product ions transitions and collision energies are listed in Table S1.

The metabolism reactions with diclofenac (DCF) and bufuralol (BFL) were monitored by a liquid chromatography-ion trap mass spectrometer (LC-IT-MS) composed of a Shimadzu LC system (Kyoto, Japan) equipped with two LC-20AD pumps, a SIL-20A autosampler, a DGU-20A5 degasser and a CBM-20A interface coupled to a 3D Ion Trap (3D IT) mass spectrometer Esquire 6000 (Bruker Daltonics, Bremen, Germany). For the MS analysis, an electrospray ionization (ESI) interface was selected and used in the positive ion mode. The 3D IT was operated under the following conditions: nebulizer gas at 30 psi, dry gas flow 7.0 L min^{-1}, dry gas temperature at 300 °C, capillary potential at 4500 V, and skimmer potential at 40 V. The flow rate was reduced to 95 µL min^{-1} using a flow rate splitter. For data acquisition, the 3D IT was operated in the full MS scan mode using an accumulation time of 50 ms, a target of 30,000, and an acquisition range from *m/z* 100 to 600 in conjugation with data-dependent MS/MS acquisitions in the most intense ions selected from the MS-scan spectrum. Data acquisition and processing were performed using the Data Analysis software (Bruker Daltonics, Bremen, Germany). The chromatography separation was performed on a Phenomenex® Phenyl-Hexyl column (50 x 2.1 mm; 5.0 µm) fitted with a phenyl-hexyl guard column (4.0 x 3.0 mm; 5 µm, Phenomenex®) at 35 °C. The mobile

phase was water (A) and methanol (B), both with 0.1 % of formic acid. A linear gradient was performed initializing at 0 min with 30 % B, reaching 90 % B in 6 min, which was kept for 1 min and returned to the initial condition at 7.01 min until 9 min.

2.3. LC-MS/MS method validation for analysis of ABZSO

The linearity of the method was evaluated by constructing an analytical calibration curve with external standards for the quantification of ABZSO. A stock solution of ABZSO (3.5 mmol L^{-1}) was prepared in methanol. Seven working standard solutions were prepared in ammonium acetate (10 mmol L^{-1}) at 1000, 800, 600, 400, 100, 50, and 10 nmol L^{-1}. Three quality controls working solutions were prepared at 900, 500, and 30 nmol L^{-1}. Calibration standards and quality controls (QCs) samples were prepared by aliquoting 20 µL of the appropriate working solution into 180 µL of ammonium acetate (10 mmol L^{-1}, pH 7.4). The samples were mixed for 30 seconds by a vortex. Aliquots of 200 µL were transferred to vials and a volume of 5 µL was injected into the LC-MS/MS system. The final concentrations of the calibration standards were 1, 5, 10, 40, 60, 80, and 100 nmol L^{-1} and the final concentrations of the QC samples were 3, 50, and 90 nmol L^{-1}.

The intra- and inter-batch precision and accuracy of the LC-MS/MS method for quantification of ABZSO were determined by analyzing five replicates of each QC sample (3, 50, and 90 nmol L^{-1}). The precision results were expressed as the coefficient of variation (CV %) of the responses obtained for each level of concentration evaluated and the accuracy of the method was evaluated as the percentage recovery of ABZSO when comparing the calculated and the nominal concentrations. The selectivity of the method was evaluated by blank samples, where no interferent ion of the same ratio *m/z* was observed.

The limit of detection (LOD) was calculated as the minimum detectable amount of compound, with a signal-to-noise (S/N) ratio of ≥three. The LOQ was

determined as the lowest calibration level of the standard calibration curve that could be determined with acceptable precision and accuracy (≤ 20 %).

The method was applied to analyze the production of ABZSO through *in vitro* metabolism. During data acquisition, the calibration curve and quality control samples were analyzed before and after the analysis of the biotransformation samples.

2.4. Preparation of the rat liver microsomes (RLM)

Rat liver microsomes (RLM) were prepared by differential high-speed centrifugation; using Wistar liver rats according to Belaz and Oliveira [108]. The animal experiment was approved by the Ethics Committee on Animal Use of the Federal University of São Carlos (protocol 2417070519). Protein concentrations were determined by the Bradford method [109]. All microsomal preparations were stored at -80 °C until analysis.

2.5. Immobilization of CYP450 enzymes from rat liver microsomes onto magnetic beads (RLM-Mbs)

Rat liver microsomal fractions were covalently linked on the surface of magnetic beads, following a previously reported protocol [99], with minor changes. For the Sigma® (1 µm diameter) – Mb1, 25 mg of magnetic beads were washed three times with 1.0 mL of phosphate buffer (100 mmol L^{-1}, pH 7.0) using a magnetic separator. The supernatant was discarded, and the magnetic beads were suspended in 1.0 mL of phosphate buffer (100 mmol L^{-1}, pH 7.0) containing 1 % of glutaraldehyde and then shaken at room temperature for 3 hours. The beads were placed in a magnetic field (2 min), and the supernatant was collected and discarded. The magnetic beads were washed three times with 1.0 mL of phosphate buffer (100 mmol L^{-1}, pH 7.0) followed by the addition of 200 µL of RLM solution (1 mg mL^{-1}) prepared in phosphate buffer (100 mmol L^{-1}, pH 7.0). The resulting reaction was allowed to proceed for 16 hours at 4.0 °C under gentle

rotation using a Rotary laboratory mixer Revolver™ (Labnet International – New Jersey, USA). The supernatant was collected, and the beads were washed three times with 1.0 mL of Tris-HCL buffer (10 mmol L^{-1}, pH 7.5). The magnetic beads were divided into five aliquots of 5 mg each.

For Captura™ N (25–106 µm diameter) – Mb2, it was weighed 5 mg of magnetic beads, and the same procedure described above was followed. All immobilized biocatalysts produced were stored in Tris-HCl buffer (10 mmol L^{-1}, pH 8.0) at 4 °C.

The immobilized rat liver microsomes in Sigma® (Mb1) and Captura™ N (Mb2) were denoted as RLM-Mb1 and RLM-Mb2, respectively. To evaluate nonspecific interactions, RLM-Mbs1-controls were also prepared. To that end, 5 mg of each immobilized biocatalyst was heated in a water bath at 80 °C for 30 min.

2.6. Activity assays of RLM-Mbs

RLM-Mbs were washed with 200 µL of ammonium acetate (10 mmol L^{-1}, pH 7.4) and the system was manually agitated and placed in contact with a magnetic separator (model WM206, Wang Yuan Biotech, China) for 2 minutes. The supernatant was discarded, and the procedure was repeated two more times. A stock solution of ABZ at 3.77 mmol L^{-1} (1mg mL^{-1}) was prepared in methanol and diluted to 200 µmol L^{-1} in ammonium acetate (10 mmol L^{-1}, pH 7.4). A solution of NADPH (10 mmol L^{-1}) was prepared in ammonium acetate (10 mmol L^{-1}, pH 7.4). Then 160 µL of ammonium acetate (10 mmol L^{-1}, pH 7.4), and 20 µL of ABZ (200 mmol L^{-1}) were added to the RLM-Mb. The immobilized biocatalyst was incubated in a shaking water bath at 37 °C for 5 minutes. The metabolism reaction was initialized by the addition of 20 µL of NADPH (10 mmol L^{-1}). The reaction was incubated in a water bath at 36 °C for 30 minutes. The system was placed in contact with a magnetic separator (2 min) and the supernatant was collected and analyzed by the LC-MS/MS method.

2.7. Doehlert design for CYP450 enzymes from rat liver microsomes immobilized onto magnetic beads

The optimization of the immobilization of CYP450 enzymes from rat liver onto magnetic beads was performed using a Doehlert design of experiment (DoE). The variables investigated were concentration of glutaraldehyde (1, 2, 3, 4 and 5 %), protein concentration (0.032, 0.188, 0.344, 0.5, 0.6, 0.8, and 0.97 mg mL^{-1}) and immobilization time (2, 5 and 8 hours). For statistical purposes, the experimental variables (X_i) were codified as χi according to the mathematical transformation described in equation 1. Where the term χi refers to the coded value for the level of factor i; X_i is its real experimental value; ΔX_i is the difference between the experimental value at the upper and lower level and α_i is the higher limit for the coded value for the variable in question. The codified and real values are depicted in Table S1.

$$\chi i = \left({X_i - X_{0i}}/{\Delta X_i}\right) * \alpha_i \qquad \textbf{Eq. 1}$$

A total of 15 experiments were performed including three replicates at the central point to evaluate the experimental error. All data processing was performed using the software Octave (version 4.2.1).

The optimal conditions were chosen considering *in vitro* metabolism experiments by monitoring the biotransformation of ABZ into ABZSO following the procedure described in the 2.6 section. The criteria adopted were to obtain the highest production of ABZSO.

2.8. Immobilization of human microsomes onto the magnetic beads (HLM-Mbs)

Human liver microsomes from 50 donors (ThermoFisher Scientific®, catalog number HMMCPL) were covalently linked on the surface of the magnetic beads, following the procedure described in section 2.5 with minor changes. Briefly, 1

mg of magnetic beads from Sigma® (Mb1) were washed three times with 200 µL of phosphate buffer (100 mmol L^{-1}, pH 7.0) using a magnetic separator. The supernatant was discarded, and the magnetic beads were suspended in 200 µL of phosphate buffer (100 mmol L^{-1}, pH 7.0) containing 1 % of glutaraldehyde and then shaken for 3 hours at room temperature. After magnetic separation, the magnetic beads were washed three more times with 200 µL of phosphate buffer (100 mmol L^{-1}, pH 7.0), followed by the addition of 200 µL of human microsomes solution (1 mg mL^{-1}) prepared in phosphate buffer (100 mmol L^{-1}, pH 7.0). The reaction was kept for 2 hours at 4.0 ºC under gentle rotation using a Rotary laboratory mixer Revolver™ (Labnet International – New Jersey, USA). After that, the supernatant was collected, and the beads were washed three times with 200 µL of Tris-HCl buffer (10 mmol L^{-1}, pH 8.0). Human liver microsomes immobilized onto magnetic beads were denominated as HLM-Mb1 (1mg beads/1mg mL^{-1} HLM). HLM-Mb1-controls were prepared by heating the immobilized biocatalyst at 80 °C for 30 min in a water bath.

2.9. Activity assay of the HLM-Mbs in different temperatures

Three batches of the HLM-Mbs (n = 3) were prepared according to section 2.8 and used for *in vitro* drug metabolism. The HLM-Mbs produced were evaluated for activity and their reuse tested in eight cycles at different temperatures of 16, 23, and 36 °C. At the end of each cycle, HLM-Mbs were washed with 200 µL of ammonium acetate (10 mmol L^{-1}, pH 7.4) and the system was manually agitated and then placed in a magnet separator for 2 minutes. The supernatant was discarded, and the procedure was repeated two more times. For the activity assay, a stock solution of ABZ at 3.77 mmol L^{-1} (1 mg mL^{-1}) was prepared in methanol and diluted to 200 µmol L^{-1} in ammonium acetate (10 mmol L^{-1}, pH 7.4). A stock solution of NADPH (10 mmol L^{-1}) was prepared in the same buffer. Then, 160 µL of ammonium acetate (10 mmol L^{-1}, pH 7.4) was added to HLM-Mbs (1mg beads/1mg mL^{-1} HLM) followed by the addition of 20 µL of ABZ (200 µmol L^{-}

[1]). The resulting mixture was incubated in a shaking water bath at 37 °C for 5 minutes. The metabolism reaction was initialized by the addition of 20 µL of NADPH (10 mmol L^{-1}). The mixture (HLM-Mbs + ABZ + NADPH) was gently agitated using a Rotary laboratory mixer Revolver™ (Labnet International – New Jersey, USA) for 30 minutes at each temperature evaluated. Then, the obtained immobilized biocatalysts were placed on the magnetic separator (model WM206, Wang Yuan Biotech, China) for 2 min, and the supernatant was collected and analyzed by LC-MS/MS using the procedure described in section 2.2.

2.10. Kinetic characterization of the HLM-Mbs

The kinetic characterization of the HLM-Mbs (1mg beads/1mg mL^{-1} HLM) was carried out in triplicate. ABZ concentrations ranged from 1 to 160 µmol L^{-1}, while NADPH solution was kept at a fixed concentration of 1 mmol L^{-1}. Both ABZ and NADPH solutions were prepared in ammonium acetate (10 mmol L^{-1}, pH 7.4). ABZ (20 µL) and NADPH (20 µL) solutions were added to the HLM-Mbs, followed by the addition of 160 µL solution of ammonium acetate (10 mmol L^{-1}, pH 7.4). The reaction was carried out for 30 min at 23 °C prior magnet separation (model WM206, Wang Yuan Biotech, China) for 2 min of the HLM-Mbs. Aliquots of 150 µL of the supernatant were collected and transferred to autosampler vials. A volume of 5 µL was injected into the LC-MS/MS system. The HLM-Mbs were used for 8 consecutive times. For that, at the end of each kinetic reaction, the HLM-Mbs were washed 3 times with ammonium acetate (10 mmol L^{-1}, pH 7.4). The concentration of ABZSO, related to the biotransformation of the ABZ, was plotted according to the Michaelis-Menten equation (Equation 2), where the term *y* is the velocity of reaction; V_{max} is the maximum rate achieved by the system; [S] is the concentration of a substrate S, and K_m is the Michaelis-Menten constant. The K_m value and V_{max} were estimated using the GraphPad Prism® software (version 5.0) by nonlinear regression analysis.

Eq. 2

$$y = \frac{V\max * [S]}{K\mathrm{m} + [S]}$$

2.11. CYP3A4 inhibition assays using the HLM-Mbs

Six batches of HLM-Mbs (n = 6) were prepared according to section 2.8 from which two batches were evaluated for each concentration of ketoconazole. A stock solution of ketoconazole at 1.88 mmol L^{-1} (1 mg mL^{-1}) was prepared in methanol and diluted to 128.1, 256.6, and 384.3 µmol L^{-1} in ammonium acetate (10 mmol L^{-1}, pH 7.4). A stock solution of ABZ (3.77 mmol L^{-1}, 1 mg mL^{-1}) was prepared in methanol and diluted to 200 µmol L^{-1} in ammonium acetate (10 mmol L^{-1}, pH 7.4), NADPH 10 mmol L^{-1} was prepared in the same buffer. For the ketoconazole inhibition assay, the activity of the HLM-Mbs (1mg beads/1mg mL^{-1} HLM) batches (n = 2) towards ABZ (20 µL of 256.2 µmol L^{-1}) was measured first in the absence (see section 2.9) and then in the presence of ketoconazole as follows: 140 µL of ammonium acetate (10 mmol L^{-1}, pH 7.4) were added to the HLM-Mbs (1mg beads/1mg mL^{-1} HLM), following by addition of 20 µL of ABZ 256.2 µmol L^{-1}, and 20 µL of ketoconazole solutions (128.1, 256.6, and 384.3 µmol L^{-1}, respectively). The HLM-Mbs (n = 2x3) were incubated in a shaking water bath at 37 °C for 5 minutes, followed by the addition of 20 µL of NADPH 10 mmol L^{-1}. The reaction mixtures were gently agitated using a Rotary laboratory mixer Revolver™ (Labnet International – New Jersey, USA) for 30 minutes at 23 °C. Then, the reactions were placed on a magnetic separator (model: WM206, Wang Yuan Biotech, China) for 2 min and the supernatants were collected and analyzed by the LC-MS/MS method, described in section 2.2. Washing procedure with ammonium acetated (10 mmol L^{-1}, pH 7.4) were carried out after each assay as described in section 2.9.

2.12. Enzyme activity-specific assays for CYP2C9 and CYP2D6 on HLM-Mbs

Enzyme activity assays were carried out for CYP2C9- and CYP2D6-specific activity-based on the hydroxylation reactions of diclofenac (DCF) and bufuralol (BFL), as probe drugs. Briefly, 3.37 mmol L^{-1} of DCF (1 mg mL^{-1}) and 3.82 mmol L^{-1} of BFL (1 mg mL^{-1}) were prepared separately in acetonitrile and diluted to 300 µmol L^{-1} in ammonium acetate (10 mmol L^{-1}, pH 7.4). *In vitro* metabolism experiments were conducted in duplicate as described in section 2.9.

2.13. Dual G6PDH-Mbs and HLM-Mbs (G6PDH-HLM-Mbs)

The immobilization of G6PDH on magnetic beads (G6PDH-Mbs), and the immobilized biocatalyst characterization were previously reported by Furlani et. al. [32]. The immobilization of the human liver microsomes on magnetic beads is described in section 2.8. Both systems were prepared, and enzymatic activity tests were carried out individually (n = 3) to verify the production of NADPH by the G6PDH-Mbs and the production of ABZSO by the HLM-Mbs (section 2.9), respectively. For the biocatalysts reuse, both immobilized G6PDH-Mbs and HLM-Mbs were washed with 200 µL of ammonium acetate (10 mmol L^{-1}, pH 7.4), as previously described in section 2.9.

After the washing procedure, it was added 200 µL of ammonium acetate (10 mmol L^{-1}, pH 7.4) in the HLM-Mbs (1mg beads/1mg mL^{-1} HLM). The immobilized biocatalyst was manually agitated and transferred to the same reactional vessel containing the G6PDH-Mbs (0.4 U/5 mg beads), originating the jointly G6PDH-HLM-Mbs. The experimental conditions for the metabolism reaction of ABZ using the G6PDH-HLM-Mbs were based on to the *in situ* production of NADPH and the *in vitro* metabolism of ABZ [32]. Briefly, stock solutions of G6P (200 mmol L^{-1}) and $NADP^+$ (2 mmol L^{-1}) were prepared in ammonium acetate (10 mmol L^{-1}, pH 7.4). Then, in the joint immobilized biocatalyst (G6PDH-HLM-Mbs) were

added 20 µL of G6P 200 mmol L^{-1}, 65 µL of $NADP^+$ 2 mmol L^{-1}, and 20 µL of ABZ 200 µmol L^{-1}, followed by the addition of 95 µL of ammonium acetate (10 mmol L^{-1}, pH 7.4). The G6PDH-HLM-Mbs was agitated under gentle rotation using a Rotary laboratory mixer Revolver™ (Labnet International – New Jersey, USA) at 23 °C for 30 minutes. Then, the G6PDH-HLM-Mbs was placed in a magnetic separator (model: WM206, Wang Yuan Biotech, China) for 2 min, and the supernatant was collected and analyzed by LC-MS/MS as described in section 2.2. Activity assays for the G6PDH-HLM-Mbs were repeated three times consecutively.

3. Results and discussions

3.1. Immobilization of CYP enzymes: Magnetic bead's size evaluation

The immobilization of supersomes has already been described using different supports and experimental procedures [17,84,110,111]. In all cases, the most challenge is to maintain the catalytic activity and ensure the required stability of the enzymes after their immobilization. To overcome this, great efforts to optimize the immobilization procedures have been employed to improve either the enzymatic stability or metabolites production; however, it requires several experimental assessments, leading to excessive consumption of consumables, including expensive enzymes and co-factors, and the generation of chemical waste, besides being a time-consuming procedure. As a practical and low-cost strategy, rat liver microsomal fractions (RLM) were chosen as a model for the immobilization of CYP P450s onto magnetic beads.

RLM were covalently immobilized onto magnetic beads as a result of the imine production when using glutaraldehyde as a linker. Covalent immobilization has as the main advantages an easy experimental design, prevention of enzyme losses, and high immobilization success rate [112].

Our group has reported on the influence of the magnetic bead's size on the immobilization of acetylcholinesterase (AChE) considering the catalytic activity and affinity assays [99]. The results demonstrated that magnetic beads with a higher surface area improved the catalytic activity; however, for ligand fishing assays magnetic beads of 1 µm were the best choice. Herein, the influence of the size of the magnetic beads was also evaluated for the immobilization of RLM.

To meet this end, different magnetic bead sizes (1 µm diameter for Mb1 and 25 - 106 µm diameter for Mb2) were tested and their influence on the resulted RLM-Mbs was assessed as: (i) RLM solutions activity prior to and after immobilization; (ii) catalytic activity of the prepared RLM-Mbs.

The biocatalytic activity of the RLM-Mbs was evaluated by LC-MS/MS following the oxidation reaction of ABZ into ABZSO, as the major biotransformation metabolite. Inactivated RLM-Mbs were used as control and no production of ABZSO was observed. For the monitoring of the generated ABZSO, the developed LC-MS/MS method was validated following a fit-for-purpose approach considering the method selectivity, linearity, inter- and intra-day precision and accuracy, limit of quantification, the limit of detection, and carryover assays. The results are presented in the Supplementary material.

The residual enzymatic activity after RLM immobilization onto Mb1 and Mb2 was 5.9 and 39.9 %, respectively. Thus, the percentage of immobilization was about 94.1% for the RLM-Mb1 and 60. 1 % for the RLM-Mb2. Moreover, RLM-Mb1 presented 93.4 % higher metabolite production when compared to RLM-Mb2. The diameters and surface area of the Mbs directly influence the immobilization process. In our studies, the greater average surface area of Mb1 provided a higher amount of protein immobilized. Also, smaller beads have higher dispersion on support promoting a higher catalyst capacity [113]. Thus, the Mb1 was chosen to continue further experiments for the CYPs immobilization.

3.2. Doehlert design of experiment for the immobilization of CYP450 and generation of the RLM-Mbs

Modeling experimental procedures that are influenced by multiple variables can highly benefit from using multivariate statistics, especially regarding the reduction of the number of experiments, development time, and costs [114]. Different matrices can be used as chemometric tools for the optimization of methods in analytical chemistry. Among the most used, Doehlert design was selected due to its flexibility in allowing the study of independent variables at different levels resulting in efficient modeling of experimental data [114,115]. In this study, the Doehlert design has been used to optimize RLM immobilization and enhance the production of metabolites. Respectively, Table S2 and Table S3 refer to the experiments carried out and to the obtained results for the biotransformation of ABZ into ABZSO, which was evaluated in terms of logarithmic scale as a normalization factor.

The immobilization of RLM was optimized through 15 experiments including three replicates in the central point (experiments 13, 14, and 15) and all experiments were analyzed randomly. The replicates (n = 3) of the central point presented an average of 6.21 ± 0.06 %, indicating the accuracy and precision of the experiments. A mathematical model was generated and evaluated by analysis of variance (ANOVA) at a 95 % of confidence level. The model obtained presented a lack of fit because the ratio between the mean square of lack of fit (MSlof) and mean square of pure error (MSpe), resulted in a $F_{calculated}$ (2800) that was higher than $F_{tabulated}$ (18). Moreover, when comparing the mean of square of regression (MSR) and mean of square of residue (MSres), the $F_{calculated}$ (2.50) should be higher than the $F_{tabulated}$ (4.75) at a 95 % confidence level. In this sense, it showed that the regression analysis was not good enough; however, it did not affect the predicting ability of the model through equation 3.

Equation 3 and the constant b_0 (0.621) show that Y is the dependent variable (production of ABZSO), b_2 is the coefficient for protein concentration (0.28), and X_2 is the codified variable for protein concentration at the highest level (0.866). Thus, Y estimated was 6.45.

$$Y = b_0 + b_2(X_2) \qquad \textbf{Eq. 3}$$

As proof of concept for the predictive capability of the model, an experiment using 0.97 mg mL^{-1} of protein concentration, 1 % (v/v) of glutaraldehyde, and 2 hours of reaction time was carried out. The difference between the estimated value and the experimental results in the production of ABZSO was only 5.6%, as a relative error and, thus, providing the necessary experimental parameters for the immobilization procedures.

3.3. Enzymatic activity assay in different temperatures for the HLM-Mb

RLM demonstrated to be a useful and low-cost strategy to design the experimental conditions for microsomal fractions immobilization onto magnetic beads. The developed experimental conditions for RLM were easily transferred to the immobilization of HLM onto magnetic beads (HLM-Mbs). HLM's importance resides in the fact that HLM are the most widely used microsomes for drug metabolism studies in the early drug discovery stage, due to their great contribution to predicting *in vivo* outcomes from *in vitro* data [16,116]. To evaluate the catalysis ability of the produced HLM-Mbs, ABZ was also used as a probe to produce ABZSO, since it is known that the major P450 enzyme catalyzing the oxidation of ABZ to ABZSO is the CYP3A4 [117]. The influence of temperature in the metabolism reactions was evaluated at 16, 23, and 36 °C in eight consecutive experiment cycles. The results are presented in Fig. 1, which shows the influence of the temperatures on the enzymatic activity and, consequently, the stability of the HLM-Mbs. The biocatalysis performed well and produced a higher concentration of ABZO (481.1 ± 17.8 µmol L^{-1}) at 36 °C but showed an activity loss of 75.8 ± 1.0 % between the first and the last cycle, after the consecutive experiments reuse. When compared to 36 °C, the production of ABZSO was much smaller at 23 and 16 °C with concentration levels of ABZSO obtained at 163.3 ±

0.84 µmol L^{-1} and 95.6 ± 11.4 µmol L^{-1}, respectively. On the other hand, the catalytic stability of the HLM-Mbs between the reuse cycles showed a better behavior, being more stable.

In accordance with the literature [29], the enzymatic stability and reuse capability of the generated HLM-Mbs increased the production of the desired metabolites and promoted a system that can be employed for different analytical assays, showing it as the major advantages for enzymes immobilization. Moreover, by reusing the same biocatalyst, it is possible to minimize the use of consumables, decrease waste generation, and promote faster experiments. Due to the catalytic stability between the reuse cycles at 23 °C, this temperature was selected for further experiments.

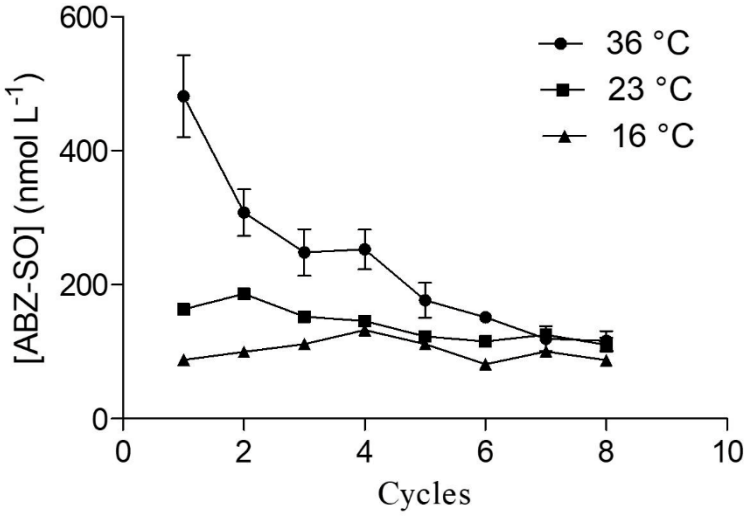

Fig. 1. Activity assays of the HLM-Mbs, targeting the biotransformation of ABZ into ABZSO. Experiments were conducted in eight consecutive experiment cycles at 16, 23, and 36 °C in ammonium acetate (10 mmol L^{-1}, pH 7.4).

3.4. Kinetic characterization and CYP3A4 inhibition assays using the HLM-Mbs

In drug metabolism assays, enzymatic kinetics are assessed by *in vitro* experiments as a suitable model to study reaction phenotyping, the production and

identification of metabolites, evaluation of metabolites stability, and inhibitors or inducers of drug-metabolizing enzymes [118]. *In vitro* research has many advantages over *in vivo* research, for example, i) a controlled physical-chemical environment; ii) a reduced cost when compared to animal and human studies; iii) higher data throughput, and iv) ethical advantages due to the reduced animal use. Considering the wide applicability of *in vitro* experiments, the HLM-Mb kinetic parameters were investigated by monitoring the CYP3A4-specific enzyme activity, which is the major enzyme involved in the ABZ metabolism. For that, eight consecutive assays were carried out with HLM-Mbs in ammonium acetate (10 mmol L^{-1}, pH 7.4) at 23 °C. The best nonlinear regression fit method was used to obtain the kinetic model for the CYP3A4 enzyme [119]. Thus, ABZSO formation was plotted according to the Michaelis-Menten equation (Equation 2) furnishing a V_{max} of 121.0 ± 6.68 µmol L^{-1}, and K_M of 25.64 ± 4.90 µmol L^{-1} (Fig. 2).

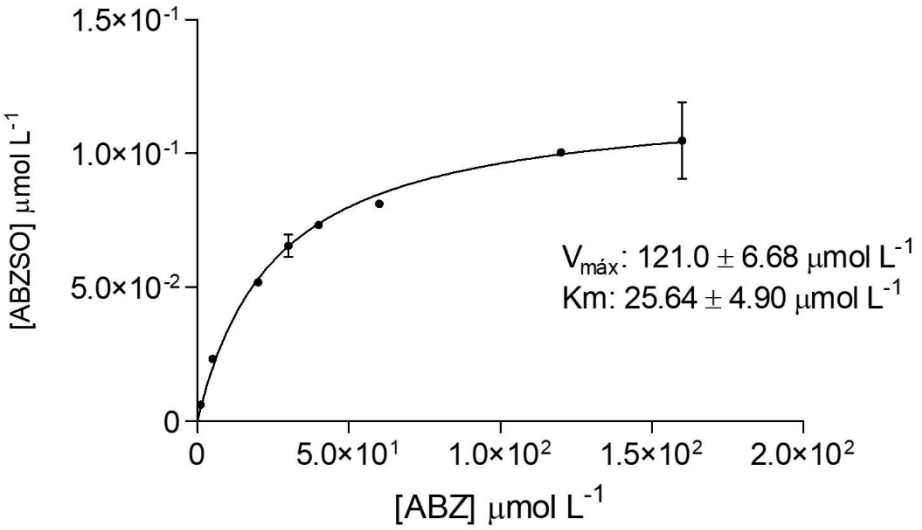

Fig. 2. HLM-Mb kinetic specific assay for CYP3A4 using ABZ from 1 to 160 µmol L^{-1}as a probe drug and monitoring of the ABZSO production. Experiments were carried out in ammonium acetate (10 mmol L^{-1}, pH 7.4), for 30 min at 23 °C.

Moreover, to demonstrate that HLM-Mbs could be used not only as a biocatalyst but also explored in *in vitro* phenotyping assays to predict a metabolite profile and ensure drug safety [31], ketoconazole (KET) was used as a CYP3A4 strong

reversible inhibitor [85]. The inhibitory effect was evaluated considering the *K*m value from the HLM-Mbs (K_M of 25.64 ± 4.90 µmol L^{-1}). First, the initial activity of HLM-Mbs (n = 6) was measured with ABZ 25.6 µmol L^{-1} (positive control) and the ABZSO production was 0.0439 ± 0.0057 µmol L^{-1}. Then, the concentration of ABZ (25.6 µmol L^{-1}) was kept fixed and the inhibition assays were carried out using ketoconazole (KET) at 12.8; 25.6; and 38.4 µmol L^{-1}. At 12.8 µmol L^{-1}, the production of ABZSO decreased by 46.8 ± 2.5 %, and this production was even lower with higher levels of KET (38.4 µmol L^{-1}). The results of the inhibition experiments using KET are presented in Fig. 3.

The inhibition of the CYP3A4 enzyme in the HLM-Mb biocatalyst by KET demonstrates the potential of the developed immobilized biocatalyst as an important and useful analytical strategy for *in vitro* drug metabolism studies, aiding versatility to the *in vitro* assays, as well as promoting new alternatives to inhibition studies [120].

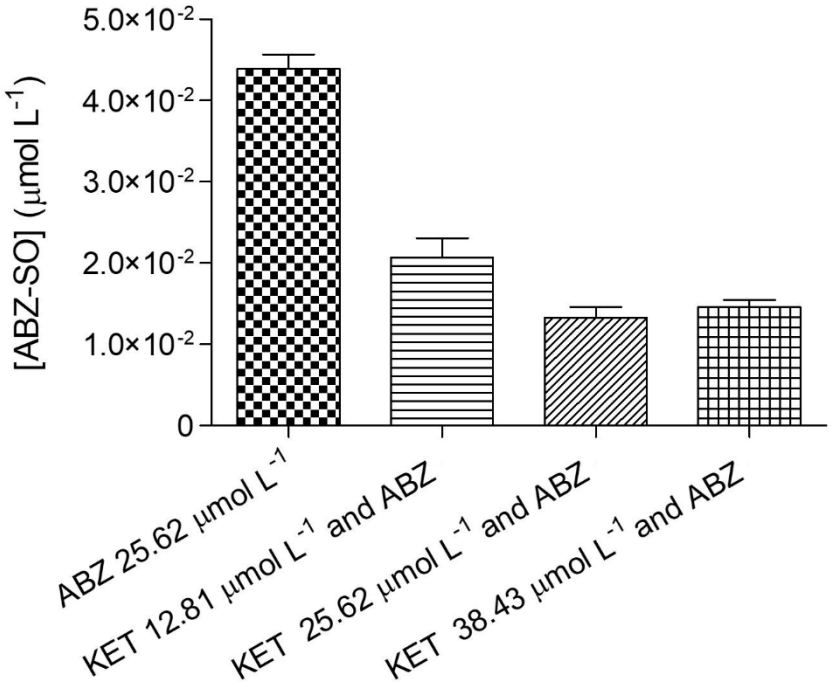

Fig. 3. CYP3A4 inhibition assays in the HLM-Mbs, using ABZ 25.6 µmol L^{-1} as a substrate and ketoconazole as an inhibitor. Experiments were carried out in ammonium acetate (10 mmol L^{-1}, pH 7.4) at 23 °C.

3.5. Specific activity assays for CYP2C9 and CYP2D6 on HLM-Mbs

The biotransformation reaction of diclofenac (DCF) to hydroxydiclofenac (DCF-OH) was chosen to monitor the CYP2C9-specific activity, while the conversion of bufuralol (BFL) into hydroxybufuralol (BFL-OH) was selected to monitor the CYP2D6-specific activity [94,121]. The produced metabolites were verified by monitoring *m/z* 312.9 for hydroxydiclofenac and *m/z* 278.4 for hydorxybufuralol in the LC-IT-MS method. Metabolism reactions were also carried out using inactivated HLM-Mbs as control and it was not observed any production of DCF-OH or BFL-OH. Base peak chromatograms for monitoring the production of DCF-OH and BFL-OH are presented in Fig. S1. These results demonstrated that the HLM-Mbs biocatalyst was able to immobilize different enzymes from the HLM fraction, and those are active as the CYP3A4 evaluated for the ABZ biotransformation. Therefore, the HLM-Mbs biocatalyst proved to be useful for the *in vitro* characterization of different enzymes that are equally important for *in vitro* metabolism studies. In this specific study, the investigated enzymes CYP3A4, CYP2D6, and CYP2C9 together are responsible for the metabolism of more than 63 % of all drugs [85].

3.6. The use of G6PDH-HLM-Mbs as one-pot strategy for NADPH production and CYP-mediated metabolism

The ability to carry out one-pot cascade enzymatic reactions has attracted attention to different processes in biotechnology by using an enzyme co-immobilization strategy. A recent review by Arana-Pena et al. [122] describes the pros and cons of different approaches, including when co-immobilization is almost compulsory and when it should be discarded. The capability of using a one-pot strategy for enzymes and cofactors is attractive because the cofactors are

expensive and are largely used in a relation to the mol of a cofactor to mol of a product, also require usually its use in excess to promote satisfactory yields.

When considering the cytochrome P450 biocatalysis, a complicated source of electrons via redox partners and NADPH are the main cofactors to mediate the oxidoreductase reactions. Therefore, it is critical to find cost-effective and practical uses to perform CYP-mediated reactions by overcoming the expensive use of NADPH. Recently, our group produced an NADPH generator system composed of the immobilization of glucose-6-phosphate dehydrogenase (G6PDH-Mbs) [8], which proved to be useful for the generation of *in situ* NADPH and drug metabolism, added to the fact that it could be re-used. Now, we report a one-pot strategy by the use of a dual biocatalyst composed of G6PDH-Mbs for the *in situ* generation of NADPH, associated with HLM-Mbs for the CYP-mediate *in vitro* metabolism. Therefore, independently immobilized biocatalysts, G6PDH-Mbs and HLM-Mbs, were prepared and combined to produce the dual G6PDH-HLM-Mbs. Application of the G6PDH-HLM-Mbs biocatalyst workflow is illustrated in Fig. 4

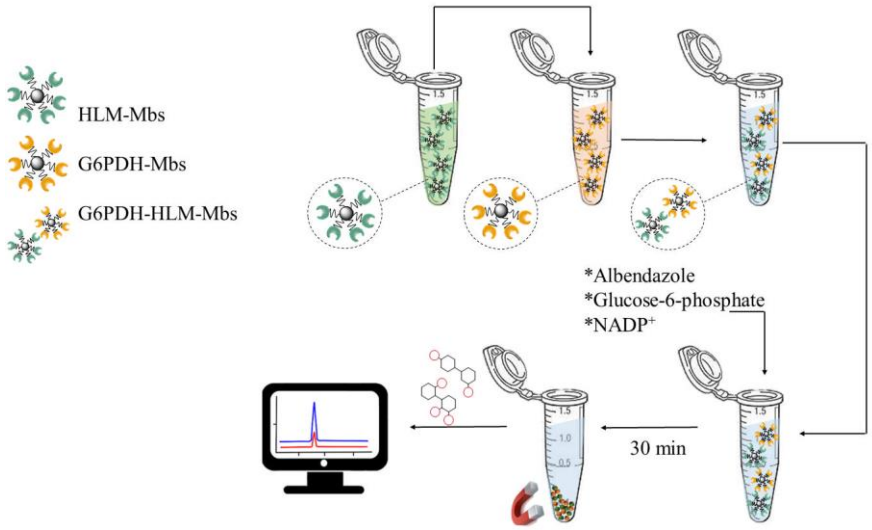

Fig 4. Development of a dual G6PDH-HLM-Mbs biocatalyst and its application in the generation of NADPH and biotransformation of ABZ to ABZSO.

ABZSO metabolite production was quantified by the LC-MS/MS method. The metabolism experiment was carried out in three cycles. When applying the G6PDH-HLM-Mbs, the production of ABZSO was 126.6 ± 5.3 nmol L^{-1} in the first experiment, and 72.8 ± 1.7 nmol L^{-1} in the third cycle (Fig. 5). Although a decrease of 42.5 % between the experiments was verified, the one-pot strategy by using G6PDH-HLM-Mbs could be an important strategy in experiments involving the use of cytochrome P450 and NADPH. Also, the application of the same immobilized biocatalyst in three consecutive experiments demonstrated the possibility of reusing the dual G6PDH-HLM-Mbs in multiple experiments.

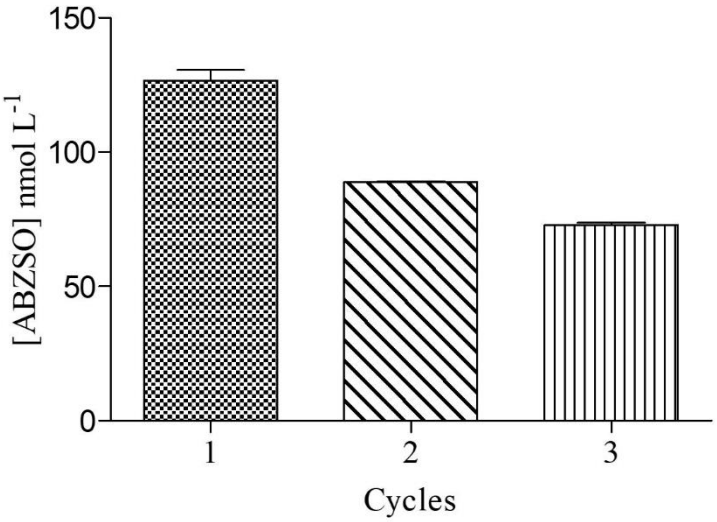

Fig. 5. Application and reuse of the dual G6PDH-HLM-Mbs in the *in vitro* metabolism of ABZ.

Conclusions

The Doehlert design showed to be a useful DoE approach for modulating the immobilization of cytochrome P450 enzymes onto magnetic beads and the RLM system demonstrated to be an economical model for the development of these experiments before moving forward to the immobilization of HLM that is more costly. The usefulness of HLM-Mbs was demonstrated by the *in vitro* metabolism of ABZ to produce ABZSO by the active CYP3A4, even after immobilization on

a solid support. Moreover, CYP3A4 inhibition assays using the HLM-Mbs and ketoconazole as a strong inhibitor, demonstrate the potential of the developed immobilized biocatalyst as new alternatives to inhibition studies. The activity of CYP2C9 and CYP2D6 in the hydroxylation reactions of diclofenac and bufuralol also illustrated that different enzymes immobilized from HLM fractions can equally keep their activity. This is especially important because purified HLM or supersomes are more expensive than a pool of microsomal fractions. The dual one-pot G6PDH-HLM-Mbs biocatalyst strategy for CYP-mediated reactions and simultaneous cofactors generation was successful applied to produce the *in vitro* metabolism of ABZ, which is an elegant solution to an old problem that is the production and generation of metabolites to be used as standards for analytical methods.

Conflicts of interest: The authors declare no conflict of interest.

Author contributions: I.L.F performed the experimental procedure, formal analysis of the data, contributed to the study conception and design, and wrote the manuscript. Q.B.C. and R.V.O conceived the study design, resources, funding acquisition supervision of the work, and formal analysis of the data. All authors gave significant contributions to the discussion and revision and agreed with the final version of the manuscript.

Founding: This research was founded by the Agency for the Improvement of Higher Education Personnel (CAPES) [Finance Code 001], the National Council for Scientific and Technological Development (CNPq) [grants 302557/2018-0 and 406064/2018-05], the São Paulo Research Foundation (FAPESP) [grants number 2014/50244-6, 2014/50249-8, 2020/05965-8, 2021/10569-7], the Ph.D. scholarships 2018/03035-3, and GlaxoSmithKline (GSK).

Acknowledge: The authors are grateful to Prof Wladimir R. Beck (Department of Physiological Sciences, Federal University of São Carlos) for furnishing livers from Wistar rats, and Prof Anderson R. M. de Oliveira (Department of Chemistry, University of São Paulo) for furnishing diclofenac and bufuralol for probes studies.

References

1. D. Valikhani, J. M. Bolivar, J. N. Pelletier, An Overview of Cytochrome P450 Immobilization Strategies for Drug Metabolism Studies, Biosensing, and Biocatalytic Applications: Challenges and Opportunities, ACS Catal. 11 (2021) 9418–9434. https://doi.org/10.1021/ACSCATAL.1C02017
2. M.T. Donato, J.V. Castell, Strategies and molecular probes to investigate the role of cytochrome P450 in drug metabolism: focus on in vitro studies, Clin. Pharmacokinet 42 (2003) 153–178. https://doi.org/10.2165/00003088-200342020-00004
3. M. Wang, D.L. Roberts, R. Paschke, T.M. Shea, B.S.S. Masters, J-J.P. Kim, Three-dimensional structure of NADPH–cytochrome P450 reductase: Prototype for FMN- and FAD-containing enzymes, Proc. Natl. Acad. Sci. 94 (1997) 8411–8416. https://doi.org/10.1073/PNAS.94.16.8411
4. U.M. Zanger, M. Schwab, Cytochrome P450 enzymes in drug metabolism: regulation of gene expression, enzyme activities, and impact of genetic variation, Pharmacol. Ther. 138 (2013) 103–141. https://doi.org/10.1016/J.PHARMTHERA.2012.12.007
5. Z . Li, Y. Jiang, X.F.P. Guengerich, L. Ma, S. Li, W. Zhang, Engineering cytochrome P450 enzyme systems for biomedical and biotechnological applications, J. Biol. Chem. 295 (2020) 833–849 . https://doi.org/10.1074/JBC.REV119.008758
6. R. Nicoli, M. Bartolini, S. Rudaz, V. Andrisano, J.L. Veuthey, Development of immobilized enzyme reactors based on human recombinant cytochrome P450 enzymes for phase I drug metabolism studies, J. Chromatogr. A. 1206

(2008) 2–10. https://doi: 10.1016/j.chroma.2008.05.080

7. E. O'Reilly, V. Köhler, S.L. Flitsch, Cytochromes P450 as useful biocatalysts: addressing the limitations, Chem. Commun. 47 (2011) 2490–2501. https://doi.org/10.1039/C0CC03165H
8. I.L. Furlani, R.V. Oliveira, Q.B. Cass, Glucose-6-phosphate dehydrogenase immobilized onto magnetic beads (G6PDH-Mb) as a generator system for production of NADPH: Development and application in metabolism studies, J. Pharm. Biomed. Anal. 219 (2022) 114901. https://doi.org/10.1016/J.JPBA.2022.114901
9. M.C. de Moraes, C.L. Cardoso, Q.B. Cass, Solid-Supported Proteins in the Liquid Chromatography Domain to Probe Ligand-Target Interactions, Front. Chem. 7 (2019) 752. https://doi.org/10.3389/fchem.2019.00752
10. R.A. Sheldon, Enzyme immobilization: The quest for optimum performance, Adv. Synth. Catal. 349 (2007) 1289–1307. https://doi.org/10.1002/adsc.200700082
11. J. Schejbal, R. Řemínek, L. Zeman, A. Mádr, Z. Glatz, On-line coupling of immobilized cytochrome P450 microreactor and capillary electrophoresis: A promising tool for drug development, J. Chromatogr. A. 1437 (2016) 234–240. https://doi.org/10.1016/J.CHROMA.2016.01.081
12. V. V. Shumyantseva, A. V. Kuzikov, R.A. Masamrekh, T. V. Bulko, A.I. Archakov, From electrochemistry to enzyme kinetics of cytochrome P450, Biosens. Bioelectron. 121 (2018) 192–204. https://doi.org/10.1016/J.BIOS.2018.08.040
13. J. Lu, D. Cui, H. Li, Y. Zhang, S. Liu, Cytochrome P450 bienzymes assembled on Au/chitosan/reduced graphene oxide nanosheets for electrochemically-driven drug cascade metabolism, Electrochim. Acta. 165 (2015) 36–44. https://doi.org/10.1016/J.ELECTACTA.2015.02.183
14. K. Wu, Y. Zhang, Q. Sun, Y. Chai, Q. He, X. Zhou, X. He, H. Ji, Preparation of cytochrome P450 enzyme-cobalt phosphate hybrid nano-flowers for

oxidative coupling of benzylamine, Enzyme Microb. Technol. 131 (2019) 109386. https://doi.org/10.1016/J.ENZMICTEC.2019.109386

15. C.H. Beckwitt, A.M. Clark, S. Wheeler, D.L. Taylor, D.B. Stolz, L. Griffith, A. Wells, Liver "organ on a chip.", Exp. Cell Res. 363 (2018) 15–25. https://doi.org/10.1016/J.YEXCR.2017.12.023
16. R. Nerimetla, G. Premaratne, H. Liu, S. Krishnan, Improved electrocatalytic metabolite production and drug biosensing by human liver microsomes immobilized on amine-functionalized magnetic nanoparticles, Electrochim. Acta. 280 (2018) 101–107. https://doi.org/10.1016/J.ELECTACTA.2018.05.085
17. K.R.A. Belaz, Q.B. Cass, R. V. Oliveira, Determination of albendazole metabolites by direct injection of bovine plasma and multidimensional achiral-chiral high performance liquid chromatography, Talanta 76 (2008) 146–153. https://doi.org/10.1016/j.talanta.2008.02.013
18. K.R.A. Belaz, R. V. Oliveira, HPLC-fluorescence Determination of EROD Activity in Wistar Rat Liver Microsomes Obtained by Two Different Extraction Procedures, Curr. Pharm. Anal. 9 (2013) 43-53. https://doi.org/10.2174/157341213804806034
19. M.M. Bradford, A rapid and sensitive method for the quantitation of microgram quantities of protein utilizing the principle of protein-dye binding, Anal. Biochem. 72 (1976) 248–254. https://doi.org/10.1016/0003-2697(76)90527-3
20. J.M. De Lima, I.L. Furlani, L.R.G. Da Silva, A.L. Valverde, Q.B. Cass, Micro- And nano-sized amine-terminated magnetic beads in a ligand fishing assay, Anal. Methods. 12 (2020) 4116–4122. . https://doi.org/10.1039/d0ay01269f
21. C.Y. Tan, H. Hirakawa, R. Suzuki, T. Haga, F. Iwata, T. Nagamune, Immobilization of a Bacterial Cytochrome P450 Monooxygenase System on a Solid Support, Angew Chem. Int. Ed. Engl. 55 (2016) 15002–15006.

https://doi.org/10.1002/ANIE.201608033

22. E. Schneider, D.S. Clark, Cytochrome P450 (CYP) enzymes and the development of CYP biosensors, Biosens. Bioelectron. 39 (2013) 1–13. https://doi.org/10.1016/J.BIOS.2012.05.043
23. V.B. Urlacher, M. Girhard, Cytochrome P450 monooxygenases: An update on perspectives for synthetic application, Trends Biotechnol. 30 (2012) 26-36. https://doi.org/10.1016/j.tibtech.2011.06.012
24. O. Barbosa, C. Ortiz, Á. Berenguer-Murcia, R. Torres, R.C. Rodrigues, R. Fernandez-Lafuente, A. Berenguer-Murcia, R. Torres, R.C. Rodrigues, R. Fernandez-Lafuente, Glutaraldehyde in bio-catalysts design: a useful crosslinker and a versatile tool in enzyme immobilization, RSC Adv. 4 (2014) 1583–1600. https://doi.org/10.1039/C3RA45991H
25. H. Veisi, M. Pirhayati, A. Kakanejadifard, P. Mohammadi, M.R. Abdi, J. Gholami, S. Hemmati, In Situ Green Synthesis of Pd Nanoparticles on Tannic Acid-Modified Magnetite Nanoparticles as a Green Reductant and Stabilizer Agent: Its Application as a Recyclable Nanocatalyst (Fe3O4 @TA/Pd) for Reduction of 4-Nitrophenol and Suzuki Reactions, Chemistry Select. 3 (2018) 1820–1826. https://doi.org/10.1002/slct.201702869
26. U.M.F.M. Cerqueira, M.A. Bezerra, S.L.C. Ferreira, R. de Jesus Araújo, B.N. da Silva, C.G. Novaes, Doehlert design in the optimization of procedures aiming food analysis – A review, Food Chem. 364 (2021) 130429. https://doi.org/10.1016/J.FOODCHEM.2021.130429
27. S.L.C. Ferreira, W.N.L. Dos Santos, C.M. Quintella, B.B. Neto, J.M. Bosque-Sendra, Doehlert matrix: A chemometric tool for analytical chemistry - Review. Talanta. 63 (2004) 1061-1067. https://doi.org/10.1016/j.talanta.2004.01.015
28. S. J. Richardson, A. Bai, A. A. Kulkarni, M. F. Moghaddam, Efficiency in drug discovery: liver S9 fraction assay as a screen for metabolic stability, Drug Metab. Lett. 10 (2016) 83–90.

https://doi.org/10.2174/1872312810666160223121836

29. A.D. Dayan, Albendazole, mebendazole and praziquantel. Review of non-clinical toxicity and pharmacokinetics, 86 (2003) 141–159. https://doi.org/10.1016/S0001-706X(03)00031-7
30. S. Nagar, U.A. Argikar, D.J. Tweedie, Enzyme kinetics in drug metabolism: fundamentals and applications, Methods Mol. Biol. 1113 (2014) 1–6. https://doi.org/10.1007/978-1-62703-758-7_1/COVER
31. A.C. Doran, W. Burchett, C. Landers, G.M. Gualtieri, A. Balesano, H. Eng, A.L. Dantonio, T.C. Goosen, R.S. Obach, Defining the Selectivity of Chemical Inhibitors Used for Cytochrome P450 Reaction Phenotyping: Overcoming Selectivity Limitations with a Six-Parameter Inhibition Curve-Fitting, Approach. Drug Metab. Dispos. 50 (2022) 1259-1271. https://doi.org/10.1124/dmd.122.000884
32. R. Walsky, S. Boldt, In vitro cytochrome P450 inhibition and induction, Curr. Drug Metab. 9 (2008) 928–939. https://doi.org/10.2174/138920008786485128
33. E.I. Minder, P.J. Meier, H.K. Müller, C. Minder, U.A. Meyer, Bufuralol metabolism in human liver: a sensitive probe for the debrisoquine-type polymorphism of drug oxidation, Eur. J. Clin. Invest. 14 (1984) 184–189. https://doi.org/10.1111/J.1365-2362.1984.TB01121.X
34. S. Arana-Peña, D. Carballares, R. Morellon-Sterlling, Á. Berenguer-Murcia, A.R. Alcántara, R.C. Rodrigues, R. Fernandez-Lafuente, Enzyme co-immobilization: Always the biocatalyst designers' choice…or not?, Biotechnol. Adv. 51 (2020) 107584. https://doi.org/10.1016/j.biotechadv.2020.107584

SUPPLEMENTARY MATERIAL

Immobilization of cytochrome P450 enzymes onto magnetic beads: an approach to drug metabolism and biocatalysts

Izadora Liranço Furlani[1], Regina Vincenzi Oliveira[1] and Quezia Bezerra Cass[1*]

[1]SEPARARE – Chromatography Research Center, Department of Chemistry, Federal University of São Carlos, São Carlos, Brazil

Table S1. LC-MS/MS acquisition parameters for albendazole (ABZ) and its metabolites.

Compound	Precursor (*m/z*) $[M+H]^+$	SRM transitions	Cone (V)	Collision (V)
ABZ	265.90	234.05	10	24
		191.16	10	38
ABZ-SO	282.10	159.04	26	38
		207.90	26	24
ABZ-SO_2	298.11	159.03	32	38
		266.00	32	20
ABZ-SO_2-NH_2	240.10	105.86	34	38
		133.08	34	30

ABZ-SO: albendazole sulfoxide; ABZ-SO_2: albendazole sulfone, ABZ-SO_2-NH_2: albendazole amino sulfone

Table S2. Codified and real values using the Doehlet design of experiments

Glutaraldehyde (% v/v)							
Codified	-1	-0.5	0	0.5	1		
Real	1	2	3	4	5		
Protein Concentration (mg mL^{-1})							
Codified	-0.866	-0.577	-0.289	0	0.289	0.577	0.866
Real	0.032	0.188	0.344	0.5	0.6	0.8	0.97
Reaction time (hours)							
Codified	-0.817	0	0.817				
Real	2	5	8				

Table S3. Matrix of Doehlert design and results for the optimization of CYP enzymes immobilized on magnetic beads.

Exp.	Variables			*In vitro* metabolism* (log)
	Glutaradehyde % (v/v)	Protein concentration (mg mL^{-1})	Time of reaction (hours)	
1	5	0.5	5	6.15
2	4	0.97	5	6.36
3	4	0.6	8	5.85
4	1	0.5	5	6.22
5	2	0.032	5	5.61
6	2	0.344	2	6.00
7	4	0.032	5	5.71
8	4	0.344	2	6.41
9	2	0.97	5	6.29
10	3	0.8	2	6.05
11	2	0.6	8	6.07
12	3	0.188	8	5.85
13	3	0.5	5	6.21
14	3	0.5	5	6.22
15	3	0.5	5	6.21

*Monitoring of albendazole-sulfoxide production.

S1. Fit-for-purpose LC-MS/MS method validation

For the quantification of ABZSO, the LC-MS/MS method was validated considering the selectivity, linearity, inter- and intra-day precision and accuracy, limit of quantification, the limit of detection, and carryover. The calibration curve obtained for ABZSO was linear with a correlation coefficient value of r^2 =0.993 and calibration equation y = 78.09x + 390.80 (n = 3). The precision (CV%) ranged from 1.6 to 9.2 % and the accuracy from 98.2 to 115.3 %. The limit of detection for ABZSO was 0.5 nmol L^{-1}, and the limit of quantification was 1 nmol L^{-1}.

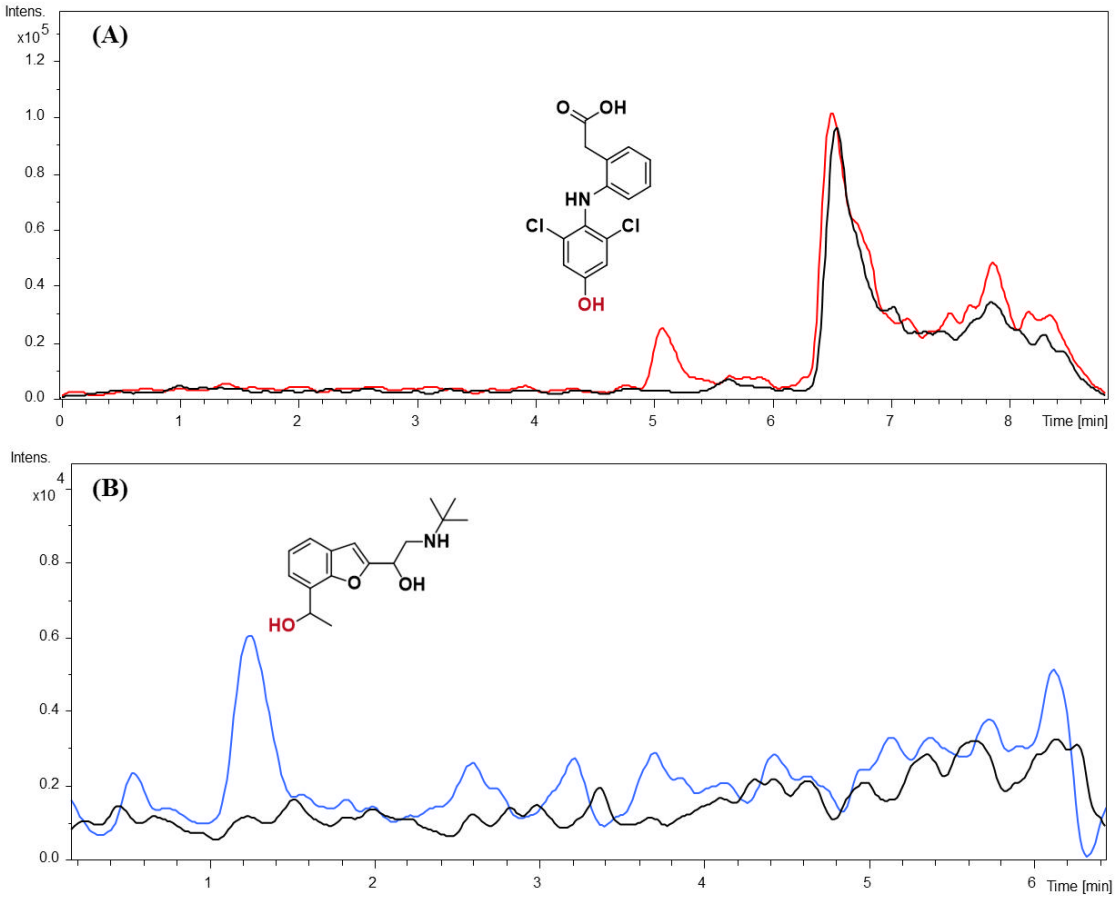

Figure S1. Base peak chromatograms for hydroxydiclofenac (red), hydroxybufuralol (blue), and Hum-Mbs inactive (black).

Chapter III

Conclusions

Chapter III | Conclusions

Considering the complex catalytic system of enzymes from cytochrome P450, herein we developed biocatalytic bioreactors aiming to boost biotransformation reactions catalyzed by those enzymes and overcome some drawbacks associated with the lack of stability, and promote an enhancement of the production of metabolites and nicotinamide adenine dinucleotide phosphate (NADPH).

Thus, as an important part of this work, a generator system based on the immobilization of glucose-6-phosphate dehydrogenase onto magnetic beads were developed and successfully applied in *in situ* production of NADPH. Also, a simple LC-UV method for separation of $NADP^+$ and NADPH was developed and qualified for the quantification of high concentrations of NADPH produced by G6PDH-Mbs. The catalytic activity, and stability of the biocatalyst bioreactor produced were evaluated, and its applicability was demonstrated in *in vitro* metabolism of albendazole and fiscalin B. Taking into account that NADPH is an important and essential substrate of several biological reactions, the application of G6PDH-Mbs goes beyond of *in vitro* drug metabolism assay, and it can be easily applied for other biocatalysts proposes.

The immobilization of CYPs onto magnetic beads were optimized through a Doehlert design. In this sense, the experiment design was applied as an important tool to optimize the immobilization conditions for CYP enzymes from rat liver microsomal fractions. Results from Doehlert design provided a significant reduction in the reaction time and in the amount of reagents typically used during the procedure. Thus, the optimized conditions were successfully applied for CYP from human liver microsomal fractions (HLM-Mbs). The catalytic activity of HLM-Mbs was studied in terms of different temperatures and cycles by monitoring the hydroxylation reaction of albendazole. A higher amount of albendazole sulfoxide was observed under 36 °C. At this temperature the

biocatalytic bioreactor can be applied as a tool in biocatalysis to enhance the concentration of metabolites produced. At 23 °C was demonstrated the reuse of HLM-Mbs in eight cycles, which allowed the application of the biocatalytic bioreactor in kinetic and inhibition studies. The experiment carried out in different temperatures clearly demonstrated that HLM-Mbs can be applied for production and generation of metabolites that can be used as standards for analytical methods and in *in vitro* drug metabolism proposes. In addition, CYP3A4 inhibition assays were carried out using the HLM-Mbs and ketoconazole as a strong inhibitor. Although the formation of albendazole-sulfoxide was clearly affected by the presence of ketoconazole, its high concentration used in this study could affect other CYP isoforms, not only CYP3A4.

Finally, as a dual one-pot strategy, both biocatalyst bioreactors produced alongside this project were jointly used (G6PDH-HLM-Mbs) promoting one system to mediate biotransformation reactions catalyzed by CYPs and by simultaneous cofactors generation. The utility of this strategy was demonstrated for *in vitro* metabolism of albendazole, and the G6PDH-HLM-Mbs were applied in three consecutive experiments. The higher concentration of metabolites produced and the possibility of reusing the system are important achievements to correlate *in vitro-in vivo* outcomes.